POWER SYSTEM STATE ESTIMATION USING CONTRACTION MAPPING AND SINGULAR VALUE DECOMPOSITION

by

Arina Aboonabi

B.Sc., K.N.T University of Technology, 2004

A THESIS SUBMITTED IN PARTIAL FULFILLMENT
OF THE REQUIREMENTS FOR THE DEGREE OF
MASTER OF APPLIED SCIENCE
in the School
of
Engineering Science

SIMON FRASER UNIVERSITY
Summer 2011

APPROVAL

Name: **Arina Aboonabi**

Degree: **Master of Applied Science**

Title of Thesis: **Power System State Estimation Using Contraction Mapping and Singular Value Decomposition**

Examining Committee:

Chair: **Dr. Carlo Menon P.Eng.**
Assistant Professor, School of Engineering Science

Dr. Mehrdad Saif P.Eng.
Senior Supervisor
Professor, School of Engineering Science

Dr. John Jones P.Eng.
Supervisor
Associate Professor, School of Engineering Science

Dr. Ahmad Rad
Examiner
Professor, School of Engineering Science

Date Approved: 20 April 2011

SFU SIMON FRASER UNIVERSITY
LIBRARY

Declaration of Partial Copyright Licence

Abstract

State estimation plays a key role in the operation of power systems. This role becomes more important considering the increasing demand of emerging power market.
Many methods have been proposed for power system state estimation, mostly based on Weighted Least Squares (WLS) approach. However, it is well known that Least Absolute Value (LAV) estimators are more efficient in terms of robustness and accuracy. For these estimators there is no closed form solution and each LAV estimator has its own criteria in choosing desired measurements. In this research, two novel LAV estimators are introduced for power system state estimation. The first estimator employs contraction mapping concepts for rejecting redundant measurements. The second estimator is introduced for systems where sparsity and ill-conditioning occur in the system matrix. In the second estimator, Singular Value Decomposition (SVD) method is combined with contraction mapping technique to find the appropriate equations for the estimation.
The application of the new estimator is studied on different IEEE power systems for verification. The estimator shows a robust performance in all the test systems, and the estimation error remains comparatively small even in the presence of significant number of bad data points.

Keywords: Power Systems, State Estimation, Least Absolute Value Estimator, Contraction Mapping, Singular Value Decomposition.

Acknowledgments

When composing this thesis I received assistance and support from many people, without whom this thesis may not come out. First of all, I want to express my deepest gratitude to my supervisor Dr. Mehrdad Saif for his support and encouragement through my studies. I also want to express my best regards to the former Dr. Gustave S. Christensen who inspired this research in many ways.

I would like to thank my defense committee members, Dr. Ahmad Rad, Dr. Carlo Menon and especially my co-supervisor Dr. John Jones for taking the time to review my work. Special acknowledgements go to Teresa Taylor and Bernard Marrocco for their comments on editing my thesis.

I would also like to thank S.M.Mahdi Alavi from Simon Fraser University and Mohammad Rasouli from University of Calgary for their valuable hints and comments on my research.

My sincere gratitude goes to my aunts, Mahvash and Mahtash for their never-ending love and support, to my father for being my rock through the life, and to my mum for her patience especially in the past few months.

Last but not least a huge thank you to my dear lab mates at control system lab, my fellows in schools of engineering and computing science, our director's secretary Roya and my wonderful friend Siamak.

Contents

List of Tables

List of Figures

List of Acronyms

LS: Least Squares
WLS: Weighted Least Squares
LAV: Least Absolute Value
WLAV: Weighted Least Absolute Value
SVD: Singular Value Decomposition
PBD: Portion of Bad Data
Iter: Iteration

Chapter 1

Introduction

1.1 State Estimation

State estimation is, by definition, the procedure in which values are assigned to unknown state variables of a system such that bad measurements of the system are filtered out during the process, and estimation error is minimized based on a specific criteria. As a result we can have accurate estimations of the states even in the presence of bad measurements [9].

State estimation plays a key role as the initial step for analyzing and controlling power networks. Contingency analysis, stability analysis, and optimal power flow all rely on the quality of the network model obtained via state estimation [2]. With the increasing demand for reliable electric energy in recent years, the growth of the size and complexity of power networks has been significant. Therefore, there is a need for more accurate and precise estimators in today's energy market [43].

To enable the state estimation, a model is built based on the information obtained from the network. In that model, if the ratio of the measurements from the system to the unknown states has an appropriate rate, the process can reduce the effect of bad data and even allow the temporary loss of measurements without affecting the quality of the estimation. Moreover, the measurements from those parts of network which are not directly metered can be estimated.

1.2 Power System Specifications

State variables in power networks are complex nodal voltages consisting of voltage magnitudes and their respective phase angles. Measurements include active and reactive power injections at network buses, and power flows in branches. In recent years, Phaser Measured Units (PMUs) are available in some power networks and they can efficiently present power angle measurements [45], although those types of measurements are not considered in this research. The state estimation process is to assign values to the unknown states such that erroneous measurements are filtered or have minor effects in state calculation.

Erroneous measurements or bad data, in this research, are referred to measurements, within the set, which are either totally different from their true values, or include a certain amount of noise in them. In real systems, these erroneous measurements are caused by various sources: A monitoring failure of a communication link can corrupt the correct value of measurement. Also it is known that some meters have intermittent fault and do not show the true values of measured quantities. Other reasons are sudden change of operating point of system and human error in some cases.

1.3 Literature Review

The most popular state estimation method in industry is Weighted Least Squares (WLS), which minimizes the weighted sum of residual squares [38]. WLS estimator is not a robust estimator since it is sensitive to bad data. Also, if the assigned weights are relatively large, the system may face numerical problems and even ill-conditioning [41]. Therefore, various bad data detection and identification methods has been developed to enhance the performance of estimator [40].

Bad data can be detected using the residuals method [1]. If the difference between the calculated and measured quantities of one measurement is large compared to other measurements, that measurement usually belongs to the bad data set. Other famous statistical tests such as chi-square and Hypothesis test can also be applied to detect bad data [6].

Other than the standard normal equations method, different solution approaches has been used to improve the numerical robustness of WLS estimator. These approaches include orthogonal methods, hybrid method, equality constrained method, Hatchel's method and sparse tableau method [39].

Least Absolute Value (LAV) estimator is an alternative estimator applied to power systems. The objective function of LAV estimators is to reduce the absolute norm of residuals. In contrast to WLS method, there is no explicit solution for LAV estimator and each LAV estimator has its own approach for finding the solution. Many LAV estimators reformulated the estimation problem as a Linear programming (LP) problem and obtained the solution by solving a sequence of LP problems [37]. Some LAV estimators, used a sequence of solutions to the L_1-regression problem employing an iteratively re-weighted least squares method and avoid Linear Programming due to its large computational time [27]. Other researchers claimed to obtain a Weighted Least Absolute Value (WLAV) estimate by applying the Newton-Raphson method to the set of equations that includes critical measurements or measurements essential for system observability and got test results competitive with standard estimators [25].

In general, methods based on Least Squares estimation are good for noise filtering when the error is Gaussian, but they fail in the presence of other types of bad data or noise. Least Absolute Value methods, on the other hand, have superior bad data suppression capability. However, they are computationally more expensive and fail in cases where bad data is associated with leverage points.

Leverage points are those measurements of a power system which have a stronger influence on the state estimation due to their location, the local measurement redundancy, the network topology, and parameters. These measurements, can distort the solution of the LAV estimation, when they carry bad data. There were LAV estimators that eliminate the leveraging effects of injection measurements via matrix stretching [26]. Linear transformation was also used to reduce the effect of leverage points on WLAV estimation [24].Also, a LAV estimator had been introduced that used integration with a sequence of L_1 regression to eliminate leverage points [27]. Although these estimators are more robust in rejecting bad data they have a poor computational time in comparison with LS based estimators. Therefore, there is still a need to develop a robust state estimator that can satisfy the conflicting requirements of speed, accuracy, and efficiency [28].

1.4 Motivations

In the late 1980s, Christensen, Soliman and Rouhi introduced a technique for curve-fitting based on Least Absolute Value (LAV) minimization technique [11]. The idea was originally developed for power system state estimation. However, the technique could address other linear/linearized systems; the advantage was being non-iterative and simple, with minimal computational requirements. Later, due to claims that the introduced method does not generally guarantee the existence of a solution or the clear relationship between estimated values [12], the authors generalized the method for cases of repeated measurements and multi optimal solutions [13]. Eventually, the approach led to a new algorithm for nonlinear L_1 norm minimization problem with applications in power systems [8]. Hence, all of these LAV estimators partially employ Least Squares (LS) techniques in the estimation process.

In 2007, Christensen, Saif and Soliman developed another algorithm for LAV estimation, without using LS techniques [7]. The methods used in this study are inspired by that algorithm. The elimination criteria are based on contraction mapping, such that it initially normalizes the matrices involved in estimation, and then eliminates the measurements with larger absolute sum of coefficients on the columns. After selecting the proper equations, the solution is found for the system and the Least Absolute Value of error is calculated for all the residuals. The method is simple and non-iterative, and its computing time and storage requirements are very small in comparison to other methods [7]. However, the mentioned algorithm has been applied for linear data-fitting applications only. For applying it to nonlinear power systems, the method needs adjustments. For instance, the equations driven from the system model should be approximated by a linearization technique and the iteration should be applied to get an acceptable result. The estimated states have a high accuracy and low estimation error in small-scale power networks [15]. In contrast, the method fails to provide an acceptable estimation in networks with more than five buses. For those networks we improve the estimator by including the Singular Value Decomposition (SVD) technique in the process [16]. As a result, the estimator enhances in estimation and provides satisfactory results, even in the presence of large portions of bad data.

Different IEEE standard networks are considered for testing the estimators. These test cases include IEEE 5 bus, IEEE 10 bus, IEEE 14 bus, IEEE 30 bus, IEEE 57 bus, and IEEE

118 bus networks [18]. Also, different types and amounts of bad data are applied to each network. The performance of suggested estimator is compared with LS estimator through various tables and figures.

1.5 Thesis Content

The remainder of this thesis is organized as follows: In chapter two state estimation for power systems is defined and the two, popular numerical approaches for a superior estimation are discussed and compared. In chapter three, the basic concepts for modeling a power network and obtaining mathematical formulation of system are introduced. Chapter four explains the suggested LAV estimators for related power networks in detail. In chapter five, the method is applied for power system state estimation on IEEE standard buses. In the last chapter, a summary of the developed methods and results is provided.

Chapter 2

The Problem and Proposed Methods

2.1 Introduction

State estimation is an essential and necessary part of power system analysis. In the real time modeling of a power system, the necessary steps before state estimation are usually data gathering, network topology processing and observability analysis. During this process, the set of measurements are gathered by Supervisory and Control Data Acquisition (SCADA) system and are transferred to the state estimator along with the pervious state of the system. The output of the state estimator provides the core information for making control decisions including contingency selection and analysis, economic dispatch calculations, optimal power flow, security assessment and other related functions [31].

In measuring and modeling a power network, diverse types of errors can occur including meter and communication errors, errors in mathematical models, and incomplete measurements. A useful estimator, is designed to reduce the effect of bad data and provide a reliable estimation of power system states. Since most of the state estimators currently used in the power industry are based on the Least Squares approach, the techniques for obtaining the solution of these estimators are presented in this chapter. In contrast to LS-based estimators, the LAV estimators are well-known representative of non-quadratic estimators with robust characteristics and are also introduced in this chapter.

2.2 State Estimation Problem

The state estimation problem in general can be addressed in a system with a number of known measurements and unknown states, represented as follows:

$$Z = H(X) + \Gamma \tag{2.1}$$

or similarly as:

$$\begin{bmatrix} z_1 \\ z_2 \\ \vdots \\ z_m \end{bmatrix} = \begin{bmatrix} h_1(x_1, \cdots, x_n) \\ h_2(x_1, \cdots, x_n) \\ \vdots \\ h_m(x_1, \cdots, x_n) \end{bmatrix} + \begin{bmatrix} \gamma_1 \\ \gamma_2 \\ \vdots \\ \gamma_m \end{bmatrix} \tag{2.2}$$

where $z_k,\ k = 1, \cdots, m$ represents the measurements obtained from the system and m gives the number of measurements. The state variables are denoted by $x_k,\ k = 1, \cdots, n$ and n is the number of unknown states. The rational polynomial functions that relate the states to the measurements are indicated by $h_k(x),\ k = 1, \cdots, m$. Therefore, matrix $H(X)$ shows the relationships between the measurements and the unknown states of system; these can be linear or nonlinear. When the relationship is linear, $H(X)$ will hereafter be shown as an $m \times n$ matrix H. The measurement errors are presented by $\gamma_k,\ k = 1, \cdots, m$. These errors are usually modeled as Gaussian errors with zero mean (E$(\gamma_k) = 0$). Also, if the measurement errors are independent and uncorrelated the covariance matrix of errors is a diagonal matrix shown by W, (cov$(\Gamma) = W$). In general, the measurement error matrix varies for different types of bad data and will be introduced more specifically in section 3.8.

Based on the ratio of measurements to unknowns, three cases can be defined: 1) If the ratio is less than one, it means that the number of measurements is less than the number of states. In this case the system is called underestimated. It is not always possible to get a unique estimate of states based on measurements for such systems. 2) If the ratio equals one, the system is called a fully determined system and the estimated states are given by solving (2.1) directly. Estimated states in such systems are usually of poor quality since all the measurements, including the erroneous ones, should be used for estimation. 3) Finally, if the ratio is larger than one, which means there are more measurements than unknown states, the system is overdetermined. The estimation problems addressed in this research are related to overdetermined systems, and the goal is to reduce the effect of erroneous measurements in the estimation process.

State estimation can reduce the effect of bad data, and allow the temporary loss of some measurements without significantly affecting the quality of the estimates. A well-known example is power system state estimation, which is mainly applied to filter redundant data, eliminate faulty measurements, and so produce a reliable state estimation [3]. The estimator can even determine the power flow in parts of the network that are not directly metered. Real-time models of power networks can also be constructed from online snapshots of system measurements and physical properties of the networks [43]. These models, which are obtained from state estimation, have a key role in various applications of the energy market, such as optimal power flow and contingency analysis.

2.3 Observability Concept

Observability in a power network means that the estimator is able to determine the unknown states based on the given measurements. If there are enough measurements and they are well distributed throughout the network in such a way that state estimation is possible, then the network is said to be observable. If a network is not observable, it is still useful to know which sections have states that can be estimated, or to determine the observable sections. Mathematically, in an observable network the system matrix is full-rank. If only some parts of a network are observable (observable islands), their related matrices should be full-rank. In the observable parts of a network, measurement redundancy is defined as the ratio of the number of measurements to the number of states. In this research, the underlying assumption is that the given networks are observable in terms of the measurements.

2.4 Normal Equations Method and Quadratic Estimators

As previously mentioned, one of the most common approaches in power system state estimation is defining the objective function as the square sum of the difference between measured values and estimated values. This approach is based on a popular statistical criteria of maximum likelihood for Gaussian distributions of measurement errors, as discussed in the next section and is categorized az the normal equations method.

There are other estimation approaches introduced for power systems. The orthogonal methods is one of the famous ones based on the P-θ and Q-V decoupling in power flow. The method is developed in order to minimize the required memory and computational time, however, the convergence rate is strongly influenced by the initial voltages [28]. Other methods, such as sparse tableau formulation and equality constrained WLS are introduced for extended problems in the field [6], however, the focus of this research is on normal equations method.

2.4.1 Maximum Likelihood and Weighted Least Squares Estimator

Consider there are m observations (or measurements) from a system and that we are interested in estimating an unknown parameter (or parameters) related to these observations. The concept of maximum likelihood is usually used in this type of context to find the unknown parameter such that it maximizes the joint probability density of observations; that is, it maximizes the probability of occurrence of observed data.

A measurement in a power system can be expressed as follows:

$$z_{meas} = z_{true} + \gamma \tag{2.3}$$

where γ represents the observation error. In most state estimation problems there is a prior knowledge of error patterns, including those for power systems. Typically, the nature of measurement error in these systems is assumed to be Gaussian [1]. If the mean value of γ is zero, the Probability Density Function (PDF) of measurement z_1 can be written as:

$$f(z_{1meas}) = \frac{1}{\sqrt{2\pi}\sigma_1} \exp\left(-\frac{(z_{1meas} - z_{1true})^2}{2\sigma_1^2}\right) \tag{2.4}$$

where σ_1 represents the standard deviation of z_{1meas}. Considering all m measurements of the system, the joint PDF of measurements is:

$$f(z) = f(z_1)f(z_2)\cdots f(z_m) \tag{2.5}$$

$$f(z) = \frac{1}{(\sqrt{2\pi})^m \prod_{i=1}^{m} \sigma_i} \exp\left(\sum_{i=1}^{m} -\frac{(z_{imeas} - z_{itrue})^2}{2\sigma_i^2}\right) \tag{2.6}$$

Instead of maximizing the joint PDF which is expressed in (2.6), we can maximize the logarithm of the joint PDF. This approach provides the same result, but is more mathematically convenient [29].

$$log(f(z)) = -\frac{1}{2}\sum_{i=1}^{m} \frac{(z_{imeas} - z_{itrue})^2}{(\sigma_i)^2} - \frac{m}{2} log(2\pi) - \sum_{i=1}^{m} log(\sigma_i) \tag{2.7}$$

Clearly, the maximization method results in minimizing the weighted sum of least squares of difference between observed values and their true values. This is the well-known Weighted Least Squares (WLS) minimization problem [2]. In an overdetermined system with m measurements and n unknowns, usually there are measurements which are less accurate. Weight is assigned to each measurement typically in proportion to the inverse of the variance of each measurement, such that the weights are smaller for the less accurate measurements (the ones with larger variances), and larger on the more accurate ones [29]. The objective is to minimize the performance index:

$$J(X) = \sum_{i=1}^{m} w_i {e_i}^2 = \sum_{i=1}^{m} w_i \left(\text{row}_i(Z - HX)\right)^2 \tag{2.8}$$

where w_i is the i_{th} diagonal element of weight matrix, such that $w_i = 1/\sigma_i^2$. Hence, the weighting matrix W is a diagonal matrix, which is the inverse covariance matrix for the measurements.

The solution to the minimization problem can be found by setting the gradient of objective function (2.8) to zero, as shown below:

$$minJ(X) = min\left((Z - HX)^T W (Z - HX)\right) \tag{2.9}$$

$$minJ(X) = min\left(Z^T W Z - Z^T W H X - X^T H^T W Z + X^T H^T W H X\right) \tag{2.10}$$

$$\nabla_X J(X) = 0 - H^T W Z - H^T W Z + H^T W H X + H^T W H X = 0 \tag{2.11}$$

$$2H^T W H = 2H^T W H X \tag{2.12}$$

$$X = (H^T W H)^{-1}(H^T W Z) \tag{2.13}$$

2.4.2 Least Squares Estimator

The Least Squares (LS) method has been used since the beginning of 18th century, and still has many applications in data-fitting and linear regression. It can be considered to be a special case of WLS with equal weights. This method is usually used in power-system state estimation when the covariance matrix of measurements is unknown, or where it may lead to singularity of product matrices in the system of equations [8].

Similar to the WLS, the LS method can be used for a linear system of overdetermined equations, where the goal is finding the best estimate for minimizing the sum of squared residuals. The approach is called LS linear, since the system is linear in its parameters and the solution is linearly dependent on the data.

$$J(X) = \sum_{i=1}^{m} {e_i}^2 = \sum_{i=1}^{m} (\mathrm{row}_i(Z - HX))^2 \tag{2.14}$$

or

$$\mathit{min} J(X) = \mathit{min} \Big((Z - HX)^T (Z - HX) \Big) \tag{2.15}$$

Following the same method used for WLS, the solution to this problem can be calculated as

$$X = (H^T H)^{-1} H^T Z \tag{2.16}$$

This solution is valid when the system matrix H is full rank, since in that case HH^T is invertible.

2.4.3 Nonlinear Systems

In AC-power system state estimation, the relationships between the measured values and states are nonlinear. The nonlinear WLS problem can be written as:

$$J(X) = \sum_{i=1}^{m} w_i e_i^2 = \sum_{i=1}^{m} \frac{(z_i - h_i(x))^2}{{\sigma_i}^2} \tag{2.17}$$

Although the linear WLS has a closed form solution, there is no closed form answer for the nonlinear WLS. Instead, the solution can be obtained through iterative methods. If the relationship between the measurements and the states is not linear, then we need to approximate the nonlinear system first, and use iterations to find an appropriate solution. Two methods commonly used for solving the minimization problem are Gauss-Newton and Newton-Raphson.

Gauss-Newton Method

To linearize a nonlinear system, we usually consider the equilibrium point of the system and write the Taylor series expansion around the equilibrium point. In the Gauss-Newton Method the first two terms of the series are considered in the linear model as follows:

$$h(x + \triangle x) \simeq h(x) + \frac{\partial h(x)}{\partial x} \triangle x \tag{2.18}$$

Then the objective function (2.17) can be written as

$$J(\triangle X) = \left(Z - H(X) - \frac{\partial H(X)}{\partial X} \triangle X \right)^T W \left(Z - H(X) - \frac{\partial H(X)}{\partial X} \triangle X \right) \tag{2.19}$$

Considering $\triangle Z = Z - H(X_0)$, and $A = \frac{\partial H(X)}{\partial X}|_{X_0}$,

$$\mathit{min} J(\triangle X) = \mathit{min} \left((\triangle Z - A \triangle X)^T W (\triangle Z - A \triangle X) \right) \tag{2.20}$$

Since equation (2.20) now matches with the linear WLS equation (2.9), its solution can be obtained by,

$$\triangle X = (A^T W A)^{-1} A^T W \triangle Z \tag{2.21}$$

During the iterative procedure, the value of X is updated to $X_1 = \triangle X + X_0$, and X_1 is considered as the new equilibrium point around which the linearization process is repeated.

Newton-Raphson Method

In approximating the nonlinear model of system, Gauss-Newton method ignores the derivative terms with order higher than one. On the other hand, Newton-Raphson method also considers the derivatives of order two. This means that the Newton-Raphson method is more precise in terms of approximating the nonlinear system. Recalling the objective function presented in (2.17), the gradient of the objective function is the non linear $g(X)$, which is expressed as:

$$g(X) = \nabla_X J(X) = -\sum_{i=1}^{m} \frac{z_i - h_i(X)}{\sigma_i} \frac{\partial h_i(X)}{\partial X} \tag{2.22}$$

The nonlinear gradient function $g(x)$ can be approximated by Gauss-Newton method as:

$$g(x + \triangle x) = g(x) + G(x)\triangle x \tag{2.23}$$

where $G(x)$ is the derivative of $g(x)$. Considering equation 2.22, and for the overdetermined system of nonlinear equations, $G(X)$ can be written as:

$$G(X) = \frac{\partial g(X)}{\partial X} = \frac{\partial^2 J(X)}{\partial^2 X} = -\left(\sum_{i=1}^{m} \frac{z_i - h_i(X)}{\sigma_i} \frac{\partial^2 h_i(X)}{\partial X^2} - \frac{\partial h_i(X)}{\partial X} \frac{1}{\sigma_i} \left(\frac{\partial h_i(X)}{\partial X}\right)^T\right) \tag{2.24}$$

Considering the matrix Z and A mentioned in (2.20), $G(X)$ can also be simplified to:

$$G(X) = \sum_{i=1}^{m} \frac{\triangle z_i}{\sigma_i} \frac{\partial^2 h_i(X)}{\partial X^2} - A^T W A \tag{2.25}$$

To minimize the objective function $J(X)$, the gradient function should be equal to zero. Considering the nonlinear gradient function $g(X)$, its linear approximation can be set equal to zero to minimize the objective function. Therefore,

$$g(X + \triangle X) = g(X) + G(X)\triangle X = 0 \tag{2.26}$$

$$G(X)\triangle X = -g(X) \tag{2.27}$$

$$\triangle X = -G^{-1}(X)g(X) = G^{-1}A^T W \triangle Z \tag{2.28}$$

and finally

$$\triangle X = \left(\sum_{i=1}^{m} \frac{\triangle z_i}{\sigma_i} \frac{\partial^2 h_i(X)}{\partial X^2} - A^T W A\right)^{-1} A^T W \triangle Z \tag{2.29}$$

Obviously, if the second derivative term $\sum_{i=1}^{m} \frac{1}{\sigma_i} \triangle z_i \frac{\partial^2 h_i(X)}{\partial X^2}$, is omitted from (2.29), it will be equivalent to (2.21). The effect of this term in nonlinear estimation is related to the difference between actual observations and their calculated values $\triangle Z$. In power system state estimation, this term is usually negligible since its effect on convergence is normally insignificant. There are exceptions in cases where strong nonlinearity of measurements is combined with topology errors, but in most practical implementations of power system state estimation, Gauss-Newton method leads to an acceptable estimation [2].

2.5 Robust Estimators

As discussed in previous sections, one of the goals of each state estimator is to reduce the influence of bad data on the estimation results. In LS-based methods, all the measurements are considered for estimation. Despite the fact that WLS estimators assign high weights to larger residuals, the estimator still considers all the measurements, including the erroneous ones, for estimation. In contrast, the robust estimator has the ability of bad data elimination.

Consider an extreme case where all the measurements except one are correct and flawless, and that the error on that one measurement tends toward being infinitely large. The objective function in the LS-based estimator tends to infinity in this case, since the estimator has to consider all the measurements, including the enormous erroneous measurement. However, an ideal robust estimator would not be sensitive to the error in a single measurement, since it is able to totally eliminate the bad measurement.

2.5.1 Least Absolute Value Estimator

The Least Absolute Value (LAV) estimator is an estimator whose objective function is minimizing norm one of the residuals, as presented in (2.30) for linear systems and in (2.31) for nonlinear systems.

$$J(X) = \sum_{i=1}^{m} |e_i| = \sum_{i=1}^{m} \text{row}_i |Z - HX| \tag{2.30}$$

$$J(X) = \sum_{i=1}^{m} |e_i| = \sum_{i=1}^{m} |z_i - h_i(x)| \tag{2.31}$$

Similar to the LS estimator, Weighted Least Absolute Value (WLAV) estimator is also defined as the absolute weighted sum of residuals.

$$J(X) = \sum_{i=1}^{m} w_i |e_i| = \sum_{i=1}^{m} w_i \left(\text{row}_i |Z - HX|\right) \tag{2.32}$$

$$J(X) = \sum_{i=1}^{m} w_i |e_i| = \sum_{i=1}^{m} w_i |z_i - h_i(x)| \tag{2.33}$$

For an overdetermined system of equations, the LAV estimator only considers n measurements among the total of m measurements. Considering the previous example of only one infinitely erroneous measurement, the LAV has the ability to ignore the bad measurement completely and present a reasonable result, in contrast to LS estimator. Therefore, LAV belongs to the group of robust estimators since it fits only the n selected data.

The selection of data points is a critical issue in LAV estimation: when an unwanted data point is selected as good data, it can affect the estimator. For larger and more complex systems, the effect is more significant. In some cases, bad data can totally effect the robustness of estimator, especially if leverage points are present in the data set. Leverage points are the data points that have strong effects on estimation. In power system state estimation, the leverage points are usually related to measurements from nodal injections and low impedance branches [5]. Therefore, the LAV bad data rejection is not perfect in all cases, and the selection criterion is a key issue in the performance of the estimator.

LAV estimator has been used in power system state estimation since the early 1970s [20, 21, 22]. Unlike the LS-based estimators, there is no explicit formula for obtaining the solution of a LAV estimator. Various LAV-based estimators were introduced, with different approaches on data fitting and bad data rejection: modifying the system matrix of WLAV by linear transformation to eliminate bad data [24], stretching the Jacobian matrix for reducing the effect of leverage points [26], developing a WLAV estimator by minor adjustments to WLS estimator to be used instead of standard Linear Programming (LP) [25], and a LAV estimator to find the L1-regression solution for power systems [27]. However, there is still a need to develop a robust state estimator that can satisfy the conflicting requirements of speed, accuracy, and efficiency [28].

2.6 Detection and Identification of Bad Data

In real time applications of a power system, state estimation is usually followed by yet another essential step: processing of bad data. The ability to detect and identify bad measurements is a valuable tool and it can enhance the performance of estimator especially in the presence of bad data among the measured quantities. The statistical methods used for detection of bad data are Largest Residuals test, Chi-Square and Hypothesis test. The general idea of these methods is that errors affecting the estimates are not usually compatible with their standard deviations [44].

2.6.1 Largest Residuals Test

To detect the presence of bad data, the largest residual test compares the residuals of state estimation with their standard deviation. The residual of each measurement is defined as the difference between its measured quantity and its calculated quantity based on state estimation. The test is also named as Largest Normalized Residual (LNR) and in that version it calculates the ratio of residual estimates to the standard deviation of the residuals. Considering the case where all the measurements are perfect except one measurement, it can be proven that no other residual has a larger residual (or normalized residual) compare to the erroneous measurement [1]. Note that even when there exists other measurements with same residual magnitude, none of them can have a larger residual.

The application of the largest residual test in not limited to the normal equations approach in state estimation. The largest residual method was used in the blocked sparse matrix approach and it was further extended to Lagrange multipliers associated with equality constraints [6].

2.6.2 Chi-Square and Hypothesis Test

Consider the performance index of the WLS as given in equation 2.17. If the measurement errors are random numbers with Gaussian distribution and zero mean, the performance index has a chi-square distribution and its degree of freedom is $k = m$ (number of measurements)$-n$ (number of states).

When a number of measurements are erroneous, their errors are frequently much larger than the assumed $|3\sigma|$ error bound for the measurement. If a threshold, t_J, is set for the performance index, $J(X)$, it can be declared that bad measurements are present when $J(X) > t_J$. The threshold test might be wrong in two situations. If t_J is set to a small value, we would get many false alarms. The false alarm means that the test would indicate the presence of bad measurements even when there were none. Also if t_J is set to a large value, the test would often detect no errors even when erroneous measurements were present. The test can be written as the following equation:

$$\text{Prob}(J(X) > t_J | J(X) \text{is a chi-square with k degrees of freedom}) = \beta \tag{2.34}$$

This type of testing is known as the Hypothesis testing and the parameter β is called the significance level of the test [1].

2.7 Summary

In this chapter, two popular numerical approaches to power system state estimation were reviewed. First, the formulation process of LS method was explained for overdetermined linear systems, and then extended to nonlinear systems, explaining the techniques for linearizing the system.

Despite the popularity of LS and its wide spread applications in industry, the LS-based estimator is not robust in the presence of bad data. Hence, the concept of LAV estimation was briefly explained as an alternative.

The estimation solution for a LAV estimator is based on its own selection technique and varies from one estimator to another. In chapter 4, a new LAV estimation approach for power system estimation will be discussed in more detail.

Chapter 3

Power System Model Description and Formulation

3.1 Introduction

This chapter reviews the fundamental components of a power network, and the nonlinear model based on those components. Then the mathematical formulation of the power system, relating the states and measurements of the system, is presented. The process of linearizing the model and finding the exact solution of states for particular operating conditions is also explained. Finally, to analyze the performance of different estimators on the network in the presence of erroneous measurements, various types of bad data points are defined. These types of bad data will be considered in chapter 4, in the process of state estimation in power systems.

3.2 Network Components and Assumptions

In this research, we assume that the power system is operating in the steady state and under balanced conditions. This assumption implies that all bus load and branch power flows are three-phase and balanced, all transmission lines are fully transposed, and all shunt devices and line charges are symmetrical in three-phase. Under these conditions, the use of single-phase positive sequence equivalent circuits for modeling the entire system is allowed [3]. Moreover, network data as well as network variables are expressed in the per-unit scale.

3.2.1 Per-Unit System

The per-unit value representation of electrical variables is a common standard in many power system problems [19].

The numerical per-unit value of any quantity is its ratio to a chosen base's quantity of the same dimension. Thus, a per-unit quantity is normalized with respect to the chosen base value. The per-unit quantity of the value is defined as:

$$\text{P.U. Value} = \frac{\text{Actual Value}}{\text{Reference or the Base Value of the same dimension}} \tag{3.1}$$

In an electrical network, the current i, the complex voltage v, the complex power s and the impedance z are the four quantities usually involved in the calculations. These four quantities are completely described by knowledge of only two of them. In other words, an arbitrary choice of two base quantities fixes the other base quantities [19]. The base units considered in this study are 100 MW for active power and 100 MVAR for reactive power. Impedance is measured in 100 MVA base.

3.2.2 Transmission Line

The equivalent two-port π model of a transmission line is shown in Figure 3.1. This figure represents the series impedance of z_{ij} and total shunt impedance of z_{si} and z_{js} at nodes i and j. The relationship between the real and imaginary components of impedance can be expressed as:

$$\begin{aligned} z_{ij} &= r_{ij} + jx_{ij} \\ y_{ij} &= z_{ij}^{-1} = g_{ij} + jb_{ij} \\ g_{ij} &= \frac{r_{ij}}{(r_{ij}^2 + x_{ij}^2)} \\ b_{ij} &= \frac{-x_{ij}}{(r_{ij}^2 + x_{ij}^2)} \end{aligned}$$

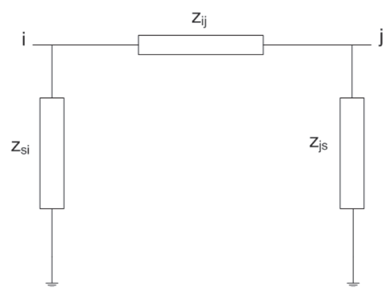

Figure 3.1: The π model of a transmission line

In above formulas, z_{ij} is the series impedance shown in Figure 3.1. The resistance and reactance of impedance z_{ij} are presented by r_{ij} and x_{ij} respectively. Similarly, the admittance of a transmission line is represented by y_{ij}. The conductance and susceptance of y_{ij} are indicated by g_{ij} and b_{ij}.
The complex voltage at node k is presented as $e_k = v_k \exp(j\theta_k)$, where v_k is the voltage magnitude at node k, and θ_k is the associated phase angle.

3.2.3 Transformer

The transformers in network branches can be modeled with an ideal transformer, with a fixed tap ratio, a_{im}, on the primary side. Also, a series impedance, z_{mj}, is added to the transformer to present resistive losses and leakage reactance. The model is shown in Figure 3.2.

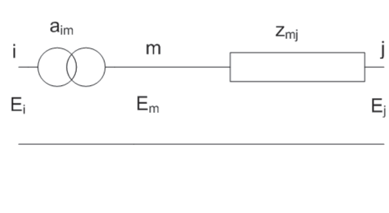

Figure 3.2: The transformer in a transmission line

In this research, we consider the ideal in-phase transformers for the network with the fixed tap ratio a_{im}. Regarding Figure 3.2, the phase angle at node i is equal to the phase angle at point m , $\theta_i = \theta_m$, and the tap ratio is $a_{im} = \frac{v_i}{v_m}$. Therefore, the relationship between the complex nodal voltages in the presence of transformer can be expressed as:

$$\frac{e_i}{e_m} = \frac{v_i \text{exp}(j\theta_i)}{v_m \text{exp}(j\theta_m)} = a_{im} \tag{3.2}$$

3.2.4 Shunt Capacitor

A static or a shunt capacitor is represented by its per unit susceptance at the related buses and is usually used for voltage/power control.

3.2.5 Loads and Generators

In modeling the network, loads and generators are considered as equivalent complex power injections and have no effect on the structure of the network model. The only exception can be a constant impedance type load, which is included as shunt admittances at the corresponding bus [3].

3.3 Problem Variables

In the basic formulation for power systems, four variables are assigned to each bus in the network:

- v_k- Voltage magnitude
- θ_k- Phase angle
- p_k- Net active power
- q_k- Net reactive power

There are different types of measurements and depending on the information provided for estimation, most commonly used measurements are: bus power injections, line power flow, bus voltage magnitudes, and line current flow magnitudes [19]. These measurements can be expressed in terms of the state variables.

The static state of an electric power system is defined as the vector of the voltage magnitudes and phase angles at all system nodes, except one node [20]. Considering a system with n_b buses, the size of the state vector is $2(n_b - 1)$, which includes voltage magnitude and phase angles at all buses except the reference bus. The reference bus (or slack bus) is a bus for which these variables are considered known. In the problem formulation, the related lines for slack bus measurements and variables are eliminated during the estimation process. Using the definitions and notations in Table 3.1 and considering the components

Table 3.1: The power system's parameters and variables

p_i	Active power of the i-th bus	MW
q_i	Reactive power of the i-th bus	MVAR
e_i	Complex voltage at the i-th bus	kV
v_i	Voltage magnitude of the i-th bus	kV
θ_i	Phase angle of the i-th bus	rad
p_{ij}	Active power flow between bus i and bus j	MW
q_{ij}	Reactive power flow between bus i and bus j	MVAR
θ_{ij}	$\theta_i - \theta_j$	rad
g_{ij}	The real part of line admittance	MVA
g_{si}	The real part of shunt admittance	MVA
b_{ij}	The imaginary part of line admittance	MVA
b_{si}	The imaginary part of shunt admittance	MVA

and assumptions described in section 3.2, the transmission line power flow can be expressed as:

$$s_{ij} = e_i i_{ij}^* = e_i \left(e_i y_{is} + (e_i - e_j) y_{ij}\right)^* = e_i e_i^* y_{si}^* + e_i (e_i - e_j)^* y_{ij}^* \tag{3.3}$$

$$s_{ij} = v_i^2 (g_{si} - j b_{si}) + v_i^2 (g_{ij} - j b_{ij}) - v_i v_j \text{exp}(\theta_{ij})(g_{ij} - j b_{ij}) \tag{3.4}$$

Since $s_i = p_i + j q_i$, the active and reactive power flows can be written separately as:

$$p_{ij} = -v_i v_j \left(g_{ij} cos(\theta_i - \theta_j) + b_{ij} sin(\theta_i - \theta_j)\right) + v_i^2 (g_{si} + g_{ij}) \tag{3.5}$$

$$q_{ij} = -v_i v_j \left(g_{ij} sin(\theta_i - \theta_j) - b_{ij} cos(\theta_i - \theta_j)\right) - v_i^2 (b_{si} + b_{ij}) \tag{3.6}$$

The net power flow at system node i is:

$$s_i = e_i i_i^* = e_i \sum_{k=1}^{m} y_{ik}^* e_k^* = v_i \text{exp}(j\theta_i) \sum_{k=1}^{m} (g_{ik} - j b_{ik}) v_k \text{exp}(-j\theta_k) \tag{3.7}$$

$$s_i = \sum_{k=1}^{m} v_i v_k (g_{ik} - j b_{ik}) [cos(\theta_i - \theta_k) + j sin(\theta_i - \theta_k)] \tag{3.8}$$

Therefore active and reactive power at bus i can be expressed as:

$$p_i = \sum_{k=1}^{m} v_i v_k \left(g_{ik} cos(\theta_i - \theta_k) + b_{ik} sin(\theta_i - \theta_k) \right) \tag{3.9}$$

$$q_i = \sum_{k=1}^{m} v_i v_k (g_{ik} sin(\theta_i - \theta_k) - b_{ik} cos(\theta_i - \theta_k)) \tag{3.10}$$

However, for finding the total power at each bus, we should also consider the generation or load power on that bus. So the total active and reactive power are given by:

$$p_{total}(i) = p_{gen}(i) - p_{load}(i) - \sum_{k=1}^{p} g_{ik} v_i v_k cos(\theta_i - \theta_k) + b_{ik} v_i v_k sin(\theta_i - \theta_k) \tag{3.11}$$

$$q_{total}(i) = q_{gen}(i) - q_{load}(i) - \sum_{k=1}^{p} g_{ik} v_i v_k sin(\theta_i - \theta_k) - b_{ik} v_i v_k cos(\theta_i - \theta_k) \tag{3.12}$$

where g_{ik} and b_{ik} are the ik-th real and imaginary elements of system admittance matrix Y_{bus}.

3.4 The Mathematical Formulation

As mentioned in the previous section, voltage magnitudes and phase angles are defined as states in our study. The vector presentation of state X therefore is given as:

$$X = \begin{bmatrix} \Theta \\ V \end{bmatrix} = \begin{bmatrix} \theta_1 \\ \theta_2 \\ \vdots \\ \theta_n \\ v_1 \\ v_2 \\ \vdots \\ v_n \end{bmatrix} \tag{3.13}$$

Now considering the active and reactive power at network nodes and branches as our measurements, we get

$$Z = \begin{bmatrix} P \\ Q \end{bmatrix} = \begin{bmatrix} p_1 \\ \vdots \\ p_n \\ q_1 \\ \vdots \\ q_n \\ p_{12} \\ \vdots \\ p_{nr} \\ q_{12} \\ \vdots \\ q_{nr} \end{bmatrix} \tag{3.14}$$

Let us now represent the relationship between states and measurements as:

$$H(X) = \begin{bmatrix} P(x) \\ Q(x) \end{bmatrix} = \begin{bmatrix} p_1(x) \\ \vdots \\ p_n(x) \\ q_1(x) \\ \vdots \\ q_n(x) \\ p_{12}(x) \\ \vdots \\ p_{nr}(x) \\ q_{12}(x) \\ \vdots \\ q_{nr}(x) \end{bmatrix} \tag{3.15}$$

The matrices in equations (3.13), (3.14), and (3.15) can now be mapped to the system of overdetermined nonlinear equations (2.2), which will be discussed in chapter 4. The remaining matrix in equation (2.2) is matrix Γ, known as measurement error that, in general, can have different patterns (Measurement error is discussed in section 3.8.) The derivation of Jacobian matrices, based on nonlinear equations from power systems, is explained in section 3.5. The Jacobian matrix will be used in the linearization procedure of nonlinear power systems in chapter 4 and 5.

3.5 Deriving the Jacobian Matrix

The Jacobian matrix contains partial derivatives of the mismatch vector (P and Q equations) with respect to the variable vector X.

$$A = \begin{bmatrix} Jn_{11} & Jn_{12} \\ Jn_{21} & Jn_{22} \\ Jb_{11} & Jb_{12} \\ Jb_{21} & Jb_{22} \end{bmatrix} \tag{3.16}$$

Matrix A is constructed on the Jacobian matrix of nodal measurements Jn, and power flow measurements Jb.

$$Jn_{11} = \frac{\partial P_{total}}{\partial \Theta}$$
$$Jn_{12} = \frac{\partial P_{total}}{\partial V}$$
$$Jn_{21} = \frac{\partial Q_{total}}{\partial \Theta}$$
$$Jn_{22} = \frac{\partial Q_{total}}{\partial V}$$

$$Jb_{11} = \frac{\partial P_{branch}}{\partial \Theta}$$
$$Jb_{12} = \frac{\partial P_{branch}}{\partial V}$$
$$Jb_{21} = \frac{\partial Q_{branch}}{\partial \Theta}$$
$$Jb_{22} = \frac{\partial Q_{branch}}{\partial V}$$

The elements of the Jacobian matrix for nodal power measurements are:

$$Jn = \begin{bmatrix} Jn_{11} & Jn_{12} \\ Jn_{21} & Jn_{22} \end{bmatrix} = \left[\begin{array}{ccc|ccc} \frac{\partial p_1}{\partial \theta_1} & \cdots & \frac{\partial p_1}{\partial \theta_n} & \frac{\partial p_1}{\partial v_1} & \cdots & \frac{\partial p_1}{\partial v_n} \\ \frac{\partial p_2}{\partial \theta_1} & \cdots & \frac{\partial p_2}{\partial \theta_n} & \frac{\partial p_2}{\partial v_1} & \cdots & \frac{\partial p_2}{\partial v_n} \\ \vdots & \ddots & & \vdots & \ddots & \\ \frac{\partial p_n}{\partial \theta_1} & \cdots & \frac{\partial p_n}{\partial \theta_n} & \frac{\partial p_n}{\partial v_1} & \cdots & \frac{\partial p_n}{\partial v_n} \\ \hline \frac{\partial q_1}{\partial \theta_1} & \cdots & \frac{\partial q_1}{\partial \theta_n} & \frac{\partial q_1}{\partial v_1} & \cdots & \frac{\partial q_1}{\partial v_n} \\ \frac{\partial q_2}{\partial \theta_1} & \cdots & \frac{\partial q_2}{\partial \theta_n} & \frac{\partial q_2}{\partial v_1} & \cdots & \frac{\partial q_2}{\partial v_n} \\ \vdots & \ddots & & \vdots & \ddots & \\ \frac{\partial q_n}{\partial \theta_1} & \cdots & \frac{\partial q_n}{\partial \theta_n} & \frac{\partial q_n}{\partial v_1} & \cdots & \frac{\partial q_n}{\partial v_n} \end{array}\right] \tag{3.17}$$

Also, the elements of active and reactive power flow measurements can be written as:

$$Jb = \begin{bmatrix} Jb_{11} & Jb_{12} \\ Jb_{21} & Jb_{22} \end{bmatrix} = \left[\begin{array}{ccc|ccc} \frac{\partial p_{1p}}{\partial \theta_1} & \cdots & \frac{\partial p_{1p}}{\partial \theta_n} & \frac{\partial p_{1p}}{\partial v_1} & \cdots & \frac{\partial p_{1p}}{\partial v_n} \\ \vdots & \ddots & & \vdots & \ddots & \\ \frac{\partial p_{nq}}{\partial \theta_2} & \cdots & \frac{\partial p_{nq}}{\partial \theta_n} & \frac{\partial p_{nq}}{\partial v_2} & \cdots & \frac{\partial p_{nq}}{\partial v_n} \\ \hline \frac{\partial q_{1p}}{\partial \theta_1} & \cdots & \frac{\partial q_{1p}}{\partial \theta_n} & \frac{\partial q_{1p}}{\partial v_1} & \cdots & \frac{\partial q_{1p}}{\partial v_n} \\ \vdots & \ddots & & \vdots & \ddots & \\ \frac{\partial q_{nq}}{\partial \theta_1} & \cdots & \frac{\partial q_{nq}}{\partial \theta_n} & \frac{\partial q_{nq}}{\partial v_2} & \cdots & \frac{\partial q_{nq}}{\partial v_n} \end{array}\right] \tag{3.18}$$

Hence, the elements of matrices Jn and Jb can be calculated by taking the partial derivatives of measurements with respect to the states, as shown in sections 3.5.1 to 3.5.8.

3.5.1 Elements of Matrix Jn_{11}

$$\frac{\partial p_i}{\partial \theta_i} = \sum_{k=1,k\neq i}^{p} -g_{ik}v_iv_ksin(\theta_i - \theta_k) + b_{ik}v_iv_kcos(\theta_i - \theta_k) \tag{3.19}$$

$$\frac{\partial p_i}{\partial \theta_k} = -g_{ik}v_iv_ksin(\theta_i - \theta_k) + b_{ik}v_iv_kcos(\theta_i - \theta_k) \tag{3.20}$$

3.5.2 Elements of Matrix Jn_{12}

$$\frac{\partial p_i}{\partial v_i} = \sum_{k=1,k\neq i}^{p} -g_{ik}v_kcos(\theta_i - \theta_k) - b_{ik}v_ksin(\theta_i - \theta_k) - 2v_ig_{ii} \tag{3.21}$$

$$\frac{\partial p_i}{\partial v_j} = -g_{ik}v_i sin(\theta_i - \theta_k) - b_{ik}v_i cos(\theta_i - \theta_k) \tag{3.22}$$

3.5.3 Elements of Matrix Jn_{21}

$$\frac{\partial q_i}{\partial \theta_i} = \sum_{k=1,k\neq i}^{p} -g_{ik}v_i v_k cos(\theta_i - \theta_k) - b_{ik}v_i v_k sin(\theta_i - \theta_k) \tag{3.23}$$

$$\frac{\partial q_i}{\partial \theta_k} = g_{ik}v_i v_k cos(\theta_i - \theta_k) + b_{ik}v_i v_k sin(\theta_i - \theta_k) \tag{3.24}$$

3.5.4 Elements of Matrix Jn_{22}

$$\frac{\partial q_i}{\partial v_i} = \sum_{k=1,k\neq i}^{p} -g_{ik}v_k sin(\theta_i - \theta_k) + b_{ik}v_k cos(\theta_i - \theta_k) + 2v_i b_{ii} \tag{3.25}$$

$$\frac{\partial q_i}{\partial v_j} = -g_{ik}v_i sin(\theta_i - \theta_k) + b_{ik}v_i cos(\theta_i - \theta_k) \tag{3.26}$$

3.5.5 Elements of matrix Jb_{11}

$$\frac{\partial p_{ij}}{\partial \theta_i} = -v_i v_j(-g_{ij} sin(\theta_i - \theta_j) + b_{ij}v_i v_j cos(\theta_i - \theta_j) \tag{3.27}$$

$$\frac{\partial p_{ij}}{\partial \theta_j} = -v_i v_j(g_{ij} sin(\theta_i - \theta_j) - b_{ij}v_i v_j cos(\theta_i - \theta_j) \tag{3.28}$$

3.5.6 Elements of Matrix Jb_{12}

$$\frac{\partial p_{ij}}{\partial v_i} = -v_j(g_{ij} cos(\theta_i - \theta_j) + b_{ij} sin(\theta_i - \theta_j) + 2v_i(g_{si} + g_{ij}) \tag{3.29}$$

$$\frac{\partial p_{ij}}{\partial v_j} = -v_i(g_{ij} cos(\theta_i - \theta_j) + b_{ij}v_i sin(\theta_i - \theta_j) \tag{3.30}$$

3.5.7 Elements of Matrix Jb_{21}

$$\frac{\partial q_{ij}}{\partial \theta_i} = -v_i v_j(-g_{ij}cos(\theta_i - \theta_j) + b_{ij}v_i v_j sin(\theta_i - \theta_j) \tag{3.31}$$

$$\frac{\partial q_{ij}}{\partial \theta_j} = v_i v_j(-g_{ij}cos(\theta_i - \theta_j) + b_{ij}v_i v_j sin(\theta_i - \theta_j) \tag{3.32}$$

3.5.8 Elements of Matrix Jb_{22}

$$\frac{\partial q_{ij}}{\partial v_i} = -v_j(g_{ij}sin(\theta_i - \theta_j) - b_{ij}cos(\theta_i - \theta_j)) - 2v_i(b_{ij} + b_{si}) \tag{3.33}$$

$$\frac{\partial q_{ij}}{\partial v_j} = -v_i(g_{ij}sin(\theta_i - \theta_j) - b_{ij}cos(\theta_i - \theta_j)) \tag{3.34}$$

3.6 Final Format of Matrices

In power system modeling, there exists a bus in each power network which is named as the slack bus. The slack bus or the reference bus is one of the generation buses of the system, whose phase angle is assumed zero. For the simplicity, the voltage magnitude of slack bus, in this research, is also considered known.

The matrix formulation of the power system as described in the pervious sections results in a system of equations with m measurements and $2n_b$ states where n_b is the number of system buses. Since the number of states is $n = 2(n_b - 1)$, the columns of the Jacobian matrix, which are related to derivatives of phase angle and voltage magnitude of the slack bus, should be eliminated in the final format of matrices. Respective rows of the state vector X should also be eliminated for the slack bus.

3.7 Newton-Raphson Method

To calculate the exact solution of the states, Newton-Raphson method is applied to the network. In Newton-Raphson method, we consider only the nodal measurements for the system; hence, the overdetermined set of nonlinear equations are reduced to a completely determined set which has an exact solution. To get the exact solution, the following steps are followed:

- Calculate ΔZ matrix using the following equation.

$$\Delta Z_n(i) = \begin{bmatrix} \Delta P_n(i) \\ \Delta Q_n(i) \end{bmatrix} = \begin{bmatrix} \Delta P_n - P_n[X(i)] \\ \Delta Q_n - Q_n[X(i)] \end{bmatrix} \tag{3.35}$$

- Find Jacobian matrix Jn, based on equation (3.17) in the previous section.
- Solve the linear set of fully determined equations:

$$\begin{bmatrix} Jn_{11} & Jn_{12} \\ Jn_{21} & Jn_{22} \end{bmatrix} \begin{bmatrix} \Delta\Theta(i) \\ \Delta V(i) \end{bmatrix} = \begin{bmatrix} \Delta P_n(i) \\ \Delta Q_n(i) \end{bmatrix} \tag{3.36}$$

- Update the value of states using

$$X(i+1) = \begin{bmatrix} \Theta(i+1) \\ V(i+1) \end{bmatrix} = \begin{bmatrix} \Theta(i) \\ V(i) \end{bmatrix} + \begin{bmatrix} \Delta\Theta(i) \\ \Delta V(i) \end{bmatrix}. \tag{3.37}$$

Regarding the operating conditions of the network, the voltage magnitudes at the generation buses are known. Therefore, their related entries in the state vector, measurement vector, and Jacobian matrix are omitted. At the end of each iteration, the generated power for generation buses should be calculated. If the calculated power at any of the generation buses exceeds the bus generation limit, that bus type is changed to a load bus with the power set at the limit [5]. Starting with initial value X_0, the procedure continues until the convergence criterion is satisfied, or the maximum number of iterations is reached. For power systems in this study, the convergence criterion for Newton-Raphson method is set to 10^{-12}, and the maximum number of iterations is set to 50. The state values obtained from this procedure are called *True Values* of states, since they are calculated in the absence of bad data and regarding the true measurements of the system.

3.8 Bad Data Definition

The presence of bad data points may severely degrade the performance of the power system static state estimators. Thus, to demonstrate the performance of state estimation, the measurement set should contain bad data points. In this research, such measurements are modeled either as outliers in the data set, or as erroneous measurements with error from a known distribution. To simulate measurement errors, a random number generating algorithm is used, with erroneous measurements obtained by adding the random errors to the base case measurements of flows, loads, and generations [1].

3.8.1 Outliers in the Measurement

There are cases where the pattern of error is not well known in the measurement set. These case are usually modeled by considering some random measurements in the set as outliers. These bad data points are significantly different from their real values. Even though the number of these bad points is not substantial, they can effectively affect the estimation in some cases.

3.8.2 Gaussian Error

The measurement errors are commonly assumed to have a Gaussian (Normal) distribution [3]. Assume z_{meas} to be the value of a measurement received from a measurement device, where z_{true} is the true value of the quantity being measured. Assigning symbol γ to measurement error, we can then represent the measured values as:

$$z_{meas} = z_{true} + \gamma \tag{3.38}$$

The random quantity, γ, is introduced to model the uncertainty in the measurement. For unbiased Gaussian error, γ is chosen from a normal distribution with zero mean. The Probability Density Function (PDF) of γ is given as,

$$f(\gamma) = \frac{1}{\sigma\sqrt{2\pi}} \exp(\frac{-\gamma^2}{2\sigma^2}) \tag{3.39}$$

where σ is the standard deviation and σ^2 is the variance. The PDF given in (3.39) is a function that describes the relative likelihood for the random variable γ to occur at a given point. A plot of $f(\gamma)$ is shown in Figure 3.3.

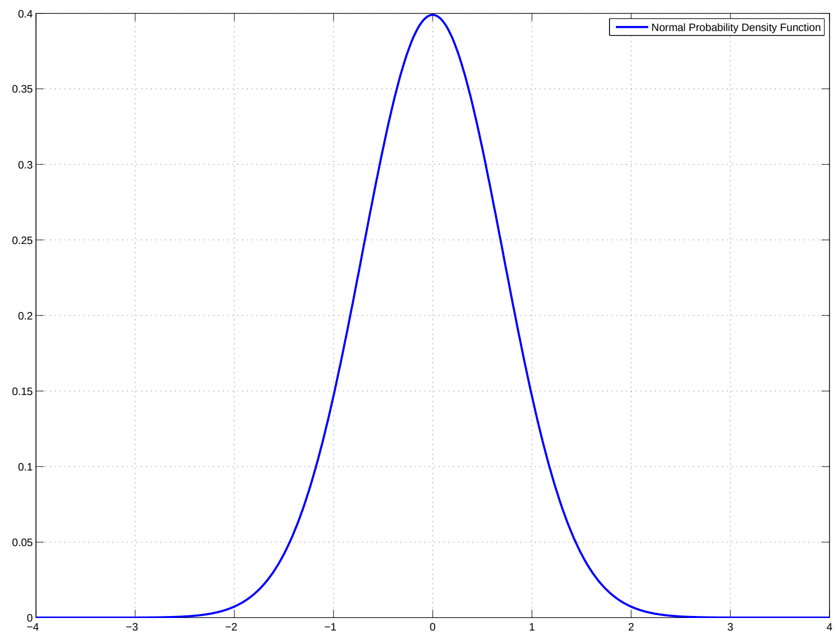

Figure 3.3: The Probability Density Function of Normal Distribution

The normal distribution is commonly used for modeling measurement errors in power systems [1]. Assuming Gaussian error for measurements, the problem of maximum likelihood estimation, or finding the most likely state of system based on erroneous measurements results in minimizing the Weighted Least Squares (WLS) error as discussed in section 2.4.1. This characteristic is one of the reasons for the common use of LS estimators in power system estimation problems.

3.8.3 Rayleigh Error

The popularity of LS-based methods continued to grow, even though it was known that it does not lead to the best possible estimates of unknown parameters when the distribution of error is other than Gaussian [9]. To model a more complicated case of bad measurements, the Rayleigh error is considered. In communication systems, the magnitude of a randomly received signal can be modeled as a Rayleigh distribution. Also if γ_1 and γ_2 represent two independent Gaussian errors in a measurement, their Euclidean norm has a Rayleigh distribution [29]. When error γ in the equation (3.38) belongs to a Rayleigh distribution, its Probability Density Function (PDF) can be expressed as,

$$\forall\gamma \geq 0, f(\gamma) = \frac{\gamma}{\sigma^2}\exp(\frac{-\gamma^2}{2\sigma^2}) \tag{3.40}$$

A plot of the PDF of a Rayleigh distribution is shown in Figure 3.4.

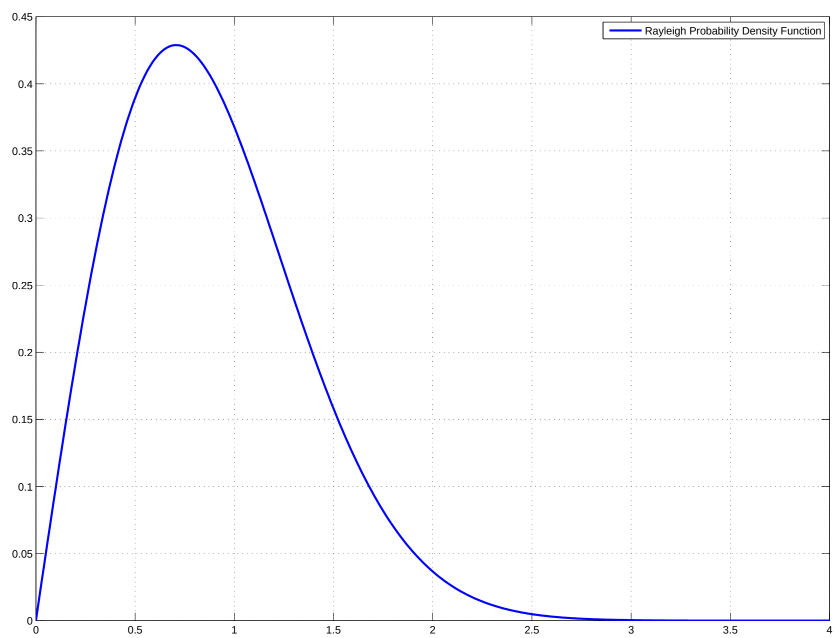

Figure 3.4: The Probability Density Function of Rayleigh Distribution

3.9 Summary

The model of a power system, and the proper formulation of system equations as an overdetermined system of nonlinear equations, were both presented in this chapter. Moreover, based on the bus branch model, the derivation of the Jacobian matrix was explained, to alter the system matrices in the proper format for state estimators. The bad data points are also defined for different types of measurement errors. Based on the information presented in this chapter, different power system test cases are modeled in chapter 5, Experiments and Results.

Chapter 3

The Modified Least Absolute Value Estimator

3.1 Introduction

This chapter discusses the development of a method which uses contraction mapping to address the problem of Least Absolute Value (LAV) static state estimation in nonlinear power systems.

In the first section, theoretical background on contraction mapping for linear state estimation is presented. The concepts are then extended to nonlinear estimation, explaining the formulation of the problem at hand, linearization technique, and necessary conditions. Finally, an algorithm is introduced based on this procedure. However, as it will be discussed later in the chapter, the proposed algorithm faces challenge when dealing with systems containing sparse matrices. To alleviate this, the method is modified by applying Singular Value Decomposition (SVD), and then employing contraction mapping selection on the resulting matrices to make it suitable for sparse systems.

3.2 Literature Review

As mentioned in the previous chapter, the Least Absolute Value (LAV) estimator is a more robust estimation approach for power systems, compared to LS-based estimator [3]. These group of estimators are usually more complex and computationally more expensive than LS estimators. However they are more robust and successful in eliminating bad data.

Unlike the LS estimator, there is no explicit solution for LAV estimators. Different estimators employ different techniques for obtaining the states. These techniques cover a wide range of methods: applying linear programming [37] and linear regression techniques [8], partial use of LS technique and weight matrix [30], employing residuals method [30], applying decoupled methods [28] or QR block decomposition method [23]. The method introduced in this research uses contraction mapping and singular value decomposition for state estimation.

The accurate performance of estimator has been verified for nonlinear power systems using a local linearization approach, and contraction mapping criteria [15]. However, when the size of the system increases, another issue appears that makes the problem difficult to solve. This issue arises from the sparse matrices in large scale power networks. As will be discussed in section 3.6, for many systems with sparse matrices, system equations needed for state estimation could not be correctly identified.

To deal with large systems with sparse matrices, a modified LAV estimator is introduced. The set of nonlinear equations describing the system is linearized by calculating Taylor Series expansion and Jacobian matrix. The system matrices are then modified by using Singular Value Decomposition (SVD) which makes it suitable for applying the LAV algorithm. applied to eliminate redundant measurements, and obtain the accurate equations essential for estimation. Finally, the estimated values of system states are computed through the iterative process of solving selected linear equations.

3.3 Theory of Contraction Mapping and Linear Systems

The state estimation problem in overdetermined linear systems can be stated as a linear relationship between system measurements Z, and its unknown states X, where the measurement set Z is corrupted by disturbance or noise Γ.

$$\begin{bmatrix} z_1 \\ z_2 \\ \vdots \\ z_m \end{bmatrix} = \begin{bmatrix} h_{11} & \cdots & h_{1n} \\ h_{21} & \cdots & h_{2n} \\ \vdots & & \vdots \\ h_{m1} & \cdots & h_{mn} \end{bmatrix} \begin{bmatrix} x_1 \\ x_2 \\ \vdots \\ x_n \end{bmatrix} + \begin{bmatrix} \gamma_1 \\ \gamma_2 \\ \vdots \\ \gamma_m \end{bmatrix} \tag{3.1}$$

$$Z = HX + \Gamma. \tag{3.2}$$

The problem can be formulated as (3.1), or as the short form equation (3.2). The objective function of LAV estimation is to assign values to unknown states X, such that the absolute sum of error given by (3.3) becomes minimum.

$$J(X) = \sum_{i=1}^{m} |e_i| = \sum_{i=1}^{m} \text{row}_i |Z - HX| \tag{3.3}$$

The LAV estimator obtains the values for states based on the following theorem.

THEOREM 1 [7], If the column rank of the matrix $H \in R^{m \times n}$ is $k \leq n$, then there exists a best LAV approximation HX_{LAV} which interpolates at least k points of the set $Z = [z_1, z_2, ..., z_m]^T$.

The theorem implies that the LAV estimator passes through at least k points in the measurement set, which makes the estimation error zero for at least k points of the objective function. This is in contrast to the LS estimator, which does not necessarily pass through exact points of the measurement set.

The way these k points are selected from the measurement set is the key difference between different LAV estimators. As mentioned before, the estimator which is studied in this research employs the contraction mapping principle so as to choose these points. To investigate features of this estimator, and the way it chooses interpolation points within the set, some concepts from linear algebra which are related to the topic are first reviewed:

Norm: A normed linear vector space is a vector space **X** on which a real-valued function called norm is defined. The norm function maps each element X in **X** into a real number $\|X\|$, satisfying the following axioms:

- $\|X\| \geq 0$ for all $X \in$ **X**, and $\|X\| = 0$ if and only if $X = 0$.
- $\|X + Y\| \leq \|X\| + \|Y\|$ for each $X, Y \in$ **X**.
- $\|\alpha X\| = |\alpha| \cdot \|X\|$ for all scalars α and each $X \in$ **X**.

In the vector space **X** with dimension n, the p-norm can be defined as:

$$\|X\|_p = (\sum_{k=1}^{n} |x_k|^p)^{1/p} \tag{3.4}$$

The norm which is used for finding the absolute value of the error is simply obtained by substituting $p = 1$ in (3.4).

Cauchy sequence: A sequence $\{x_n\}$ in a normed space is said to be a Cauchy sequence if $\|x_n - x_m\| \to 0$ as $n, m \to \infty$.

Complete Space: A normed linear vector space is complete if every Cauchy sequence in space has its limit within the space.

Banach Space: A complete normed linear vector space is called Banach space.

Orthogonal Matrix: An $n \times n$ real matrix Q is called an orthogonal matrix if it satisfies the following condition:

$$QQ^T = Q^T Q = I_n \tag{3.5}$$

where Q^T represents the transpose of Q and I_n is the $n \times n$ identity matrix.

Unitary matrix: An $n \times n$ complex matrix U is called a unitary matrix if it satisfies the following condition:

$$UU^+ = U^+ U = I_n \tag{3.6}$$

where U^+ represents the conjugate transpose of U and I_n is the $n \times n$ identity matrix. In other words, a unitary matrix has an inverse which is equal to its conjugate transpose.

Right and Left Singular Vectors: The n eigenvectors of A^+A are called the right singular vectors of A, where A is an $m \times n$ complex matrix and A^+ is its complex conjugate transpose. The m eigenvectors of AA^+ are called left singular vectors of A.

Distance Function: Considering two elements X and Y from an n-dimensional Banach space, the distance between X and Y can be defined as:

$$d(X,Y) = \sum_{j=1}^{n} |x_j - y_j| = \|X - Y\| \tag{3.7}$$

The distance function can also be considered as a norm since it is the 1-norm for the vector $X - Y$ from the space.

Fixed point: The solution X for equation $X = T(X)$ is said to be a fixed point of the transformation T when X leaves the transformation invariant.

Based on the above definitions, we can now introduce the contraction mapping condition for a Banach space with distance norm as follows,

THEOREM 2-Contraction mapping theorem [4]: Let **S** be a subset of a normed space **X** and let T be a transformation mapping from **S** into **S**. Then T is said to be contraction mapping if there is an α, $0 \leq \alpha < 1$ such that

$$\forall X, Y \in S, \exists \alpha : \|T(X) - T(Y)\| \leq \alpha \|X - Y\| \tag{3.8}$$

Thus, a contraction mapping brings every two elements in space **S** closer together. Furthermore, every contraction mapping in the Banach space has one and only one fixed point which is the unique solution of equation

$$X = T(X). \tag{3.9}$$

Recalling the LAV estimator which interpolates k points of measurement set, we know that for these points the measurement error is considered zero since the estimator passes through them directly. If these points are chosen such that their related rows of matrix H forms a contraction mapping, then X will become the fixed point of the transformation.

The condition for the transformation H to become a contraction mapping can be derived as:

$$\begin{aligned} d(HX, HY) &= \|(HX, HY)\| \\ &= \textstyle\sum_{i=1}^{n} |\sum_{j=1}^{n} h_{ij}(x_j - x_j)| \\ &\leq \textstyle\sum_{i=1}^{n} \sum_{j=1}^{n} |h_{ij}||x_j - x_j| \\ &\leq max_j \textstyle\sum_{i=1}^{n} |h_{ij}| d(X, Y) \end{aligned}$$

So the condition obtained comparing the above formulas with the contraction mapping theorem is given as:

$$\alpha_j = \sum_{i=1}^{n} |h_{ij}| \leq \alpha < 1 \tag{3.10}$$

Furthermore, it is proved in [7] that the set which has the smallest α in H, leads to the optimal solution of LAV estimation.

3.4 Extension to Non-Linear Systems

In this section it is further assumed that the system dynamic is nonlinear. The compact form of (2.2) is given by

$$Z = H(X) + \Gamma. \tag{3.11}$$

where, $Z = [z_1 \ \ z_2 \ \ \cdots z_n]^T$, $X = [x_1 \ \ x_2 \ \ \cdots x_n]^T$, $H(x) = [h_1(x) \ \ h_2(x) \ \ \cdots h_n(x)]^T$ and $\Gamma = [\gamma_1 \ \ \gamma_2 \ \ \cdots \gamma_n]^T$.

The objective of the LAV estimator for nonlinear systems is to minimize the total absolute error, $J(X)$, of all state variables as follows:

$$J(X) = \sum_{i=1}^{m} |e_i| = \sum_{i=1}^{m} |z_i - h_i(x)| \tag{3.12}$$

By using the Gauss-Newton linearization technique explained in section 2.4.3, matrix $H(X)$ is approximated around its equilibrium point, X_0, by:

$$H(X) = H(X_0) + A\ \Delta X \tag{3.13}$$

where $A = \frac{\partial H(X)}{\partial X}|_{X=X_0}$ is the $m \times n$ Jacobian matrix of $H(X)$ at X_0, and $\Delta X = X - X_0$. For power-system state estimation, the Jacobian matrix is calculated as discussed in section 3.5.

By substituting (3.13) into (3.11) and defining $\Delta Z = Z - H(X_0)$, the estimation error, E, is given by:

$$E = \Delta Z - A\,\Delta X \tag{3.14}$$

The equation (3.14) presents an approximation of the state estimation error around the equilibrium point which consists of m simultaneous locally linearized equations with n state variables.

Regarding the contraction mapping condition in linear systems (3.10), for the linearized system given by (3.14), the transformation is a contraction mapping if

$$\alpha_j = \sum_{i=1}^{n} |a_{ij}| < 1 \tag{3.15}$$

where a_{ij} are the elements of A, the Jacobian matrix, i.e., $A = [a_{ij}]$. If (3.15) is satisfied, the estimation error converges to zero by the method of successive approximations, starting from an arbitrary initial vector from the subspace.

Note that the selected set should include enough critical measurements from equation (3.14), to make the system observable. In that case, the selected $n \times n$ $A_{selected}$ matrix becomes full rank. Otherwise, we should select another set with the second smallest α_j, and continue in this manner.

After selecting the desired set of equations from the linearized model, the estimation error E is set to zero for those equations. Then, the following expression for ΔX can be obtained by:

$$\Delta X = A_{selected}^{-1} \Delta Z_{selected}. \tag{3.16}$$

The value of vector X is also updated as:

$$X(i+1) = X(i) + \Delta X. \tag{3.17}$$

For the nonlinear systems, the method should be iterated for the new value of X until the desired convergence criterion or a certain number of iterations is reached.

3.5 The Proposed Algorithm

In order to achieve a contraction mapping of (3.14), the condition (3.15) must be satisfied for A. In this section, an algorithm is proposed which will be applied to nonlinear power systems in chapter 5.

1. Consider the system equation (3.11), including nonlinear matrix $H(X)$.

2. Read power system parameters and all the available measurements. Construct the matrices in (3.11) based on the given system data, and the method explained in section 3.4.

3. Assign initial values to the state variables. In power-system state estimation, a flat start is considered as the initial state, where all the voltage magnitudes have the value of one per-unit, and all phase angles are zero.

4. Calculate the Jacobian matrix A, and construct the linearized model around the initial state, based on equation (3.14).

5. Normalize the linearized equations such that all the elements of vector ΔZ (the vector of difference between actual and calculated measurements) are normalized, and the absolute values of all elements in Jacobian matrix A become less than one .

6. Compute α_i for each column of normalized matrix A. If any of these α_i's are larger than one, repeat the normalization process by dividing the equations by a power of 10 until the contraction mapping condition (3.15) is satisfied.

7. If there are identical equations, only consider one of them and disregard the rest. Assuming that there are identical equations in the system, the number of equations is reduced to m_1.

8. In the final set, choose n equations that have the smallest α_i's, and make the system observable. By choosing these equations, the corresponding Jacobian matrix is full rank.

9. Find ΔX in (3.14) by assigning the measurement error E equal to zero for the selected equations and by using equation (3.16).

10. Update the value of X by adding the estimated value of ΔX to the previous value of X, as stated in (3.17).

11. If the calculated ΔX is smaller than the convergence criterion, or if the maximum number of iterations is reached, continue, otherwise repeat steps 4 to 10. The convergence criterion we considered for power-system state estimation is 0.001 p.u. The maximum number of iterations is set 20 for the networks.

12. Calculate the final Least Absolute Error as stated in (3.12).

3.6 Challenges in Sparse Matrices

Definition: A sparse matrix is a matrix populated primarily with zeros.

In chapter 5, the algorithm introduced in section 3.5 is applied to power systems for state estimation. It is shown there that the method results in satisfactory estimation for networks with a few buses. However, when system dimensions increase, such as in the 10 bus power system, the algorithm based on contraction mapping fails to succeed, due to sparsity in the system matrices.

Consider a system of nonlinear equations formulated as in (2.2). If a measurement z_i is only related to a few unknown states, partial derivatives for a large number of states becomes zero. Hence, the row related to z_i in a Jacobian matrix has a significant number of zeros in it. Now, as the number of measurements which have the same nature as z_i increases, the number of rows in the Jacobian matrix that have many zeros in them increases. As a result, the Jacobian matrix is primarily populated by zeros, or becomes sparse.

The above scenario commonly occurs in large-scale power networks. In those networks, each bus is related to a limited number of other buses within the system [10]. Regarding the huge size of such networks, the node and branch measurements are dependent on a few states, and their partial derivatives for other states will become zero. Therefore, the physical structure of the network gives the related Jacobian matrix a sparse nature.

Applying the proposed algorithm in section 3.5 to a linearized system with sparse Jacobian matrix is challenging, since finding the desired n equations for estimation is challenging. The algorithm suggests that we find the contraction mapping coefficients for the columns of Jacobian matrix based on equation (3.15), and choose the set of equations which is related to the smallest coefficient. Now, consider that for most of the columns in the Jacobian matrix the number of states, n, is less than the number of non-zero elements. The smallest contraction mapping coefficients for those columns can belong to different sets of equations, since there is no preference between the zero elements. As a result, the estimator gains a random feature in selecting the equations, which is not desired. To overcome this problem and render the method precise, Singular Value Decomposition technique modifies system matrices such that the contraction mapping can be applied.

3.7 Singular Value Decomposition (SVD)

Singular Value Decomposition (SVD) is a matrix factorization with many applications in data processing and statistics. This factorization can be looked upon as a method for transforming correlated variables into a set of uncorrelated ones that better expose the various relationships among the original data items. The SVD is based on a theorem from linear algebra which proves that a rectangular m by n matrix ($m > n$) can be broken down into the product of three matrices. Those are: an orthogonal matrix U, a diagonal matrix S and the transpose of an orthogonal matrix D:

$$A = USD^T \tag{3.18}$$

In (3.18), S is a diagonal $m \times n$ matrix where the elements on its diagonal are called singular values of A. Matrices U and D are $m \times m$ and $n \times n$ unitary matrices respectively where $U^T U = I$ and $D^T D = I$. Moreover, the columns of U and D contain left and right singular vectors of diagonal elements of S respectively.

3.8 Modified Contraction Mapping Estimator

Since the SVD technique deals with matrices and equations which are singular, or very close to singularity [17], the technique can be used to resolve the issue of zero elements in the Jacobian matrix.

When SVD factorization is applied to the sparse Jacobian matrix A, matrix B (which is a non-sparse $m \times n$ matrix), can be constructed as the product of unitary matrix U and singular value matrix S. Therefore, the non-sparse matrix B is closely related to the sparse Jacobian matrix A in terms of including all of its singular values, and their related right singular vectors.

$$B = US \tag{3.19}$$

The linearized system equation (3.14) is then written as,

$$\Delta Z = A\Delta X + \Gamma = BD^T \Delta X + \Gamma \tag{3.20}$$

Regarding the relevance between matrices A and B, the contraction mapping criteria can be applied to matrix B to choose the desired set of n equations.

By equalizing the measurement error to zero for selected n equations from contraction mapping criteria, the states can be estimated by,

$$\Delta X = (DS^T SD^T)^{-1} D(B)^T_{selected} \Delta Z_{selected}. \tag{3.21}$$

In equation (3.21) $B_{selected}$ represents an $n \times n$ matrix related to the n system selected equations and $\Delta Z_{selected}$ is an $n \times 1$ row-vector presenting the corresponding measurements.

3.9 The Modified Algorithm

In this section an algorithm is proposed regarding the modified contraction mapping concept. The algorithm is developed for power-system state estimation, and it eliminates most of the bad data points within the set.

1. Consider the system equation (3.11) with nonlinear matrix $H(X)$.

2. Read the power system data and all the available measurements that include redundant measurements. Build matrices in (3.11), based on the given data and the method explained in section 3.4.

3. Assign initial values to the state variables. The flat start which sets all the phase angles equal to zero and all the voltage magnitudes equal to one, is considered.

4. Find the Jacobian matrix A and construct the linearized model (3.14) around the state vector.

5. Use SVD factorization as stated in (3.18) to find matrices U, S and V for the Jacobian matrix A.

6. Compute B matrix by using (3.19).

7. Compute the contraction coefficients , $\alpha_j = \sum_{i=1}^{n} |b_{ij}|$, for the n smallest elements of each column in the B matrix.

8. Compare the α_j s for different columns of matrix B: Pick up n equations related to the smallest α_j within the columns which result in a full rank $B_{selected}$ matrix, which is of $n \times n$ order. By choosing these equations, we know that the related system is observable.

9. Find ΔX by using (3.21).

10. Update the value of X by (3.17).

11. If the calculated ΔX is larger than the convergence criteria and if the maximum number of iterations is not reached, repeat steps 4 to 10.

12. Calculate the LAV estimation error given by (3.12).

3.10 Summary

Least Absolute Value estimator methodology, for selecting desired data points in an overdetermined state estimation problem, can rely on contraction mapping concepts such that the smallest contraction coefficients within the system matrices lead to the optimal solution of estimation. For estimation problems with a sparse system matrix, the SVD should first be applied to pre-process the system sparse matrix, and then the contraction mapping criteria are applied to the processed matrices to find the desired set for LAV state estimation. Two algorithms were introduced in sections 3.5 and 3.9, based on these concepts for non-linear state estimation problems in power systems. The applications of these algorithms are presented in chapter 5 through various examples of state estimation in different power networks.

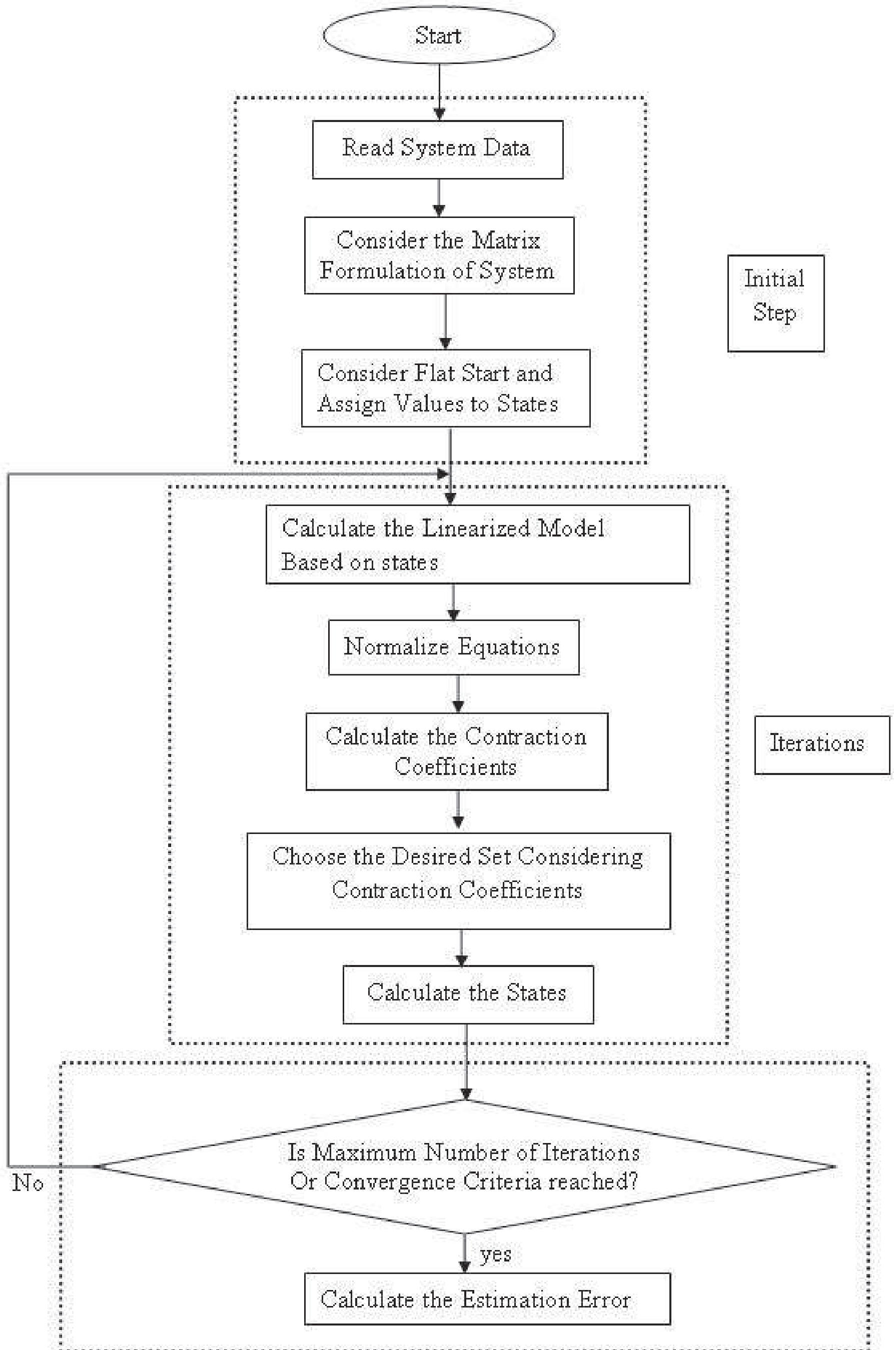

Figure 3.1: The proposed algorithm flowchart

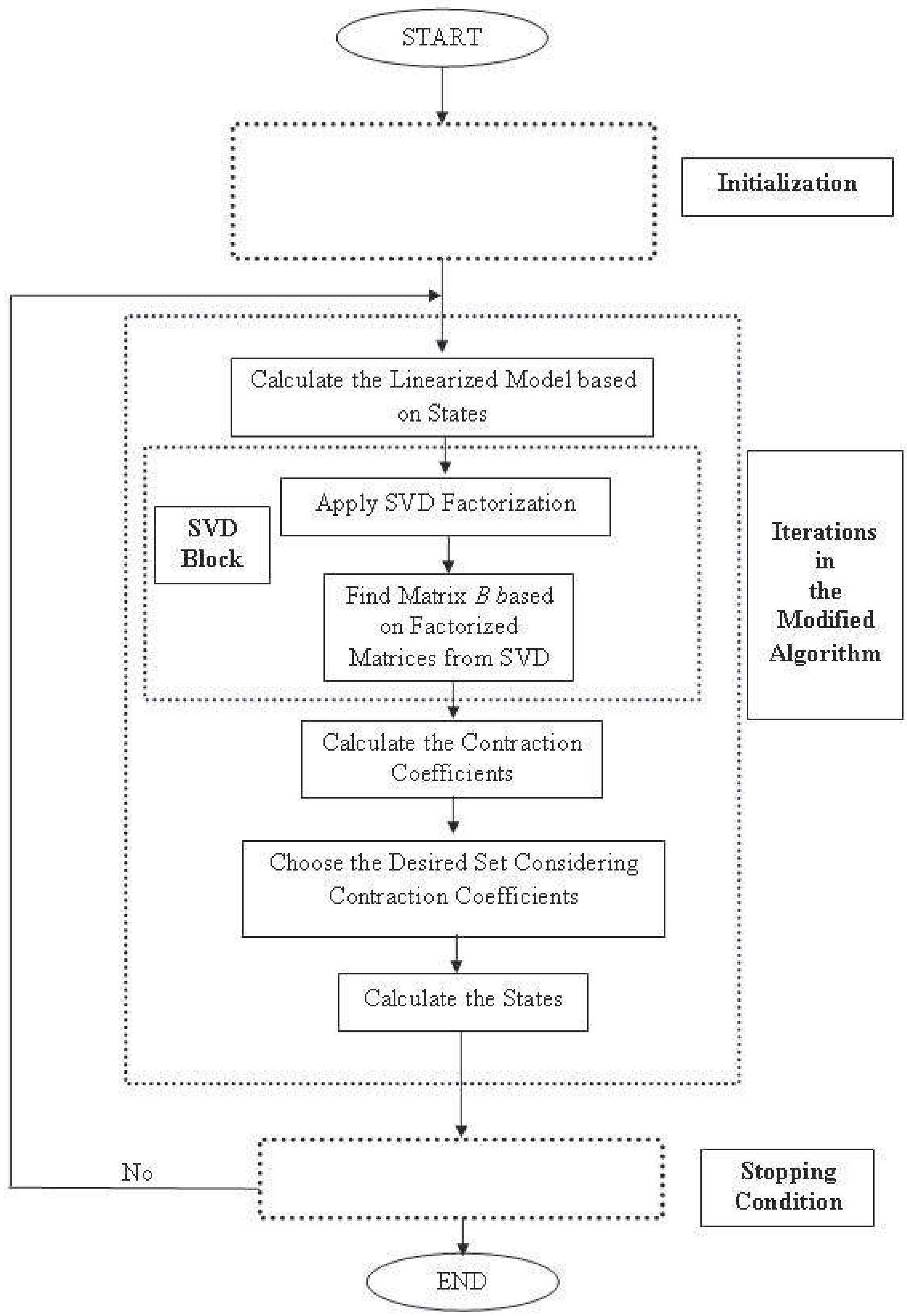

Figure 3.2: The modified algorithm flowchart

Chapter 4

Experiments and Results

4.1 Introduction

In this chapter, the proposed algorithms for modified LAV state estimation are verified on power systems. The first set of experiments, includes small-scale power networks and LAV estimation is obtained by applying the nonlinear contraction mapping algorithm. This algorithm demonstrates satisfactory results; however, when the size of the network increases, the algorithm loses its robustness due to its inability to omit bad data. Therefore, for the large-scale systems discussed in section 4.4, the modified contraction mapping algorithm is employed. Different sets of bad data are considered for each network, and the estimation results are presented and evaluated. Finally the method is compared with a more developed LS-based method which uses residuals analysis to eliminate bad data. The discussion of advantages and disadvantages is also presented in the chapter.

4.2 Small-Scale Power Networks

A 5 bus and a 10 bus power network are examined in this section. For both examples, the nonlinear dynamic is considered. The system information, i.e., the measurements, bad data, as well as the systems operating conditions, are adopted from [9]. The true values of states are calculated for each network. The measurements considered for calculation of true values, are nodal active power, and nodal reactive power at all the system buses, in the absence of bad data. The true states are obtained by using Newton-Raphson's method. The maximum number of iterations is set to 50 and the convergence criterion is 1×10^{-12}. The proposed LAV is then applied to each system to obtain an estimation of the states. The software used for coding is MATLAB. Toolboxes used during simulation process are Symbolic Math toolbox and Statistics toolbox. The accuracy of the proposed estimator is evaluated by comparing the estimated states and the true states, and calculating the LAV error. For comparative study, the estimation error of the proposed LAV estimation is compared with the LS-based estimation, and the results are discussed.

4.2.1 The IEEE 5 Bus Power Network

The schematic of the IEEE 5 bus system is shown in Figure 4.1. The generation buses are bus one and two, where bus one is considered as slack bus. The specification tables related to the physical parameters and the working condition of network are given in appendix A.

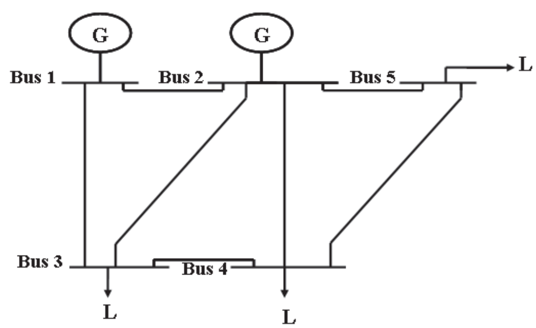

Figure 4.1: The schematic diagram of the 5-bus power system.

The state estimation experiment, with basic contraction mapping algorithm, has been tested on this network with different measurement sets A and B. For each set, three different groups of bad measurements are considered. The features of each set, in terms of its measurement specifications, are expressed in section C.1.1 of appendix C. The LAV estimation technique, based on the local linearization approach, is applied to to all the data sets. In the following, the estimation results for each test are presented and discussed.

Set A

Set A is the first set considered for the experiments. The specifications of the set can be expressed as:

- number of buses : $n_b = 5$
- number of states : $n = 2(n_b - 1) = 8$
- number of measurements: $m = 23$
- redundancy ratio: $\eta = 2.875$

In set A, the ratio of measurements to unknowns (redundancy ratio) is 2.875. As mentioned earlier, three sets of bad data points are defined on set A, which can be named as A_1, A_2 and A_3. These sets, which include different bad data points, are employed for state estimation. For data set A_1, the bad data point is generated by reversing p_2. This experiment is one of the simple examples to check the outlier-rejection ability presented in the new LAV algorithm. The error of estimated values for voltage magnitudes and phase angles are presented in Figure 4.2(a) for each bus, which shows that the proposed method is more successful in reducing the error in the presence of the bad data point p_2.

The next bad data set is generated by inverting p_{3-1}, and halving q_{5-4}. These bad data points influence the estimation at buses three, four, and five. The results of state estimation are given in Figure 4.2(b). For set A_3, bad data points are generated by inverting p_{3-1}, halving q_{5-4} and equalizing p_{5-4} to zero, which affects almost all of the buses in the network. The results are shown in Figure 4.3.

Figure 4.2 and 4.3 illustrate that the proposed LAV estimation technique results in better estimation in comparison with the LS-based estimation technique. The difference between two estimators is more noticeable in phase estimation, especially for the last two sets that have more inaccurate measurements. The estimation errors for each experiment are presented in Table 4.1, expressing that the proposed estimator successfully shows less estimation error.

Table 4.1: The table of estimation error for 5 bus system - data set A

Bad data Set	Estimation error of LAV estimator	Estimation error of LS estimator
A_1	0.1323	0.3602
A_2	0.2729	0.7361
A_3	0.7877	1.1959

Set B

The second set of measurements tested on 5 bus system, is set B. For this set we have the same number of buses and states, however the number of measurements and therefore the redundancy ratio is different:

- number of measurements: $m = 21$
- redundancy ratio: $\eta = 2.625$

For set B, the redundancy ratio decreases to 2.625. The first group of bad data points, B_1, is generated by inverting p_2 and p_{3-4}. The value of q_3 is also halved. The second bad data set, B_2, is generated by setting q_4 and q_{3-4} to zero, doubling p_{3-4}, and halving the value of p_5. The last bad data set, B_3, is also produced by setting q_4 and q_{3_4} to zero, doubling p_{3-4} and p_{2-4}, inverting the value of q_{4-2}, and halving the value of p_5.

The estimation errors on buses, shown in Figures 4.4 and 4.5, demonstrate that within these data sets, the estimation results are more accurate for both estimators. However, the calculated values of the proposed estimator exactly match the true state values where LS estimator encounters minor errors in estimating states, such as the voltage magnitude estimation errors in Figure 4.4(a).

Since the 5 bus system is a comparatively small network, and its Jacobian matrix in the linearized model is not sparse, the algorithm is able to approximate the states precisely, and obtain a smaller estimation error in comparison with the LS estimator.

Table 4.2: The table of estimation error for 5 bus - data set B

Bad data Set	Estimation error for proposed estimator	Estimation error for LS estimator
B_1	0.4868	1.1156
B_2	0.4843	0.9396
B_3	0.4843	1.0840

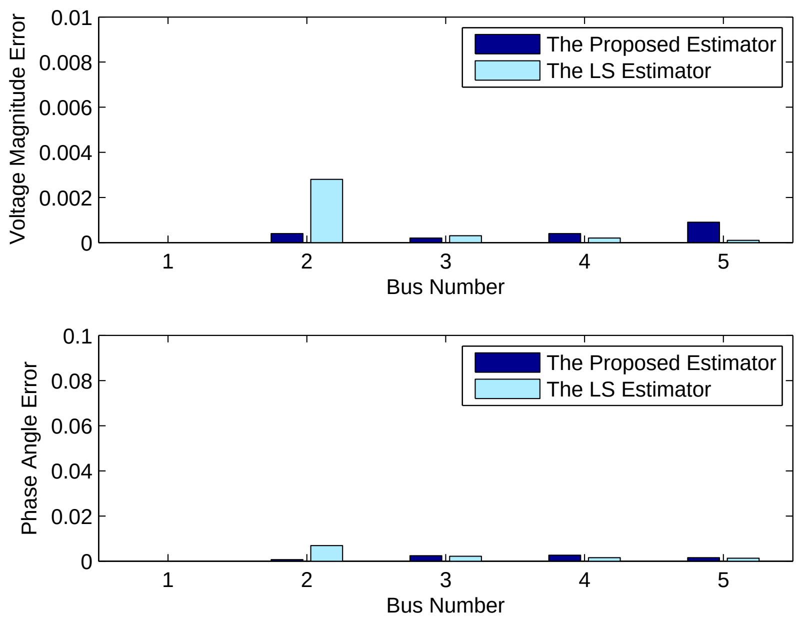

(a) Set A1

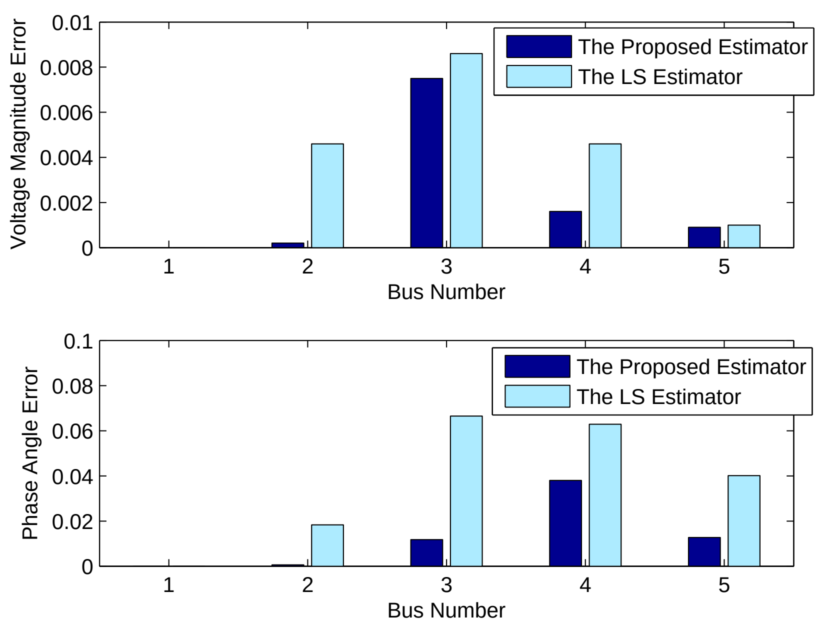

(b) Set A2

Figure 4.2: The Voltage and Phase Error for the 5-bus power system with measurement set A1 and A2.

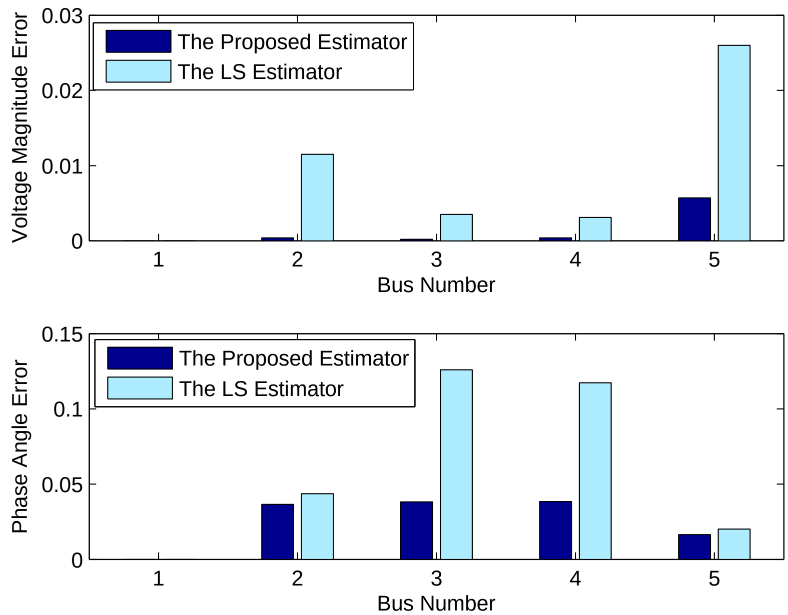

Figure 4.3: The Voltage and Phase Error for the 5-bus power system with measurement set A3.

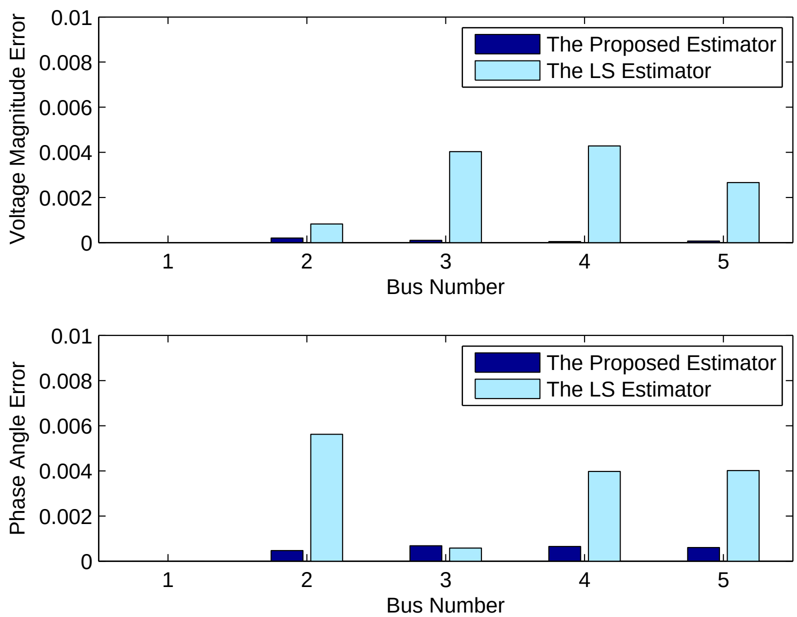

(a) Set B1

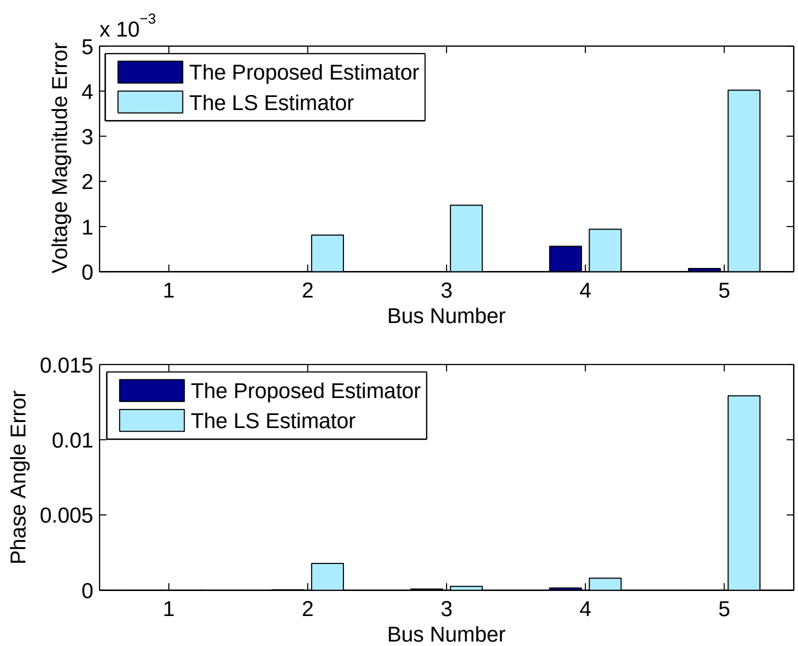

(b) Set B2

Figure 4.4: The Voltage and Phase Error for the 5-bus power system with measurement set B1 and B2.

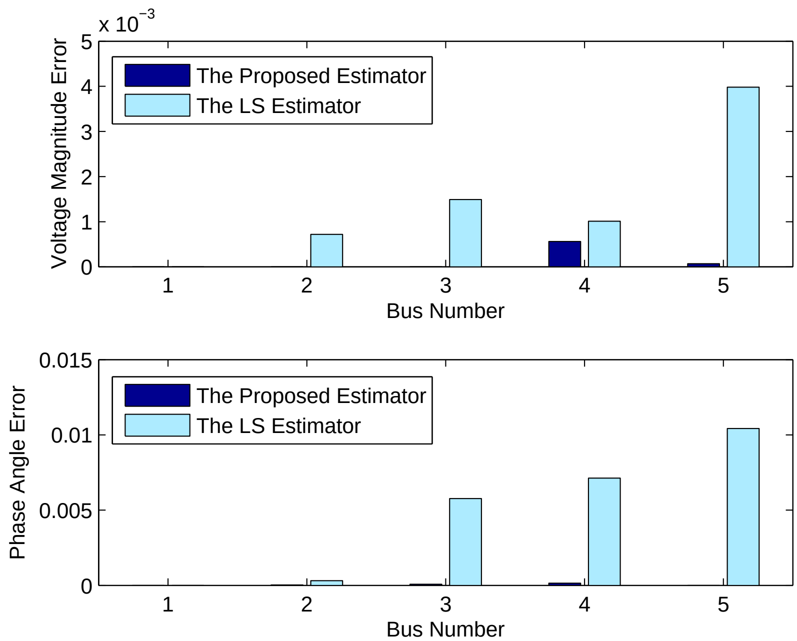

Figure 4.5: The Voltage and Phase Error for the 5-bus power system with measurement set B3.

4.2.2 The IEEE 10 Bus Power Network

In Figure 4.6, the simplified graphic of the IEEE 10 bus system is shown, with generation buses one, two, and four. More detailed information about this system is given in appendix A.

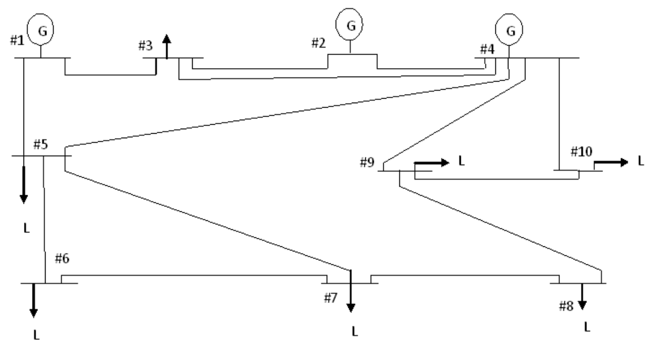

Figure 4.6: The schematic diagram of the 10-bus power system.

Similar to the state estimation experiments in section 4.2.1, the network is analyzed with different sets of measurements and bad data. These measurements and their bad data points are fully described in section C.1.2 of appendix C. The simulation results are obtained by applying the original contraction mapping algorithm, and presented through related figures and tables. The proposed estimator shows a different behavior in this network, and the accuracy of estimation reduces in comparison to the 5 bus system.

Set A

The first set considered for experiments is set A. The basic specifications of the set are:

- number of buses : $n_b = 10$
- number of states : $n = 2(n_b - 1) = 18$
- number of measurements: $m = 53$

- redundancy ratio: $\eta = 2.944$

Three sets of bad data points are investigated for state estimation in A, grouped as set A_1, set A_2 and set A_3. The results can be viewed through Figure 4.7 and Figure 4.8(a).

The first set of bad data points is produced by reversing P_{10-4} and Q_{5-6}. The voltage magnitude and phase angle at bus 10 are greatly affected by these bad data points, and the error is significant on this bus when applying the proposed estimation algorithm.

The second set of bad data is generated by reversing Q_{5-6} and P_{10-4}, and halving Q_7 and Q_9. The measurement Q_{8-9} is set to zero, and Q_{1-3} is doubled. Here the estimation is obviously affected by bad data points at buses 6, 7, 8, and 9. As shown in Figure 4.7(b), the LS estimator has a better performance for this set, in terms of estimation errors on network buses.

The last set of bad data points is obtained by doubling and reversing P_3, setting P_9 to zero, and halving P_{2-4}. The estimation is more accurate here, compared to the second set, however in the buses 2, 3, 4, and 9 that are affected by bad measurements, the results of the proposed algorithm are very close to the those of LS estimator.

In power systems, each bus is connected to a limited number of other buses, as can be seen in Figure 4.6. Since each nonlinear relationship between measurements from each bus is dependent upon buses connected to it, the number of zeros increases in the Jacobian matrix as the network expands. As discussed in chapter 3, the proposed contraction mapping algorithm gains a random feature dealing with a sparse matrix, since the number of states is larger than the number of nonzero elements in most of the columns. Therefore, the estimator could not differ between these zero elements, and a larger estimation error occurs in experiments within set A.

Set B

The next set considered for 10 bus network is described as set B. The measurements are different in this set, and their redundancy ratio is larger, compared to set A.

- number of measurements: $m = 54$
- redundancy ratio: $\eta = 3.00$

For the measurement set B, the redundancy ratio is 3.00. Bad data points are considered such that P_2 and P_{5-7} are reversed, P_6 is halved and Q_{4-9} is zero.

For this set, the bad measurements again affect the LAV estimation greatly, as shown in Figure 4.8(b). However, applying the modified algorithm which uses SVD factorization technique changes the estimation values, and resolves the issue in most of the buses. By using SVD and following the steps of modified algorithm, the sparse Jacobian matrix is factorized to non sparse matrices and transforms in the appropriate format for applying the contraction mapping criteria. The modified estimator is also tested on larger networks in the next section.

4.3 Discussion of Results for Small-Scale Systems

The performance of the proposed LAV estimator and the LS estimator were tested on IEEE 5 bus and IEEE 10 bus power systems as explained in sections 4.2.1 and 4.2.2. The true states of these systems were computed by applying Newton-Raphson method in the absence of bad data. The algorithms, employed for state estimation in the presence of bad data, were Least Squares and Least Absolute Value using contraction mapping.

For the IEEE 5 bus system, the proposed LAV estimator illustrates low estimation error and low average error in comparison with LS estimator. This better performance was visible in both sets of measurements (set A and set B).

For the IEEE 10 bus system, the LS estimator established more accurate results. The total estimation error of the proposed LAV estimator was high in both sets, and the estimator lost its superior estimation accuracy for the larger network. The reason as explained in section 3.6 is the inability of the contraction mapping algorithm to pick the accurate measurements required for estimation.

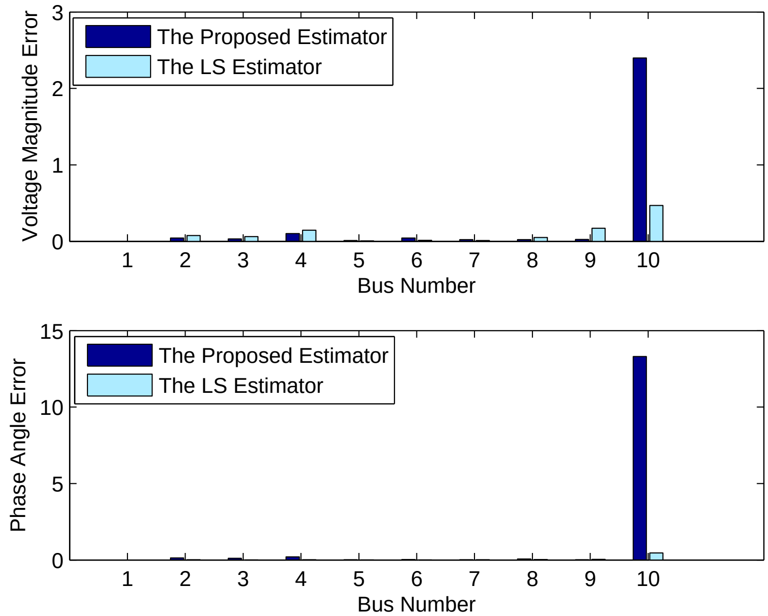

(a) Set A1

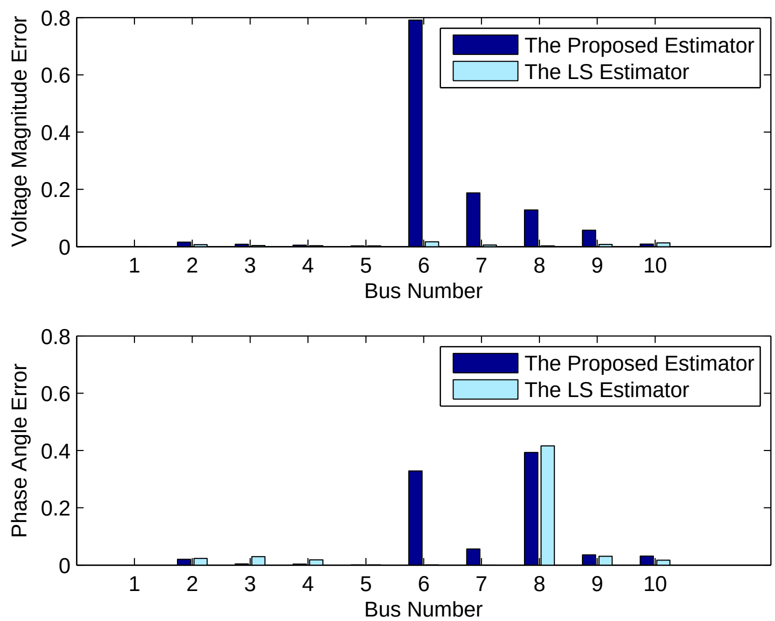

(b) Set A2

Figure 4.7: The Voltage and Phase Error for the 10-bus power system with measurement set A2 and A2.

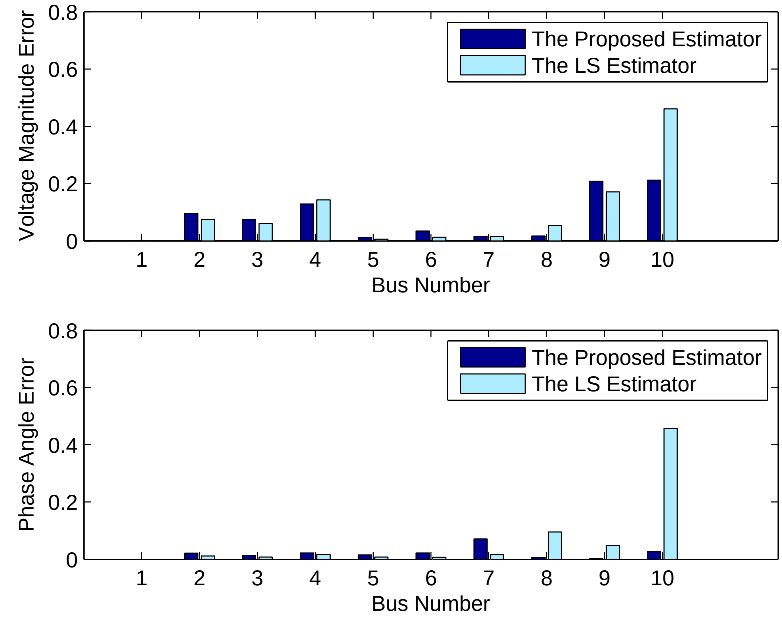

(a) Set A3

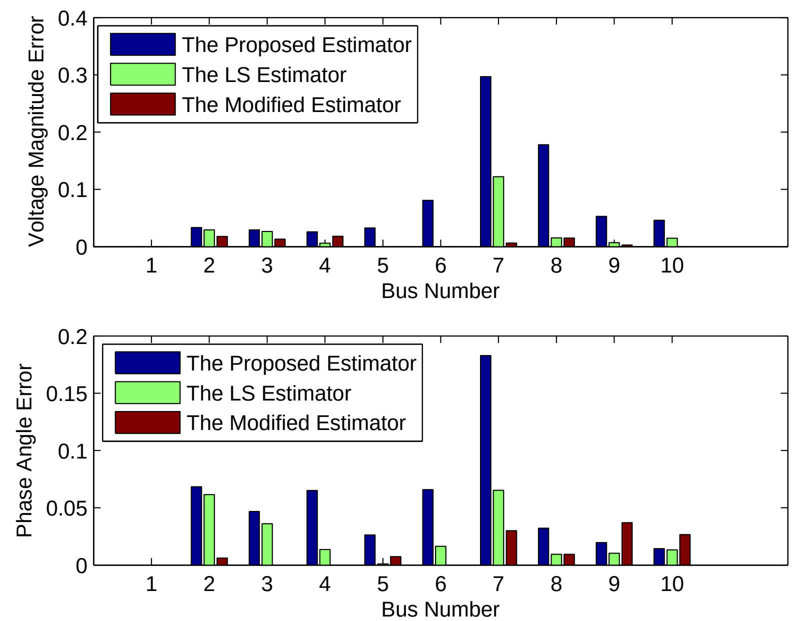

(b) Set B

Figure 4.8: The Voltage and Phase Error for the 10-bus power system with measurement set A3 and B.

4.4 Large-Scale Power Networks

In the next series of experiments, large scale power networks are considered as test benchmarks. As explained for the 10 bus network in section 4.2.2, the proposed LAV estimation technique fails to obtain accurate results when the size of the power network expands. This failure is the reason for using a more developed LAV estimator for large-scale power systems, referred to as the modified LAV estimator in section 3.8. The nonlinear dynamic is considered for each power network in the following. The system information including bus data (network generation power and load power at nodes, bus types, and values of static capacitors), and branch data (resistance, reactance and line charges between branches, and transformer ratios), are given in Appendix B. Similar to Small-scale power networks, true states are calculated using the Newton-Raphson method as explained in section 3.7. The general measurement set is then constructed based on the true state values and system information, such that all the bus and branch measurements are considered.

The measurements obtained from a real system are not perfect. The measurement errors can be larger on some of the buses in the network. To simulate the effect of these measurement errors in the network, m_1 elements of the total measurement set are corrupted with noise. For corruption a random-generator algorithm has been used to produce random errors. The errors were created so as to be the representative of values drawn from a set of numbers having a Gaussian PDF (4.1) for the *first experiment*, and Rayleigh PDF (4.2) for the *second experiment*. In equations (4.1) and (4.2), μ and σ present mean and variance, respectively. These generated values have been added to m_1 measurements in the original set, to construct a new set of measurements with erroneous data. This set represents a situation where only some of the measurements in the network contain bad data. The properties of bad data and measurement set are expressed in appendix C in more details.

$$f(\gamma) = \frac{1}{\sqrt{2\pi\sigma^2}} \exp(\frac{-(\gamma-\mu)^2}{2\sigma^2}) \tag{4.1}$$

$$f(\gamma) = \frac{-\gamma}{\sigma^2}\exp(\frac{-\gamma^2}{2\sigma^2}) \tag{4.2}$$

Since the measurement error is not consistent in all measurements, the traditional Weighted

Least Squares method is not applicable. The LS estimation technique also leads to significant estimation errors in buses for which the measurements contain noise.

State estimation using the modified LAV estimator is summarized as follows:

- Considering the related measurement set, system equations are linearized around the flat start, and the initial matrix format of the system is created.
- SVD factorization is applied to the Jacobian matrix to modify it for contraction-mapping selection.
- The processed matrices are examined to find the observable set with the smallest contraction mapping coefficient.
- The values of states are updated after solving the equations related to the selected set.
- The procedure is iterated until it satisfies the estimation convergence criterion or exceeds the maximum number of iterations.

4.4.1 The IEEE 14 Bus Power Network

The schematic of IEEE 14 bus system is presented in Figure 4.9.

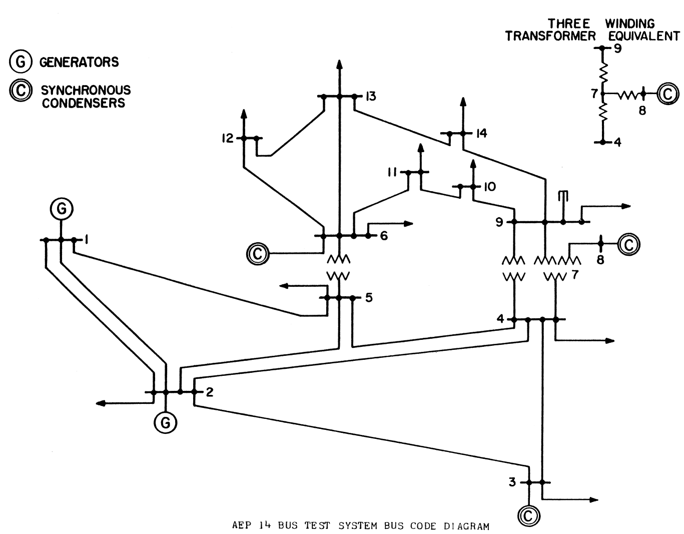

Figure 4.9: The schematic diagram of the 14 bus power system.

The network specification tables are fully presented in Appendix B. The basic features of network are:

- number of buses : $n_b = 14$
- number of states : $n = 2(n_b - 1) = 26$
- number of measurements: $m = 68$
- redundancy ratio: $\eta = 2.615$

In this network, bus number 1 is the slack bus and buses two, three, six, and eight are system-generation buses. The redundancy ratio of the measurements is 2.615. The Gaussian noise has been added to 1/5, 1/4 and 2/3 of data in the measurement set (the total number of 4,5, and 9 buses of network) during 100 independent trials. The corrupted measurements are majorally placed on buses one to four (for the first experiment), one to five (for the second experiment), and one to nine (for the last experiment) and their related branches in the system. The average estimation results for state vector, containing the voltage magnitudes and phase angles, are presented in Figure 4.10 and Figure 4.11. The true states obtained from the original measurement set using the Newton-Raphson method and estimated states using the LS estimator are also shown in those figures.

LAV estimation error for actual measurements and their calculated values is compared to the LS estimator in the Table 4.3. The average voltage magnitude error, and phase angle error on each bus, are also given in Table D.1 of appendix D. The estimation error is significantly less for the modified LAV estimator. The error does not change drastically for different portions of Gaussian noise and it seems that the estimator is successful in eliminating bad data within the measurement set. The simulation results show that even in the case where two-thirds of the measurements are affected by noise, the modified estimator is successful in calculating the states.

The convergence data, for both estimators, are provided in Table 4.4. We can conclude from the table that the modified LAV estimator is converging faster than the LS estimator and even provides a better convergence in fewer iterations. As a results, the estimation time required by the modified LAV estimator is less than the time required by LS estimator.

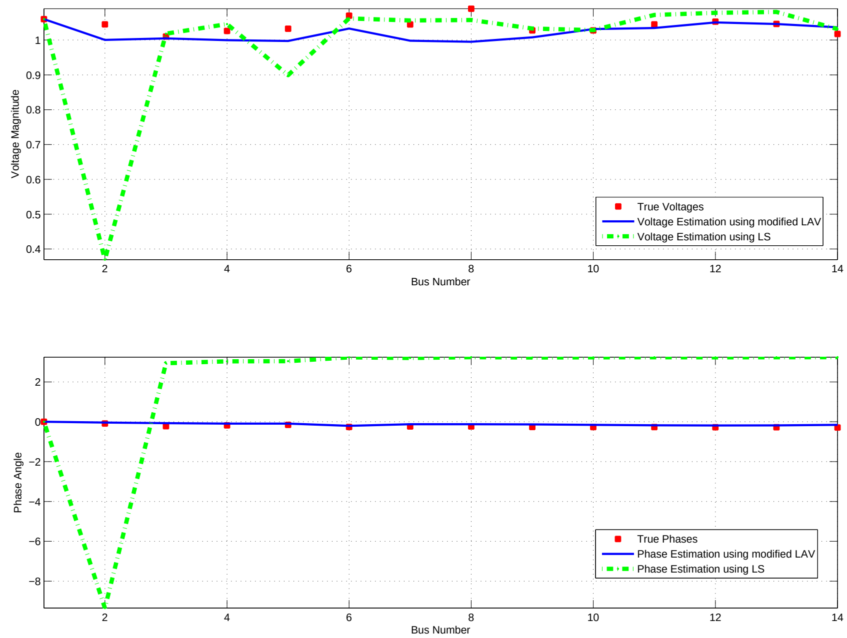

(a) Noise on 1/5 of measurement set

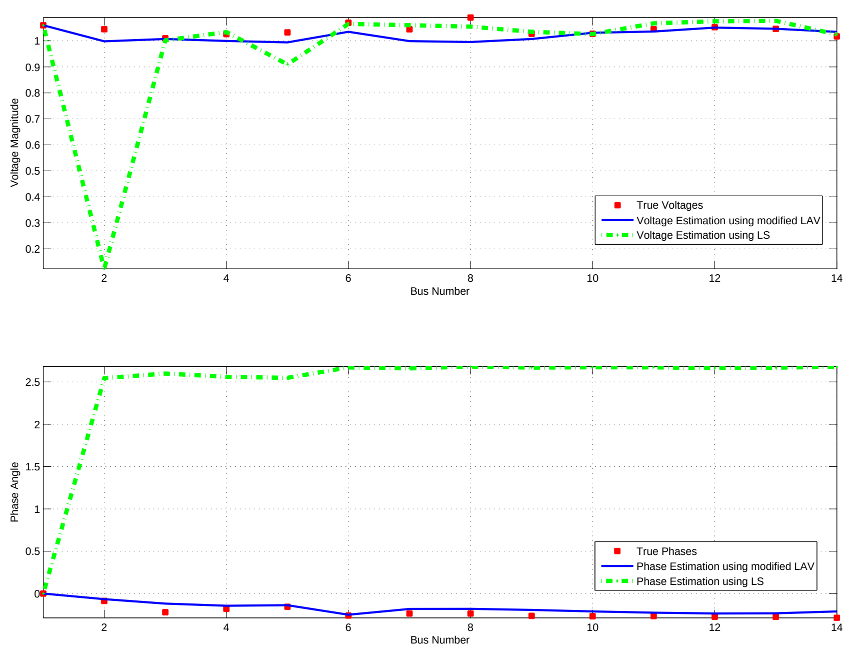

(b) Noise on 1/4 of measurement set

Figure 4.10: The Voltage and Phase estimation for the 14-bus power system with Gaussian noise.

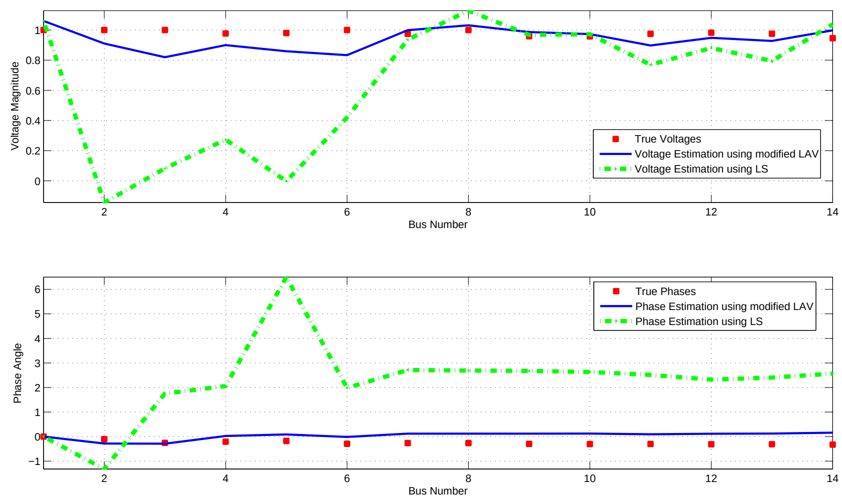

Figure 4.11: The Voltage and Phase estimation for the 14-bus power system - Gaussian noise on 2/3 of measurement set.

Table 4.3: The estimation error of 14 bus system with Gaussian noise

Portion of bad data	Estimation error of modified LAV estimator	Estimation error of LS estimator
1/5	24.1372	111.4573
1/4	24.2962	114.6033
2/3	25.3749	224.9231

To view the robustness of the estimator in the presence of other types of bad data, the experiments are repeated using the measurement set which is corrupted by Rayleigh noise. Regarding the nature of the Rayleigh distribution, the average value of noise is larger compared to the Gaussian distribution. The estimation becomes inaccurate for both estimators when the percentage of bad data increases. This change is more noticeable in the modified LAV estimator with the PBD equal to 2/3. However, the modified LAV estimator still predicts the states with less error compared to the LS estimator as shown in Table 4.5.

Table 4.4: The estimation convergence of 14 bus system with Gaussian noise

Portion of Bad Data	Modified LAV			LS		
PBD	Iter[1]	Log of convergence	Time	Iter	Log of convergence	Time
1/5	2	-3.4815	0.0180	20	-0.5811	0.0920
1/4	3	-3.2185	0.0247	20	-0.3945	0.0931
2/3	4	-3.3175	0.0318	20	1.3898	0.1100

Table 4.6 provides the information related to the convergence and simulation time for the Rayleigh noise. For the smallest portion of bad data (PBD equals to 1/6) the modified LAV estimator converges after five iterations and its simulation time is therefore three times smaller than the LS estimator. As the portion of Rayleigh noise increases, the number of iterations also increases for the LAV estimator. The commotional time required by the LAV estimator to provide same number of iterations is more than the required time of LS estimator. The modified LAV algorithm is more convergent though in comparison with the LS estimator and considering similar number of iterations.

Table 4.5: The estimation error of 14 bus system with Rayleigh noise

Portion of bad data	Estimation error for modified LAV estimator	Estimation error for LS estimator
1/6	41.6196	111.2667
1/5	51.5723	122.1543
2/3	280.2665	328.5404

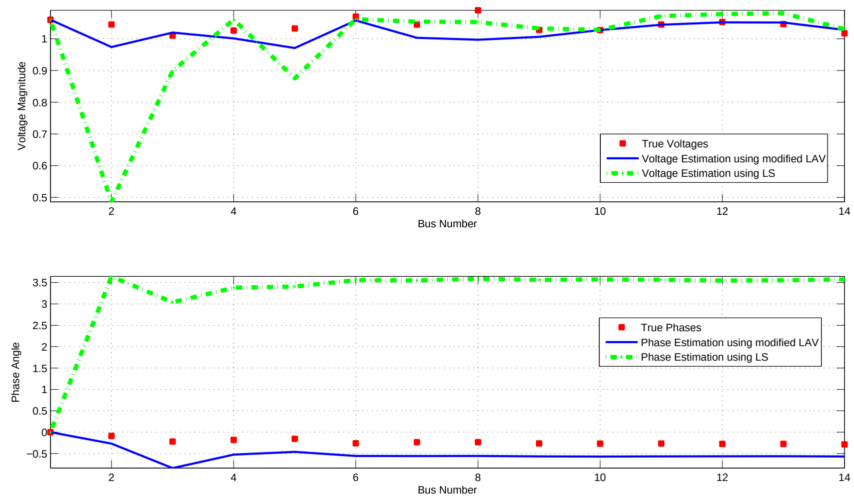

(a) Noise on 1/6 of measurement set

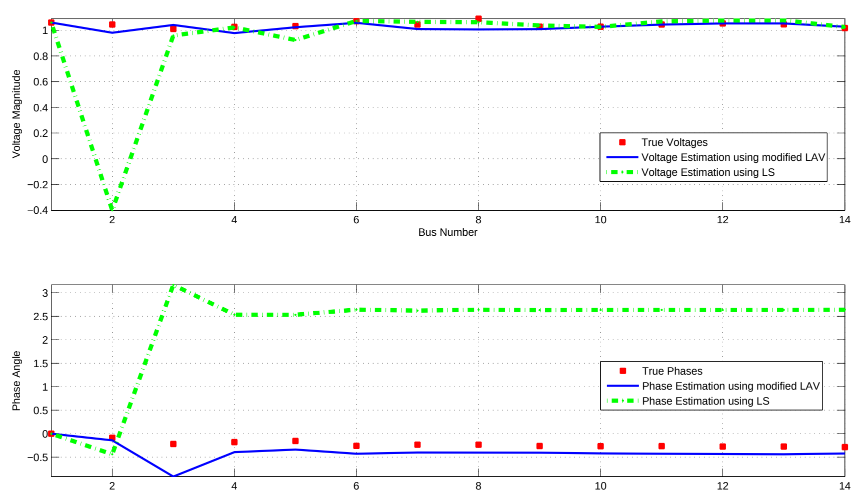

(b) Noise on 1/5 of measurement set

Figure 4.12: The Voltage and Phase estimation for the 14-bus power system with Rayleigh noise.

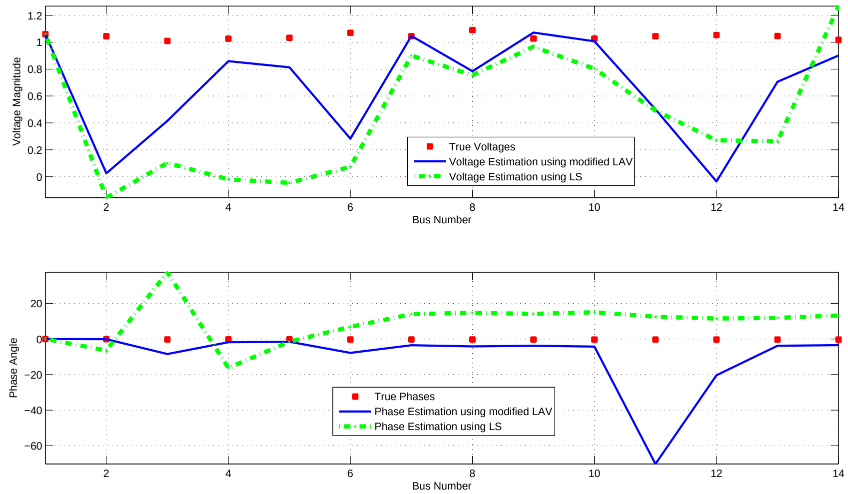

Figure 4.13: The Voltage and Phase estimation for the 14-bus power system - Rayleigh noise on 2/3 of measurement set.

Table 4.6: The estimation convergence of 14 bus system with Rayleigh noise

Portion of Bad Data	Modified LAV			LS		
PBD	Iter	Log of convergence	Time	Iter	Log of convergence	Time
1/6	5	-3.0008	0.0352	20	-0.4960	0.0920
1/5	20	-2.8357	0.1091	20	-0.4014	0.0931
2/3	20	0.0057	0.1312	20	1.6204	0.1226

4.4.2 The IEEE 30 Bus Power Network

The next test system employed in this study is the IEEE 30 bus, which is shown in figure 4.14. The number of network states and measurements are described as:

- number of buses : $n_b = 30$
- number of states : $n = 2(n_b - 1) = 58$
- number of measurements: $m = 142$
- redundancy ratio: $\eta = 2.448$

The specification tables of network physical properties are given in appendix B. The measurement set and bad data points are fully described in section C.2.2 of appendix C.

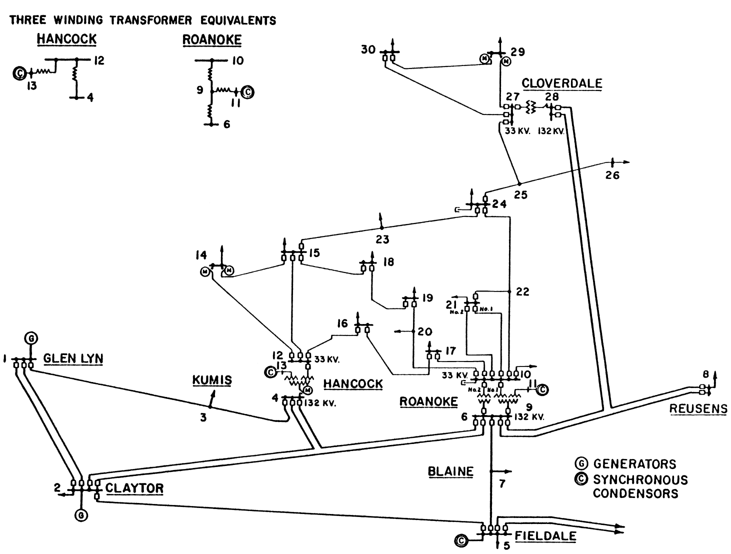

Figure 4.14: The schematic diagram of the 30-bus power system.

The redundancy ratio of this network is 2.448. The Gaussian noise corrupts 1/6, 1/5, and 1/2 of measurement set for the first round of experiments. The noise has been added to the middle buses of the system such that, when the portion of bad data is 1/6, noisy measurements affect buses four to fourteen. For the ratio of 1/5 bad data, buses four to fifteen are involved. For the ratio of 1/2, most of the buses in the system, from bus four to

Table 4.7: The estimation error of 30 bus system with Gaussian noise

Portion of bad data	Estimation error of modified LAV estimator	Estimation error of LS estimator
1/6	93.7931	223.6825
1/5	118.9552	221.1685
1/2	171.1282	298.5043

Table 4.8: The estimation convergence of 30 bus system with Gaussian noise

Portion of Bad Data	Modified LAV			LS		
PBD	Iter	Log of convergence	Time	Iter	Log of convergence	Time
1/6	8	-4.4738	0.1281	20	-1.2538	0.1707
1/5	8	-3.7564	0.1304	20	-0.0890	0.1736
1/2	20	-2.4146	0.2979	20	-0.0878	0.1828

twenty-four, are more or less affected. The average simulation results for 100 independent trials are shown in Figures 4.15(a).

When 1/6 or 1/5 of the measurements are corrupted by noise, the modified estimator faces minor challenges in predicting the states at bus thirteen. For the rest of the states, it is quite superior to the LS estimator.

In case of half-noisy measurements, bad data points affect both estimators, because the number of exact (non-corrupted) measurements is now less than the number of states. The modified estimator shows a larger error in this case, as a result of having some bad data points in its selected set. However, it still presents a closer estimation to true values in almost all of the states in comparison to LS estimator.

The estimation errors are compared in Table 4.7 for the three cases. Again, the modified estimator has smaller error in all cases. Same results are obtained by comparing the average voltage and phase errors in Table D.3 of appendix D. As expected, the average voltage estimation error and average phase estimation error increase along with the ratio of bad

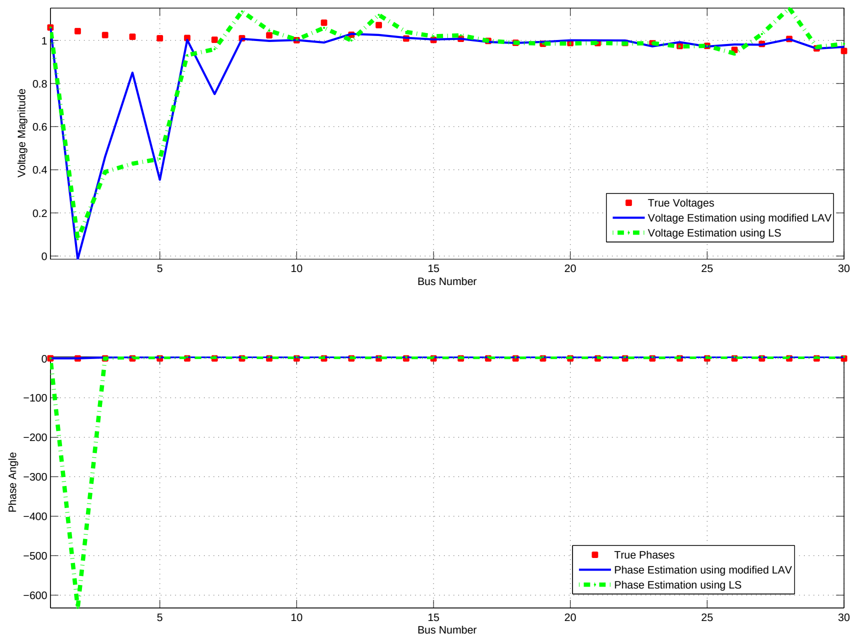

(a) noise on 1/6 of measurement set

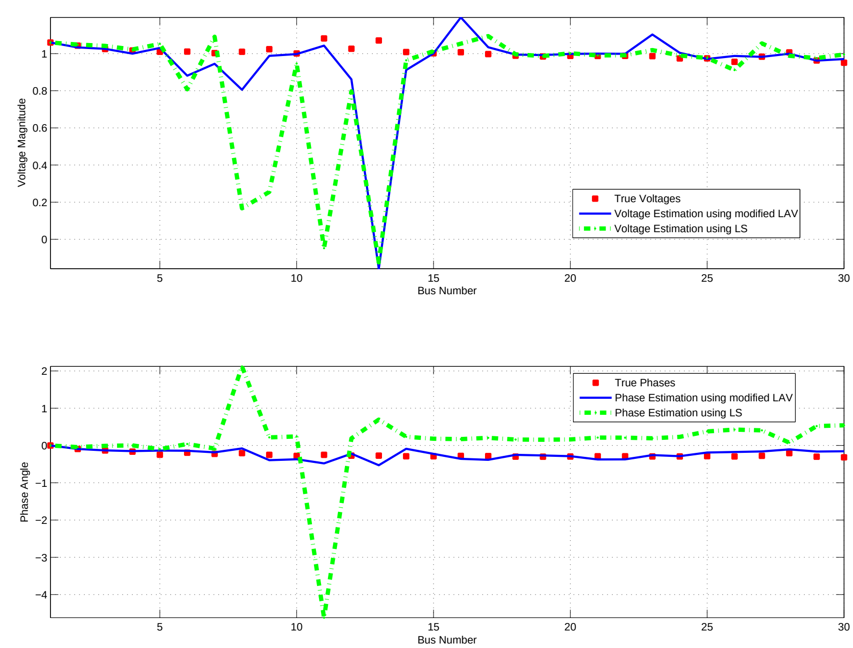

(b) noise on 1/5 of measurement set

Figure 4.15: The Voltage and Phase estimation for the 30-bus power system with Gaussian noise.

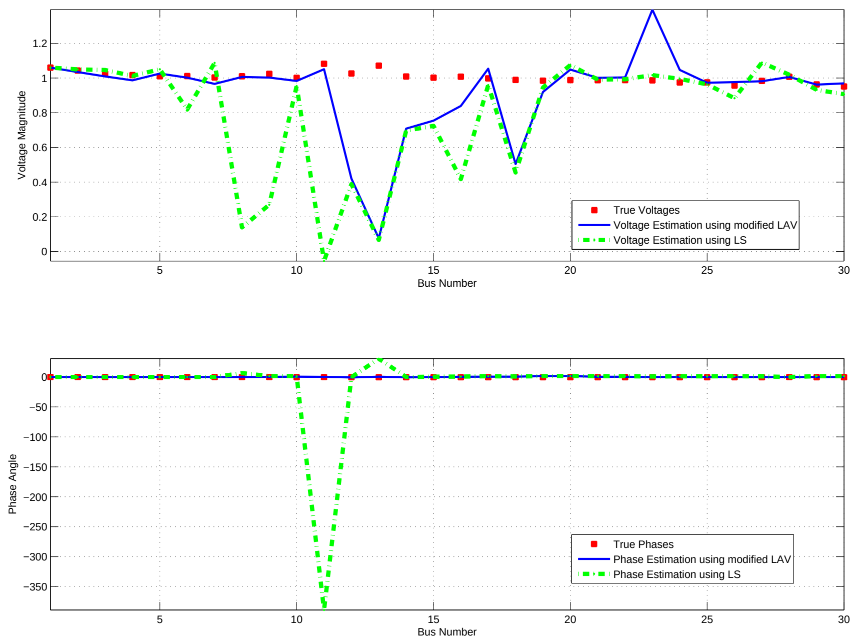

Figure 4.16: The Voltage and Phase estimation for the 30-bus power system - Gaussian noise on 1/2 of measurement set.

data. The modified LAV estimator illustrates a better performance, with approximately five times smaller average error for smaller portions of bad data, and four times smaller average error for larger portions, compared to LS estimator.

Table 4.8 compares the estimation results in terms of convergence rate of each method. The parameters present in the table are the number of iterations used for 30 bus test case, the logarithm of obtained convergence, and the overall time of estimation. For portions of bad data equal to 1/6 and 1/5, the modified LAV estimator converges faster than the LS estimator, reaching the convergence criterion after eight iterations. The LAV estimator also provides a smaller simulation time in both experiments. When the portion of bad data increases to more than half, however, the simulation time of LAV estimator exceeds the simulation time of LS estimator. The LAV estimator still remains more convergent in comparison to the LS estimator.

In conclusion, the modified LAV estimator provides a fast convergent algorithm for smaller portions of bad data in terms of simulation time, convergence value and number of iterations. For larger portions of bad data, the LAV estimator has a more precise convergence rate but needs more simulation time for the same number of iterations.

Figures 4.17 and 4.18 show the results for different portions of bad data from a Rayleigh distribution. The estimation errors are also demonstrated in Table 4.9. In Table D.4 of appendix D, the average error on each bus, regarding the voltage magnitude and phase angle, are presented. During 100 independent trails for each set of bad data points, corrupted measurements are mainly placed at buses one to seven and their related branches, for the first and second experiments (1/6 and 1/5 of set contains bad data), and buses one to eighteen and their branches, for the last experiment (1/2 of set contains bad data).

In the first two experiments, as shown in Figure 4.17, with the exception of bus two, the LAV estimator predicts the states better than the LS estimator. The robustness of the modified estimator is more noticeable in phase estimation. Even for the last experiment, where more than half of the buses in the network are affected by noise, the modified estimator remains closer to real states, as shown in Figure 4.18.

Table 4.9: The estimation error for 30 bus system with Rayleigh noise

Portion of bad data	Estimation error of modified LAV estimator	Estimation error of LS estimator
1/6	188.6926	325.7247
1/5	209.5714	367.6843
1/2	597.8723	704.5947

The average estimation errors on each bus is shown in Table D.4 of appendix D. The table indicates that the average errors with Rayleigh noise are greater than their corresponding values with Gaussian noise. The average phase estimation error increases significantly for LS estimator due to large phase estimation errors on three buses of network. As a result,

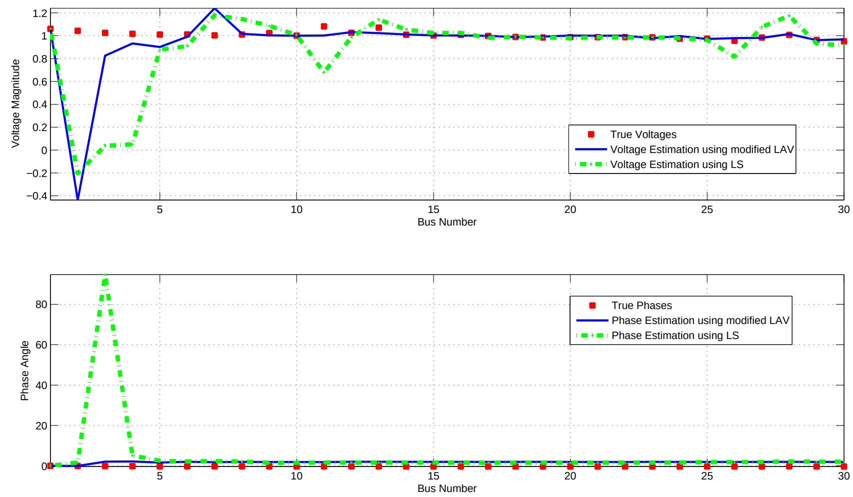

(a) noise on 1/6 of measurement set

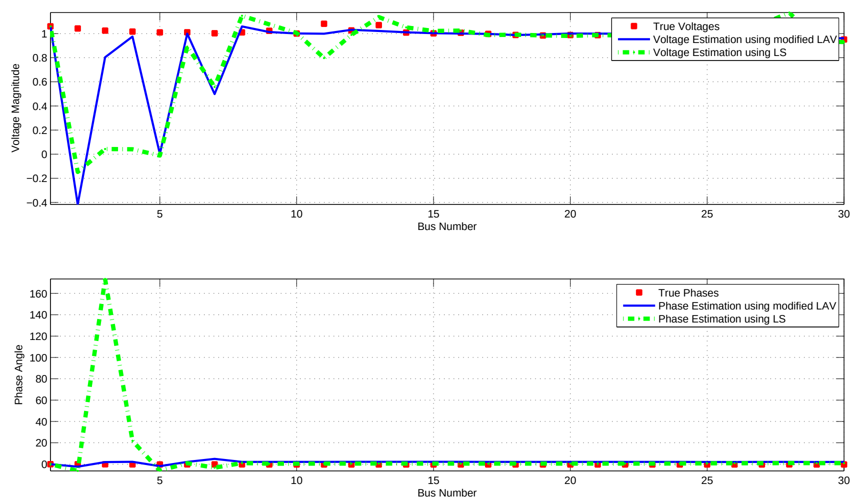

(b) noise on 1/5 of measurement set

Figure 4.17: The Voltage and Phase estimation for the 30-bus power system with Rayleigh noise.

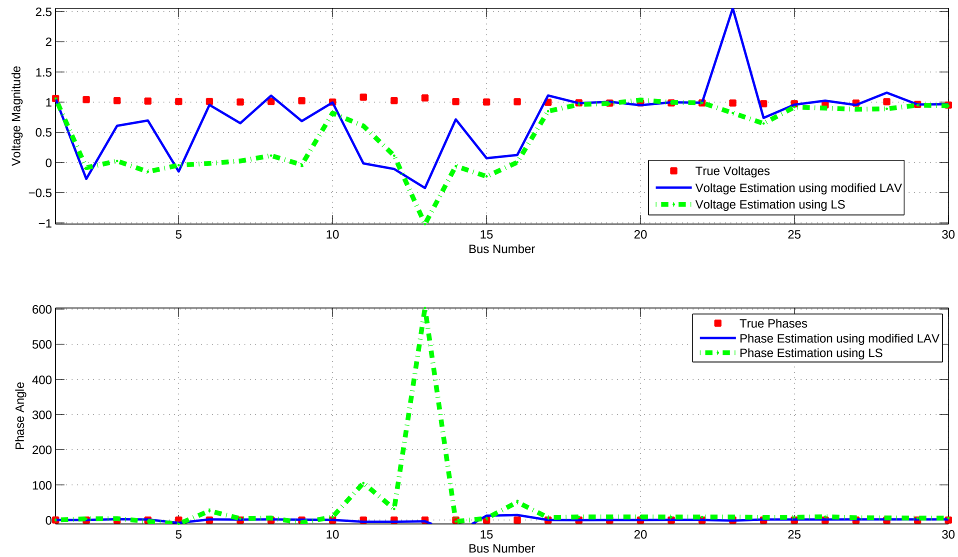

Figure 4.18: The Voltage and Phase estimation for the 30-bus power system - Rayleigh noise on 1/2 of measurement set.

Table 4.10: The estimation convergence of 30 bus system with Rayleigh noise

Portion of Bad Data	Modified LAV			LS		
PBD	Iter	Log of convergence	Time	Iter	Log of convergence	Time
1/6	20	-2.4675	0.2779	20	0.2494	0.1721
1/5	20	-0.7962	0.2968	20	0.8384	0.1827
1/2	20	0.9609	0.3206	20	1.9275	0.2051

the average error of LS estimator exceeds the average error of LAV estimator, in all the experiments.

The performance of both estimators in terms of convergence rate and simulation time are shown in Table 4.10. The noise, in these experiments, has a Rayleigh distribution. As the ratio of noise increases in three different experiments, both estimators become less convergent. Their simulation times, on the other hand, grows with more Bad data in the measurement set. As a result, the estimation errors, shown in Table 4.9, are enlarged comparing the rows from top to bottom. In general, the convergence value is smaller in the modified LAV estimator. Hence, the LS estimator provides a smaller simulation time.

4.4.3 The IEEE 57 Bus Power Network

Another power network studied in this research is the IEEE 57 bus system, as shown in Figure 4.19. More detailed information about this system can be found in appendix B. Section C.2.3 of appendix C describes the measurement set used in simulations.

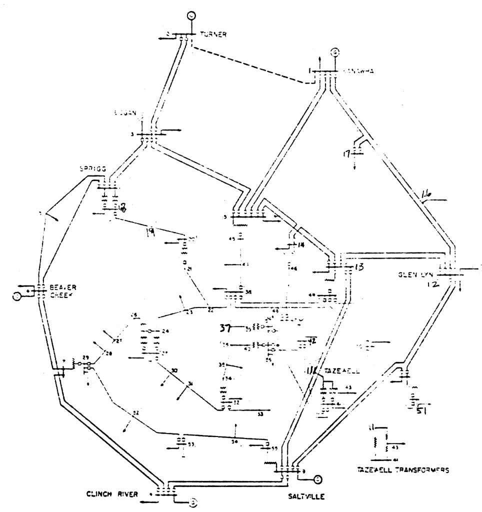

Figure 4.19: The schematic diagram of the 57-bus power system.

The network states and measurements can be summarized as:

- number of buses : $n_b = 57$
- number of states : $n = 2(n_b - 1) = 112$
- number of measurements: $m = 274$
- redundancy ratio: $\eta = 2.446$

The redundancy ratio of this network is 2.446. The Gaussian noise corrupts 1/9 and 1/3 of the measurement set for the first round of experiments. The noise has been added to the measurements of the system such that when the portion of bad data is 1/9, noisy measurements involve buses one to six (half of the generator buses). The noise also affects measurements related to branches between buses nineteen to twenty-eight. For the ratio of 1/3, buses thirty to forty-nine are involved, and related branch measurements between buses eighteen to forty-four, including bus seven and bus eleven. The average simulation results for 50 independent trials are shown in Figure 4.20.

The phase estimation is smooth and almost flawless for the modified estimator compared to the LS estimator. In the estimation of voltage magnitudes, the modified estimator remains near the initial values of states where the LS estimator varies between 0.5 p.u. to 1 p.u. at the noisy section as shown in Figure 4.20(a). When the proportion of bad data increases, the accuracy of estimation decreases for both estimators, as shown in Figure 4.20(b). However, the modified estimator still has a smaller estimation error, and smaller average error, compared to the LS estimator, as described in Table 4.11 and Table D.5 of appendix D.

The performance of estimators in terms of convergence rate and computation time are compared in Table 4.12. As shown in the table, for the portion of noise equals to 1/9, the modified LAV estimator converges after only four iterations and therefore its computational time becomes us reduced to half the time needed for LS estimation. For larger portion of bad data (PBD equals to 1/3), the modified LAV estimator enhances in convergence after similar number of iterations but it also has a greater computational time regarding the LS estimator.

Table 4.11: Estimation error for 57 bus system with Gaussian noise

Portion of bad data	Estimation error of modified LAV estimator	Estimation error of LS estimator
1/9	217.9808	301.4502
1/3	408.6627	654.4023

The same arguments are true for the system with Rayleigh noise, as is shown in Figure 4.21. Table 4.13 demonstrates the estimation error in the presence of Rayleigh noise. The average voltage magnitude and phase angle errors on each bus are given in Table D.6 of appendix D. The estimation error increases for Rayleigh noise. The average error also increases for both estimators. The modified LAV estimator becomes more sensitive to noise for larger portion

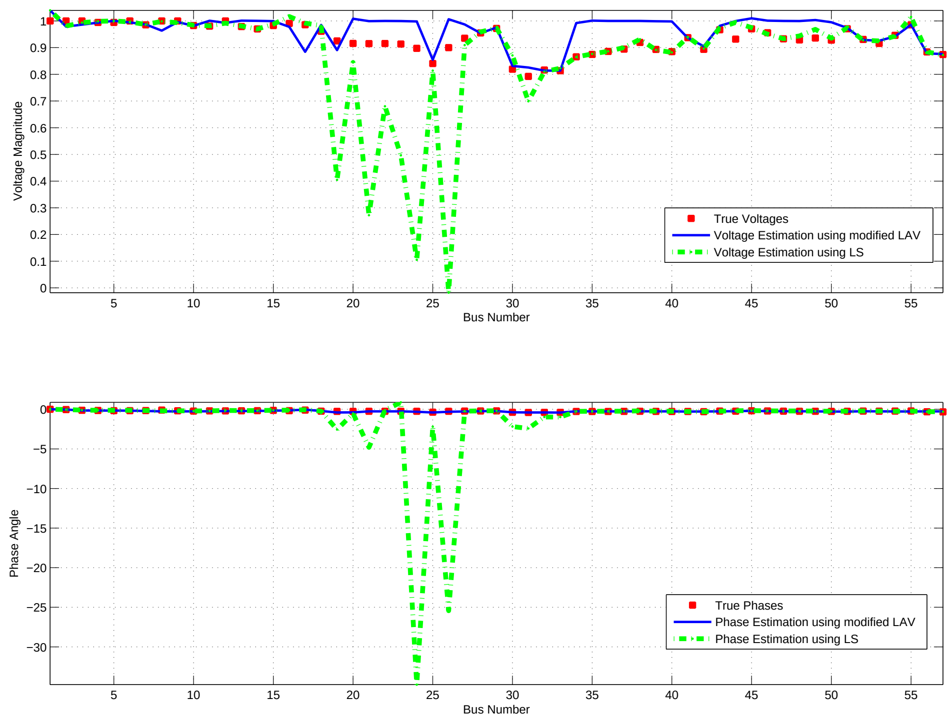

(a) Noise on 1/9 of measurement set

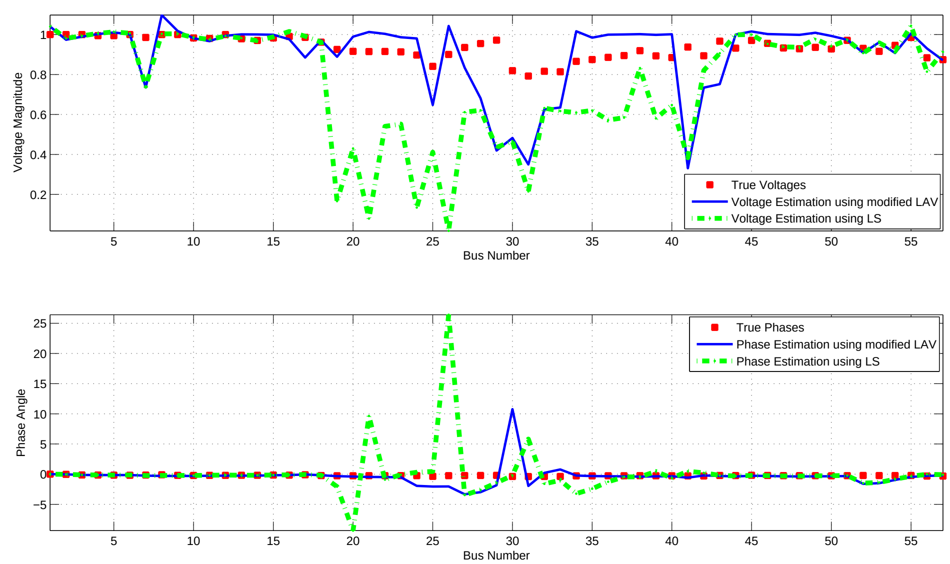

(b) Noise on 1/3 of measurement set

Figure 4.20: The Voltage and Phase estimation for the 57-bus power system with Gaussian noise.

Table 4.12: The estimation convergence of 57 bus system with Gaussian noise

Portion of Bad Data	Modified LAV			LS		
PBD	Iter	Log of convergence	Time	Iter	Log of convergence	Time
1/9	4	-3.0980	0.1932	20	-0.1276	0.3459
1/3	20	-0.5440	0.5808	20	2.0233	0.3511

of Rayleigh noise, however, its estimation error is almost half of the estimation error for LS-based estimator in both cases.

Table 4.13: Estimation error for 57 bus system with Rayleigh noise

Portion of bad data	Estimation error of modified LAV estimator	Estimation error of LS estimator
1/9	234.1623	471.5403
1/3	693.5311	1110

Table 4.14 demonstrates the convergence rate and the overall estimation time for both estimators. The estimation time of modified LAV estimator exceeds the estimation time of LS estimator. Hence, the convergence rate reached within the same number of iterations for LAV estimator significantly improves in comparison to LS estimator.

Table 4.14: The estimation convergence of 57 bus system with Rayleigh noise

Portion of Bad Data	Modified LAV			LS		
PBD	Iter	Log of convergence	Time	Iter	Log of convergence	Time
1/9	20	-2.8865	0.5998	20	1.0623	0.3508
1/3	20	-1.5604	0.600	20	1.8888	0.3532

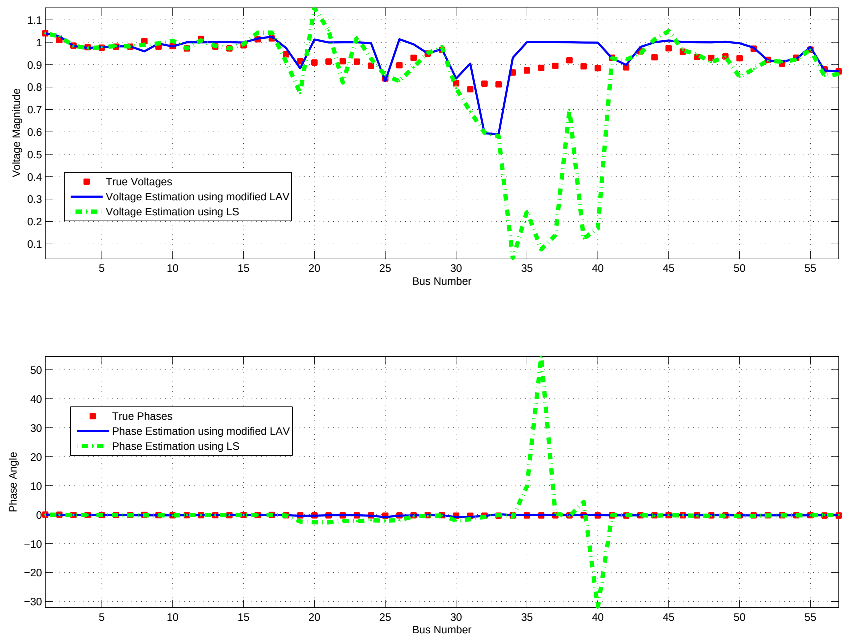

(a) Noise on 1/9 of measurement set

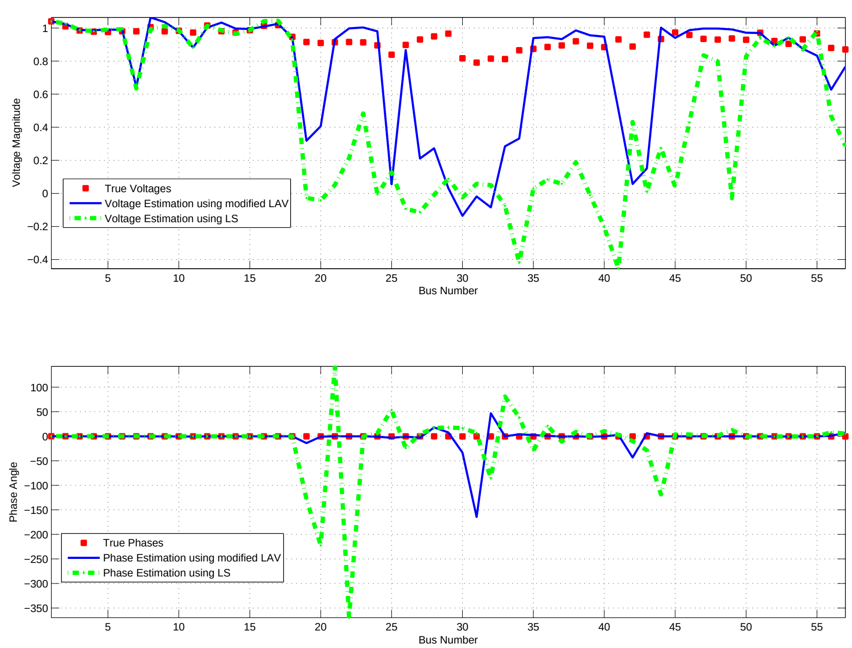

(b) Noise on 1/3 of measurement set

Figure 4.21: The Voltage and Phase estimation for the 57-bus power system with Rayleigh noise.

4.4.4 The IEEE 118 Bus Network

The last power network tested in this study is the IEEE 118 bus system, as shown in Figure 4.22, with specification tables given in appendix B.

- number of buses : $n_b = 118$
- number of states : $n = 2(n_b - 1) = 234$
- number of measurements: $m = 606$
- redundancy ratio: $\eta = 2.5897$

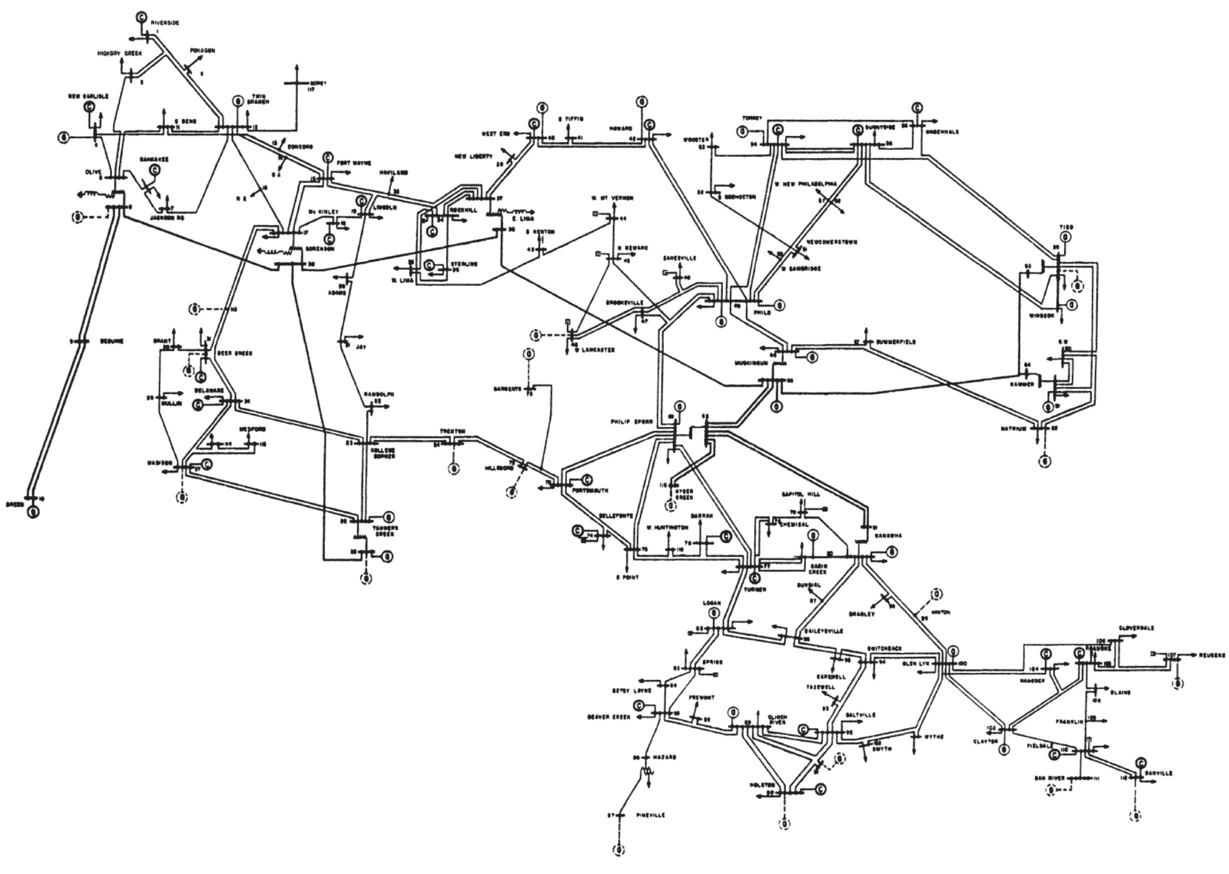

Figure 4.22: The schematic diagram of the 118-bus power system

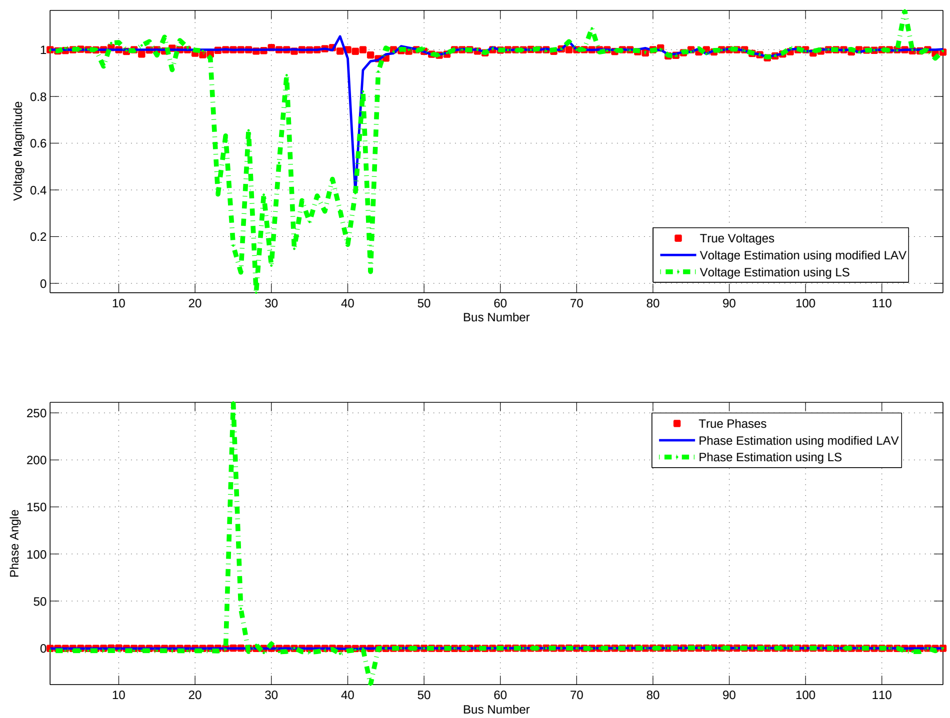

(a) Noise on 1/6 of measurement set

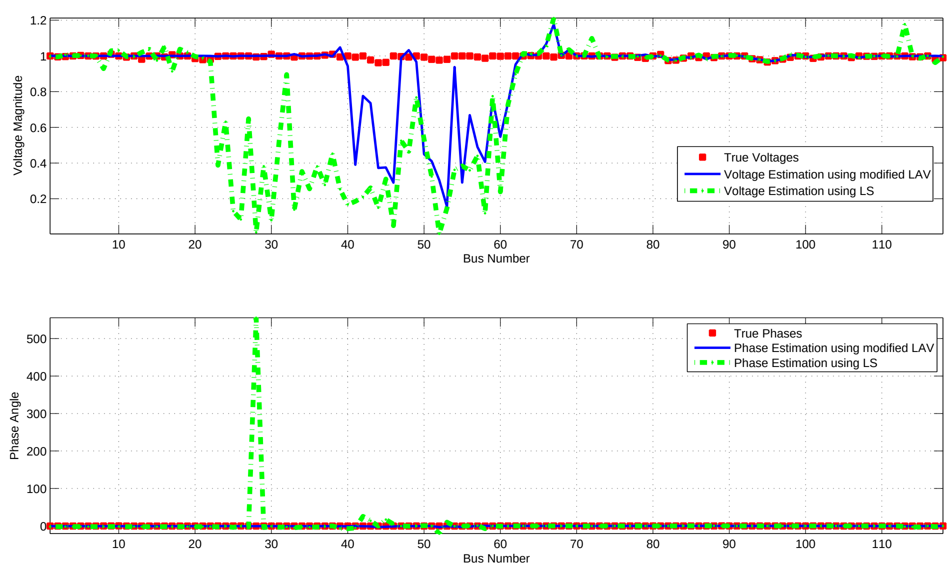

(b) Noise on 1/3 of measurement set

Figure 4.23: The Voltage and Phase estimation for the 118-bus power system with Gaussian noise.

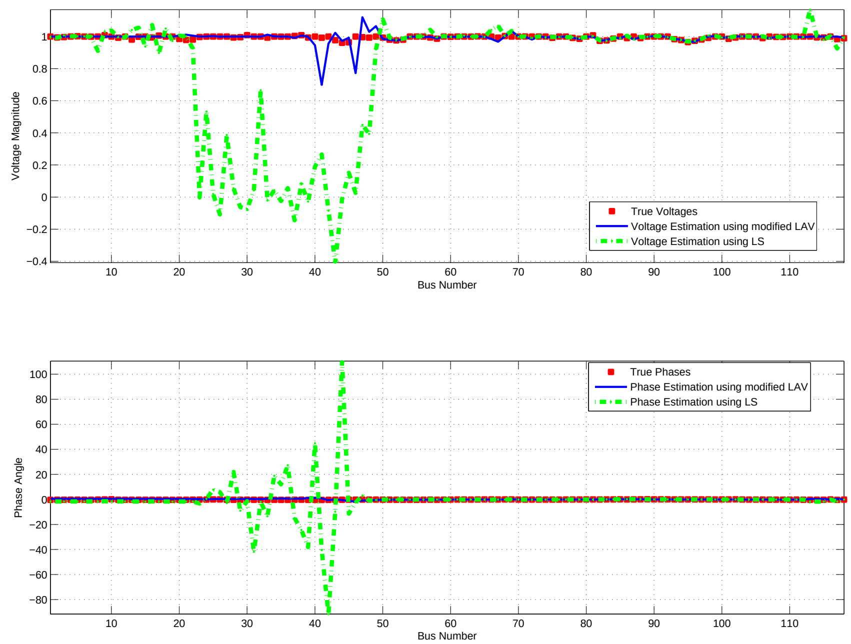

(a) Noise on 1/6 of measurement set

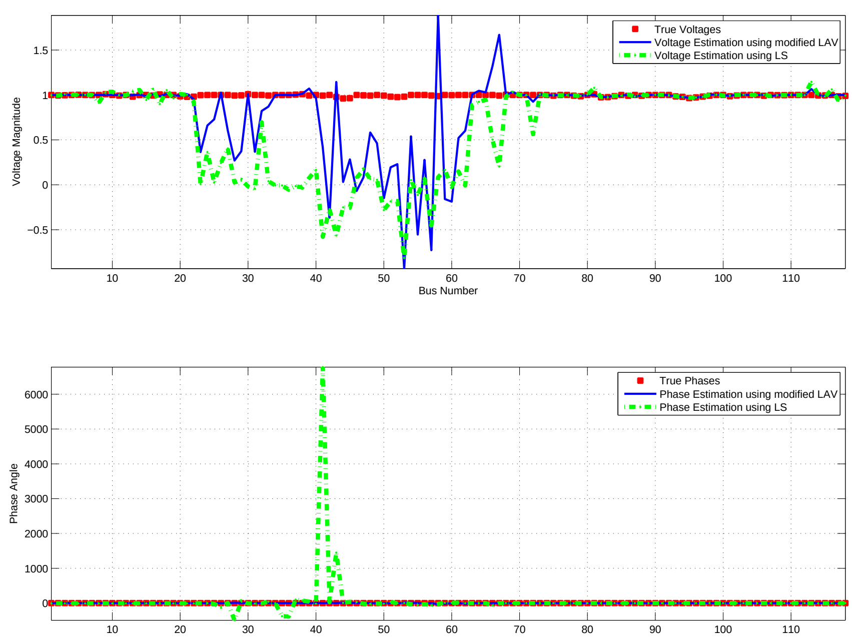

(b) Noise on 1/3 of measurement set

Figure 4.24: The Voltage and Phase estimation for the 118-bus power system with Rayleigh noise.

For this network, the redundancy ratio is 2.5897. The Gaussian noise corrupts 1/6, and 1/3 of the measurement set for the first round of experiments. The noise has been added to the measurements of the system such that when the portion of bad data is 1/6, noisy measurements involve buses thirty to fifty . The noise also affects measurements related to branches between buses twenty to forty-five. For the ratio of 1/3, buses thirty to sixty-nine are involved and related branch measurements between buses twenty-three to sixty-nine, including bus seven, bus eight and bus nineteen. The average simulation results for 50 independent trials are shown in Figure 4.23.

As shown in Figure 4.23(a), the modified estimator is tolerant to Gaussian noise in buses twenty to forty, and it only swings for buses forty to forty-five. With this portion of Gaussian noise, the estimation error is approximately five times smaller for the modified estimator regarding Table 4.15. With a higher amount of noise on the measurement set, as seen in Figure 4.23(b), more states are getting further from their true values. Nonetheless, those related to the LAV modified estimator are always closer to true states in comparison to the LS estimator. The only exception is bus number 55. The total estimation errors are compared in Table 4.15. The average errors on buses are also compared in Table D.7 of appendix D. As expected, the average estimation errors for both voltage magnitude and phase angle are also reduced employing the modified LAV estimator instead of LS estimator. This argument is consistent in both test cases with different portions of bad data.

Table 4.16 provides the simulation time and convergence rate for both estimators. For the smaller portion of Gaussian noise, the modified LAV estimator is approximately seven times more convergent than the Ls estimator. On the other hand, LS estimator is almost 1.6 times faster in computing the estimation results. For the higher PBD, the simulation time does not change drastically but both estimators become less convergent.

Same bad data points are considered for the second experiment, but the noise added to the system comes from the Rayleigh distribution this time. The results can be viewed in Figure 4.24. Hence the difference between the actual measurements and the noisy ones is growing for Rayleigh noise; estimation error also increases, as stated in Table 4.17. The average voltage magnitude errors and phase angle errors, as shown in Table D.8 of appendix D, are greater than their values for Gaussian noise.

Voltage estimation in the presence of Rayleigh noise also depends on the amount of bad data. For the portion of 1/6, the modified estimator can exactly picks the flawless measurements, and therefore the estimation is four times more precise than for the LS estimator. For the portion of 1/3, where almost half the buses in the network are affected with noise in some degrees, the noisy measurements affect the accuracy of estimation. As it can be seen in Table 4.17, the error increases significantly. Yet it remains less than the estimation error of the LS estimator.

For both types of noise, the phase estimation is significantly more robust in comparison with the LS estimator, as shown in Figure 4.23 and Figure 4.24.

The last table of the section describes the convergence and time data of the experiment with different portions of Rayleigh noise. The LAV estimator reaches the convergence criterion in ten iterations and hence its estimation time is less than LS estimator. The convergence rate is the reason for its better accuracy in terms of estimation error and average error on each bus. For PBD equals to 1/3, the simulation time of LAV estimator increases and it exceeds the time used by LS estimator. The convergence rate remains higher than the LS estimator but it does not satisfy the convergence criterion for either one of the estimators.

Table 4.15: Table of estimation error for the 118 bus system with Gaussian noise

Portion of bad data	Estimation error of modified LAV estimator	Estimation error of LS estimator
1/6	317.5387	1781.5
1/3	1286.5	3020.2

Table 4.16: The estimation convergence of 118 bus system with Gaussian noise

Portion of Bad Data	Modified LAV			LS		
PBD	Iter	Log of convergence	Time	Iter	Log of convergence	Time
1/6	20	-2.7309	1.3113	20	0.4592	0.8114
1/3	20	-0.6552	1.3263	20	0.2585	0.8134

Table 4.17: Table of estimation error for the 118 bus system with Rayleigh noise

Portion of bad data	Estimation error of modified LAV estimator	Estimation error of LS estimator
1/6	519.4886	2159.9
1/3	2777.5	3721.5

Table 4.18: The estimation convergence of 118 bus system with Rayleigh noise

Portion of Bad Data	Modified LAV			LS		
PBD	Iter	Log of convergence	Time	Iter	Log of convergence	Time
1/6	10	-3.3256	0.8086	20	1.5034	0.8127
1/3	20	-0.0074	1.3211	20	2.5566	0.8161

4.5 Discussion of Results for Large-Scale Systems

In the pervious sections of this chapter, different estimators were tested on IEEE large-scale networks with various sets of measurements. As discussed in section 4.4 the measurements are corrupted during independent experiments with two types of bad data: Gaussian noise, and Rayleigh noise. The experiments involve 14 bus, 30 bus, 57 bus and 118 bus networks. The true states of these systems were gained by applying Newton-Raphson method to the systems in the absence of noise. The estimators used with redundant measurement sets, were the LS estimator and the modified LAV estimator. The results were shown in various figures and tables. The estimated states of selected experiments were given in Appendix E.

Both estimators gained smaller estimation errors when the ratio of noise was smaller. The results is reasonable since we get a more precise estimation with a more accurate measurement set. Also the estimation errors became larger for Rayleigh noise in comparison with Gaussian noise. This result could be explained regarding the nature of Rayleigh noise and the larger magnitude of noise caused by its distribution.

The two estimators had noticeable differences as well. The modified LAV estimator had a superior performance in terms of estimation error and average error in all the test cases. The modified LAV estimator also converged faster, especially in situations where the portion of bad data was small. Even where the convergence criterion was not satisfied, the modified LAV estimator gained better convergence for the same number of iterations. The fact that the modified LAV estimator employs contraction mapping and SVD techniques before selecting the requires measurements for estimation, enhances the estimation in this regard. However, the more complex procedure effects the computational time of the estimator.

The modified LAV estimator follows a more complex algorithm for selecting a number of measurements for estimation but by selecting those equations the algorithm also reduces the size of the problem. Therefore, if the modified LAV estimator reaches the convergence criterion in a few iterations, its computational time is less than the LS estimator. As the number of iterations increases, the effect of computational complexity factor overcomes the effect of size reduction. As a result, the LS estimator provides a smaller simulation time for the larger number of iterations.

As an alternative, a more developed LS algorithm is tested with the IEEE 14 bus on the next section.

4.6 The IEEE 14 bus Power Network - Another Approach

In this section the IEEE 14 bus power system with similar characteristics described in section 4.4.1 is employed for experiments. A more developed LS estimator is used in the test and the simulation results include the estimates provided by that estimator.

The new LS-based estimator uses a bad data processing technique in each iteration to detect non critical erroneous measurements and remove them for the next iteration. The detection technique is based on the Largest Residual test explained in section 2.6.1. The residuals of estimation are calculated. Their standard deviation is then computed and the normalized ratio of each residual to standard deviation is obtained. In the end, the measurements with larger ratio are eliminated in the next iteration. Note that these measurements should not include critical measurements of system since removing the critical measurements from the measurement set, makes the system unobservable.

The estimation results of the original LS estimator, the modified LAV estimator and the modified LS estimator are presented in Figure 4.25 and Figure 4.26 for different portions of Gaussian noise. The estimation errors are given in Table 4.19. The figures clearly show that the performance of the original LS estimator improves by applying the bad data processing step. The modified LS estimation plot gets closer to the modified LAV estimator especially for smaller portions of bad data. The estimation error follows the same pattern and it almost matches the estimation error of the modified LAV for PBD equals to 1/5. In general though, the modified LAV estimation still performs better in terms of estimation error.

Table 4.19 also presents the convergence and time data of the simulations. Comparing this table with Table 4.4, the modified LS algorithm converges for all three portions of Gaussian bad data, and its convergence rate is close to the modified LAV estimator. The number of iterations before reaching the convergence criterion are also close to each other for smaller portions of bad data. However, the estimation time of the modified LS is greater than the estimation time needed by the modified LAV algorithm.

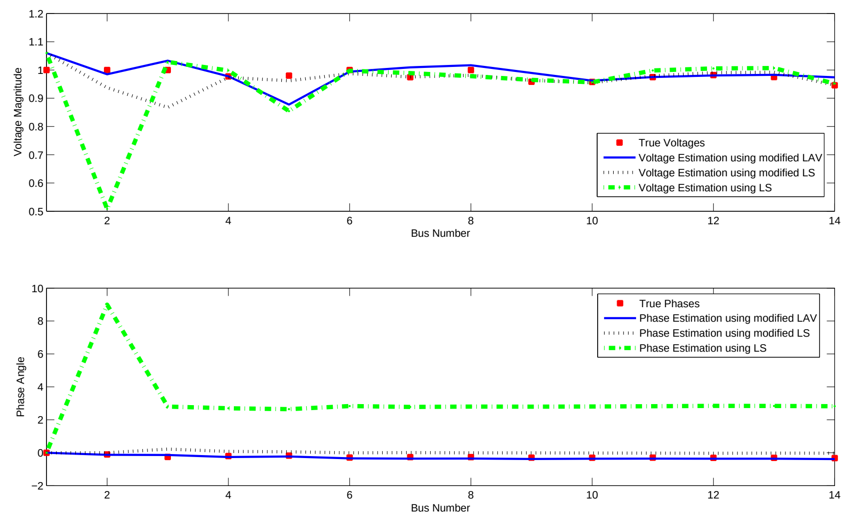

(a) Noise on 1/5 of measurement set

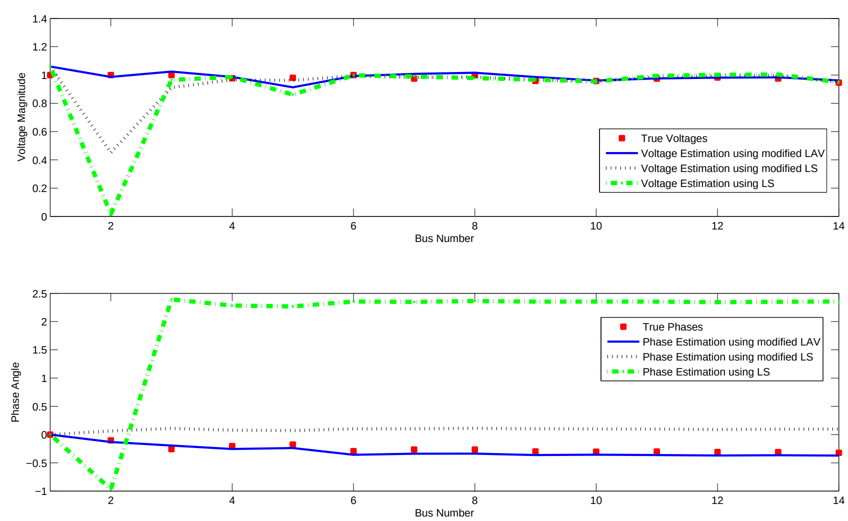

(b) Noise on 1/4 of measurement set

Figure 4.25: The Voltage and Phase estimation for the 14-bus power system with Gaussian noise and three estimators.

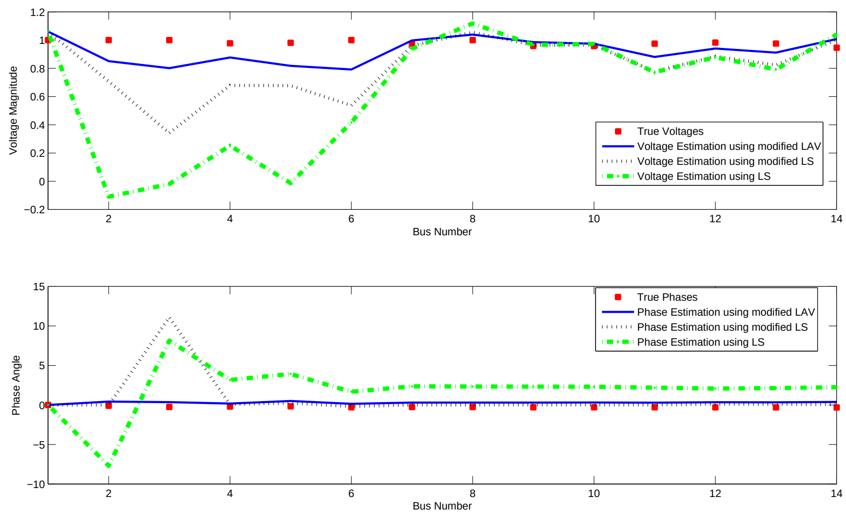

Figure 4.26: The Voltage and Phase estimation for the 14-bus power system with three estimators- Gaussian noise on 2/3 of measurement set.

Figure 4.6 shows the simulation results for voltage magnitude and phase angle estimation in 14 bus system which includes the results of the modified LS estimator in the presence of Rayleigh noise. Similar to results obtained for the Gaussian noise, the modified LS estimator is close to the modified LAV estimator when the portion of bad data is smaller. In the case when 2/3 of measurements are affected by Rayleigh noise, both estimators get further from the true states. The estimation error of the LAV estimator remains smaller than the relative value for the modified LS estimator as given in Table 4.20.

For Rayleigh noise, the modified LS estimator provides a better convergence compare to the original estimator. The simulation time is however larger than the LS estimator or even the LAV estimator. Similar to Gaussian noise, this feature is more noticeable for PBD equals to 2/3. In conclusion, although the modified LS estimator is more accurate and convergent than the original LS estimator, its accuracy and convergence is still less than the modified LAV estimator. The computational time of the estimator also exceeds the time required by the two other estimators.

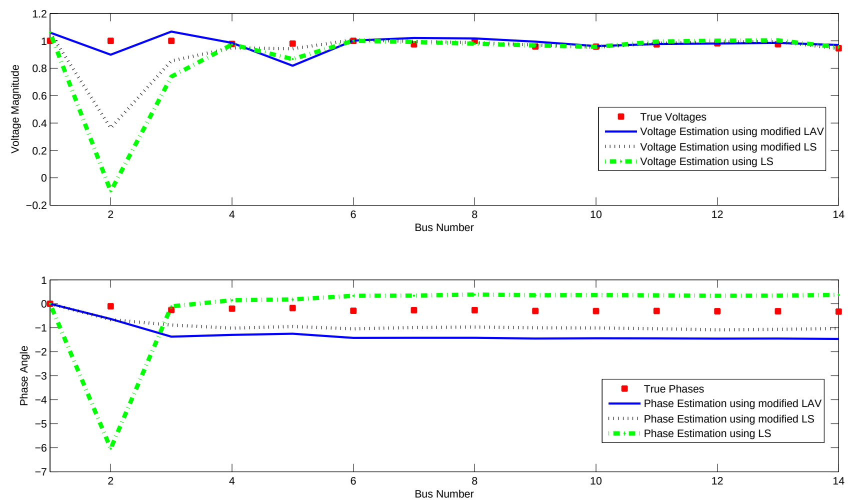

(a) Noise on 1/5 of measurement set

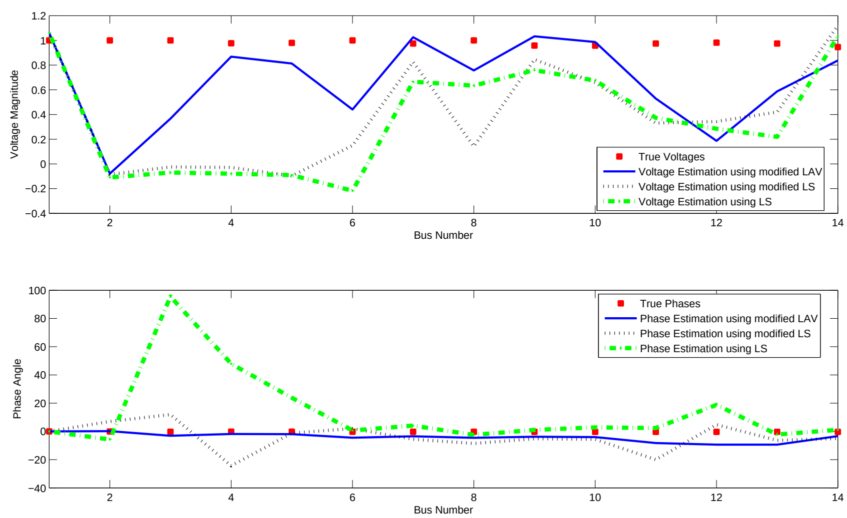

(b) Noise on 2/3 of measurement set

Figure 4.27: The Voltage and Phase estimation for the 14-bus power system with Rayleigh noise and three estimators.

Table 4.19: The estimation convergence of 14 bus system with Gaussian noise and the modified LS estimator

Portion of Bad Data	Modified LS			
PBD	Estimation Error	Iter	Log of convergence	Time
1/5	34.3959	3	-3.1079	0.0284
1/4	57.5984	5	-3.1953	0.0416
2/3	110.3498	12	-3.0803	0.0958

Table 4.20: The estimation convergence of 14 bus system with Rayleigh noise and the modified LS estimator

Portion of Bad Data	Modified LS			
PBD	Estimation Error	Iter	Log of convergence	Time
1/5	81.2759	20	-1.9272	0.1572
2/3	289.1801	20	0.4933	0.1610

4.7 Summary

In this chapter, the effectiveness of the suggested LAV estimation techniques have been assessed on several IEEE power systems benchmarks. First, it was shown that the LAV estimation technique based on the locally linearization concepts works well for small-scale nonlinear power networks. However, it was practically shown that this LAV estimation approach fails for power networks that include more than 5 buses, because of the sparse conditions of the system matrices. It was then shown that the application of the proposed modified LAV estimation technique can significantly address this issue. A comprehensive comparative study confirms the better performance of the proposed LAV technique in comparison with the LS estimation, in the presence of different noise conditions.

Chapter 5

Conclusion

The primary focus of this thesis was to introduce a LAV estimator for power system state estimation regarding the fundamentals of contraction mapping and Singular Value Decomposition.An introduction to fundamentals of modeling and formulating power networks, and state estimation in those networks using numerical methods, were the subjects of the first three chapters. Chapter four discussed a method which uses contraction mapping to address the problem of LAV static state estimation in nonlinear power networks. The novel contributions can be listed as:

- Introducing an algorithm for LAV state estimation in nonlinear power systems using the contraction mapping.
- Modifying the algorithm by SVD technique to extend the application to larger power networks.

Simulations were carried out in chapter five to assess the performance of the new LAV estimator in different test cases and with different types and amounts of bad data. Significant improvements were seen in all cases in terms of estimation error. The future work can be extended in various ways and directions such as:

- Adjusting the algorithms to the Weighted LAV estimator.
- Analyzing the convergence rate.

- Modifying the method for applications in real time state estimation problems.
- Extension to other state estimation problems with similar nature.

Appendix A

The Parameters of IEEE Small-Scale Systems

A.1 The IEEE 5 Bus Test System

Table A.1: The 5-bus Power System Operating Conditions

Line	Resistance(P.U)	Reactance(P.U)	Line Charging (P.U)
1-2	0.02	0.06	0.030
1-3	0.08	0.24	0.025
2-3	0.06	0.18	0.020
2-4	0.06	0.18	0.020
2-5	0.04	0.12	0.015
3-4	0.01	0.03	0.010
4-5	0.08	0.24	0.025

Table A.2: The 5-bus Power System Parameters

Bus Number	Active Power Net Generation MW	Reactive Power Net Generation MVAR
2	20.0	20.0
3	-45.0	-15.0
4	-40.0	-05.0
5	-60.0	-10.0

A.2 The IEEE 10 Bus Test System

Table A.3: The 10-bus Power System Operating Conditions

Line	Resistance(P.U)	Reactance(P.U)	Line Charging (P.U)
1-3	0.004	0.032	0.000
1-5	0.005	0.042	0.000
2-3	0.001	0.010	0.000
2-4	0.003	0.028	0.000
3-4	0.054	0.151	0.000
4-5	0.143	0.364	0.000
4-9	0.044	0.112	0.000
4-10	0.029	0.073	0.000
5-6	0.055	0.140	0.000
5-7	0.073	0.185	0.000
6-7	0.132	0.336	0.000
7-8	0.029	0.073	0.000
8-9	0.033	0.084	0.000
9-10	0.033	0.084	0.000

Table A.4: The 10-bus Power System Parameters

Bus Number	Active Power Net Generation MW	Reactive Power Net Generation MVAR
2	380.0	-70.0
3	-90.0	55.0
4	160.0	-80.0
5	-50.0	25.0

Continued on the next page

Table A.4 – continued from the previous page

6	-10.0	-15.0
7	-70.0	20.0
8	-50.0	25.0
9	-100.0	50.0
10	-40.0	-100.0

Appendix B

The Parameters of IEEE Large-Scale Systems

B.1 The IEEE 14 Bus Test System

Table B.1: The 14-bus Power System Operating Conditions

Bus Number	Bus Type	P gen(p.u.)	Q_g(p.u.)	P_l(p.u.)	Q_l(p.u.)	Capacitor
1	3	2.324	-0.169	0	0	0
2	2	0.4	0.424	0.217	0.127	0
3	2	0	0.234	0.942	0.19	0
4	0	0	0	0.478	-0.039	0
5	0	0	0	0.076	0.016	0
6	2	0	0.122	0.112	0.075	0
7	0	0	0	0	0	0
8	2	0	0.174	0	0	0
9	0	0	0	0.295	0.166	0.19
10	0	0	0	0.09	0.058	0
11	0	0	0	0.035	0.018	0

Continued on the next page

Table B.1 – continued from previous page

12	0	0	0	0.061	0.016	0
13	0	0	0	0.135	0.058	0
14	0	0	0	0.149	0.05	0

Table B.2: The 14-bus Power System Parameters

From Bus	To Bus	r_{ij} (p.u.)	x_{ij} (p.u.)	Line Charging (p.u.)	Tap Ratio
1	2	0.01938	0.05917	0.0528	0
1	5	0.05403	0.22304	0.0492	0
2	3	0.04699	0.19797	0.0438	0
2	4	0.05811	0.17632	0.034	0
2	5	0.05695	0.17388	0.0346	0
3	4	0.06701	0.17103	0.0128	0
4	5	0.01335	0.04211	0	0
4	7	0	0.20912	0	0.978
4	9	0	0.55618	0	0.969
5	6	0	0.25202	0	0.932
6	11	0.09498	0.1989	0	0
6	12	0.12291	0.25581	0	0
6	13	0.06615	0.13027	0	0
7	8	0	0.17615	0	0
7	9	0	0.11001	0	0
9	10	0.03181	0.0845	0	0
9	14	0.12711	0.27038	0	0
10	11	0.08205	0.19207	0	0
12	13	0.22092	0.19988	0	0
13	14	0.17093	0.34802	0	0

B.2 The IEEE 30 Bus Test System

Table B.3: The 30 Bus Power System Operating Conditions

Bus Number	Bus Type	P_g(p.u.)	Q_g(p.u.)	P_l(p.u.)	Q_l(p.u.)	Capacitor
1	3	2.602	-0.161	0	0	0
2	2	0.4	0.5	0.217	0.127	0
3	0	0	0	0.024	0.012	0
4	0	0	0	0.076	0.016	0
5	2	0	0.37	0.942	0.19	0
6	0	0	0	0	0	0
7	0	0	0	0.228	0.109	0
8	2	0	0.373	0.3	0.3	0
9	0	0	0	0	0	0
10	0	0	0	0.058	0.02	0.19
11	2	0	0.162	0	0	0
12	0	0	0	0.112	0.075	0
13	2	0	0.106	0	0	0
14	0	0	0	0.062	0.016	0
15	0	0	0	0.082	0.025	0
16	0	0	0	0.035	0.018	0
17	0	0	0	0.09	0.058	0
18	0	0	0	0.032	0.009	0
19	0	0	0	0.095	0.034	0
20	0	0	0	0.022	0.007	0
21	0	0	0	0.175	0.112	0
22	0	0	0	0	0	0

Continued on the next page

Table B.3 – continued from the previous page

23	0	0	0	0.032	0.016	0
24	0	0	0	0.087	0.067	0.043
25	0	0	0	0	0	0
26	0	0	0	0.035	0.023	0
27	0	0	0	0	0	0
28	0	0	0	0	0	0
29	0	0	0	0.024	0.009	0
30	0	0	0	0.106	0.019	0

Table B.4: The 30-bus Power System Parameters

From Bus	To Bus	r_{ij} (p.u.)	x_{ij} (p.u.)	Line Charging (p.u.)	Tap Ratio
1	2	0.0192	0.0575	0.0528	0
1	3	0.0452	0.1652	0.0408	0
2	4	0.057	0.1737	0.0368	0
3	4	0.0132	0.0379	0.0084	0
2	5	0.0472	0.1983	0.0418	0
2	6	0.0581	0.1763	0.0374	0
4	6	0.0119	0.0414	0.009	0
5	7	0.046	0.116	0.0204	0
6	7	0.0267	0.082	0.017	0
6	8	0.012	0.042	0.009	0
6	9	0	0.208	0	0.978
6	10	0	0.556	0	0.969
9	11	0	0.208	0	0
9	10	0	0.11	0	0
4	12	0	0.256	0	0.932

Continued on the next page

Table B.4 – continued from the previous page

12	13	0	0.14	0	0
12	14	0.1231	0.2559	0	0
12	15	0.0662	0.1304	0	0
12	16	0.0945	0.1987	0	0
14	15	0.221	0.1997	0	0
16	17	0.0524	0.1923	0	0
15	18	0.1073	0.2185	0	0
18	19	0.0639	0.1292	0	0
19	20	0.034	0.068	0	0
10	20	0.0936	0.209	0	0
10	17	0.0324	0.0845	0	0
10	21	0.0348	0.0749	0	0
10	22	0.0727	0.1499	0	0
21	22	0.0116	0.0236	0	0
15	23	0.1	0.202	0	0
22	24	0.115	0.179	0	0
23	24	0.132	0.27	0	0
24	25	0.1885	0.3292	0	0
25	26	0.2544	0.38	0	0
25	27	0.1093	0.2087	0	0
28	27	0	0.396	0	0.968
27	29	0.2198	0.4153	0	0
27	30	0.3202	0.6027	0	0
29	30	0.2399	0.4533	0	0
8	28	0.0636	0.2	0.0428	0
6	28	0.0169	0.0599	0.013	0

B.3 The IEEE 57 Bus Test System

Table B.5: The 57 Bus Power System Operating Conditions

Bus Number	Bus Type	P_g(p.u.)	Q_g(p.u.)	P_l(p.u.)	Q_l(p.u.)	Capacitor
1	3	1.289	-0.161	0.55	0.17	0
2	2	0	-0.008	0.03	0.88	0
3	2	0.4	-0.01	0.41	0.21	0
4	0	0	0	0	0	0
5	0	0	0	0.13	0.04	0
6	2	0	0.008	0.75	0.02	0
7	0	0	0	0	0	0
8	2	4.5	0.621	1.5	0.22	0
9	2	0	0.022	1.21	0.26	0
10	0	0	0	0.05	0.02	0
11	0	0	0	0	0	0
12	2	3.1	1.285	3.77	0.24	0
13	0	0	0	0.18	0.023	0
14	0	0	0	0.105	0.053	0
15	0	0	0	0.22	0.05	0
16	0	0	0	0.43	0.03	0
17	0	0	0	0.42	0.08	0
18	0	0	0	0.272	0.098	0.1
19	0	0	0	0.033	0.006	0
20	0	0	0	0.023	0.01	0
21	0	0	0	0	0	0
22	0	0	0	0	0	0
23	0	0	0	0.063	0.021	0
24	0	0	0	0	0	0
25	0	0	0	0.063	0.032	0.059

Continued on the next page

Table B.5 – continued from the previous page

26	0	0	0	0	0	0
27	0	0	0	0.093	0.005	0
28	0	0	0	0.046	0.023	0
29	0	0	0	0.17	0.026	0
30	0	0	0	0.036	0.018	0
31	0	0	0	0.058	0.029	0
32	0	0	0	0.016	0.008	0
33	0	0	0	0.038	0.019	0
34	0	0	0	0	0	0
35	0	0	0	0.06	0.03	0
36	0	0	0	0	0	0
37	0	0	0	0	0	0
38	0	0	0	0.14	0.07	0
39	0	0	0	0	0	0
40	0	0	0	0	0	0
41	0	0	0	0.063	0.03	0
42	0	0	0	0.071	0.044	0
43	0	0	0	0.02	0.01	0
44	0	0	0	0.12	0.018	0
45	0	0	0	0	0	0
46	0	0	0	0	0	0
47	0	0	0	0.297	0.116	0
48	0	0	0	0	0	0
49	0	0	0	0.18	0.085	0
50	0	0	0	0.21	0.105	0
51	0	0	0	0.18	0.053	0
52	0	0	0	0.049	0.022	0
53	0	0	0	0.2	0.1	0.063
54	0	0	0	0.041	0.014	0

Continued on the next page

Table B.5 – continued from the previous page

55	0	0	0	0.068	0.034	0
56	0	0	0	0.076	0.022	0
57	0	0	0	0.067	0.02	0

Table B.6: The 57-bus Power System Parameters

From Bus	To Bus	r_{ij} (p.u.)	x_{ij} (p.u.)	Line Charging (p.u.)	Tap Ratio
1	2	0.0083	0.028	0.129	0
2	3	0.0298	0.085	0.0818	0
3	4	0.0112	0.0366	0.038	0
4	5	0.0625	0.132	0.0258	0
4	6	0.043	0.148	0.0348	0
6	7	0.02	0.102	0.0276	0
6	8	0.0339	0.173	0.047	0
8	9	0.0099	0.0505	0.0548	0
9	10	0.0369	0.1679	0.044	0
9	11	0.0258	0.0848	0.0218	0
9	12	0.0648	0.295	0.0772	0
9	13	0.0481	0.158	0.0406	0
13	14	0.0132	0.0434	0.011	0
13	15	0.0269	0.0869	0.023	0
1	15	0.0178	0.091	0.0988	0
1	16	0.0454	0.206	0.0546	0
1	17	0.0238	0.108	0.0286	0
3	15	0.0162	0.053	0.0544	0
4	18	0	0.555	0	0.97
4	18	0	0.43	0	0.978

Continued on the next page

Table B.6 – continued from the previous page

5	6	0.0302	0.0641	0.0124	0
7	8	0.0139	0.0712	0.0194	0
10	12	0.0277	0.1262	0.0328	0
11	13	0.0223	0.0732	0.0188	0
12	13	0.0178	0.058	0.0604	0
12	16	0.018	0.0813	0.0216	0
12	17	0.0397	0.179	0.0476	0
14	15	0.0171	0.0547	0.0148	0
18	19	0.461	0.685	0	0
19	20	0.283	0.434	0	0
21	20	0	0.7767	0	1.043
21	22	0.0736	0.117	0	0
22	23	0.0099	0.0152	0	0
23	24	0.166	0.256	0.0084	0
24	25	0	1.182	0	1
24	25	0	1.23	0	1
24	26	0	0.0473	0	1.043
26	27	0.165	0.254	0	0
27	28	0.0618	0.0954	0	0
28	29	0.0418	0.0587	0	0
7	29	0	0.0648	0	0.967
25	30	0.135	0.202	0	0
30	31	0.326	0.497	0	0
31	32	0.507	0.755	0	0
32	33	0.0392	0.036	0	0
34	32	0	0.953	0	0.975
34	35	0.052	0.078	0.0032	0
35	36	0.043	0.0537	0.0016	0
36	37	0.029	0.0366	0	0

Continued on the next page

Table B.6 – continued from the previous page

37	38	0.0651	0.1009	0.002	0
37	39	0.0239	0.0379	0	0
36	40	0.03	0.0466	0	0
22	38	0.0192	0.0295	0	0
11	41	0	0.749	0	0.955
41	42	0.207	0.352	0	0
41	43	0	0.412	0	0
38	44	0.0289	0.0585	0.002	0
15	45	0	0.1042	0	0.955
14	46	0	0.0735	0	0.9
46	47	0.023	0.068	0.0032	0
47	48	0.0182	0.0233	0	0
48	49	0.0834	0.129	0.0048	0
49	50	0.0801	0.128	0	0
50	51	0.1386	0.22	0	0
10	51	0	0.0712	0	0.93
13	49	0	0.191	0	0.895
29	52	0.1442	0.187	0	0
52	53	0.0762	0.0984	0	0
53	54	0.1878	0.232	0	0
54	55	0.1732	0.2265	0	0
11	43	0	0.153	0	0.958
44	45	0.0624	0.1242	0.004	0
40	56	0	1.195	0	0.958
56	41	0.553	0.549	0	0
56	42	0.2125	0.354	0	0
39	57	0	1.355	0	0.98
57	56	0.174	0.26	0	0
38	49	0.115	0.177	0.003	0

Continued on the next page

Table B.6 – continued from the previous page

38	48	0.0312	0.0482	0	0
9	55	0	0.1205	0	0.94

B.4 The IEEE 118 Bus Test System

Table B.7: The 118 Bus Power System Operating Conditions

Bus Number	Bus Type	P_g(p.u.)	Q_g(p.u.)	P_l(p.u.)	Q_l(p.u.)	Capacitor
1	2	0	0	0.51	0.27	0
2	0	0	0	0.2	0.09	0
3	0	0	0	0.39	0.1	0
4	2	-0.09	0	0.3	0.12	0
5	0	0	0	0	0	-0.4
6	2	0	0	0.52	0.22	0
7	0	0	0	0.19	0.02	0
8	2	-0.28	0	0	0	0
9	0	0	0	0	0	0
10	2	4.5	0	0	0	0
11	0	0	0	0.7	0.23	0
12	2	0.85	0	0.47	0.1	0
13	0	0	0	0.34	0.16	0
14	0	0	0	0.14	0.01	0
15	2	0	0	0.9	0.3	0
16	0	0	0	0.25	0.1	0
17	0	0	0	0.11	0.03	0
18	2	0	0	0.6	0.34	0
19	2	0	0	0.45	0.25	0
20	0	0	0	0.18	0.03	0
21	0	0	0	0.14	0.08	0
22	0	0	0	0.1	0.05	0
23	0	0	0	0.07	0.03	0
24	2	-0.13	0	0	0	0
25	2	2.2	0	0	0	0

Continued on the next page

Table B.7 – continued from the previous page

26	2	3.14	0	0	0	0
27	2	-0.09	0	0.62	0.13	0
28	0	0	0	0.17	0.07	0
29	0	0	0	0.24	0.04	0
30	0	0	0	0	0	0
31	2	0.07	0	0.43	0.27	0
32	2	0	0	0.59	0.23	0
33	0	0	0	0.23	0.09	0
34	2	0	0	0.59	0.26	0.14
35	0	0	0	0.33	0.09	0
36	2	0	0	0.31	0.17	0
37	0	0	0	0	0	-0.25
38	0	0	0	0	0	0
39	0	0	0	0.27	0.11	0
40	2	-0.46	0	0.2	0.23	0
41	0	0	0	0.37	0.1	0
42	2	-0.59	0	0.37	0.23	0
43	0	0	0	0.18	0.07	0
44	0	0	0	0.16	0.08	0.1
45	0	0	0	0.53	0.22	0.1
46	2	0.19	0	0.28	0.1	0.1
47	0	0	0	0.34	0	0
48	0	0	0	0.2	0.11	0.15
49	2	2.04	0	0.87	0.3	0
50	0	0	0	0.17	0.04	0
51	0	0	0	0.17	0.08	0
52	0	0	0	0.18	0.05	0
53	0	0	0	0.23	0.11	0
54	2	0.48	0	1.13	0.32	0

Continued on the next page

Table B.7 – continued from the previous page

55	2	0	0	0.63	0.22	0
56	2	0	0	0.84	0.18	0
57	0	0	0	0.12	0.03	0
58	0	0	0	0.12	0.03	0
59	2	1.55	0	2.77	1.13	0
60	0	0	0	0.78	0.03	0
61	2	1.6	0	0	0	0
62	2	0	0	0.77	0.14	0
63	0	0	0	0	0	0
64	0	0	0	0	0	0
65	2	3.91	0	0	0	0
66	2	3.92	0	0.39	0.18	0
67	0	0	0	0.28	0.07	0
68	0	0	0	0	0	0
69	3	5.164	0	0	0	0
70	2	0	0	0.66	0.2	0
71	0	0	0	0	0	0
72	2	-0.12	0	0	0	0
73	2	-0.06	0	0	0	0
74	2	0	0	0.68	0.27	0.12
75	0	0	0	0.47	0.11	0
76	2	0	0	0.68	0.36	0
77	2	0	0	0.61	0.28	0
78	0	0	0	0.71	0.26	0
79	0	0	0	0.39	0.32	0.2
80	2	4.77	0	1.3	0.26	0.1
81	0	0	0	0	0	0
82	0	0	0	0.54	0.27	0
83	0	0	0	0.2	0.1	0

Continued on the next page

Table B.7 – continued from the previous page

84	0	0	0	0.11	0.07	0
85	2	0	0	0.24	0.15	0
86	0	0	0	0.21	0.1	0
87	2	0.04	0	0	0	0
88	0	0	0	0.48	0.1	0
89	2	6.07	0	0	0	0
90	2	-0.85	0	0.78	0.42	0
91	2	-0.1	0	0	0	0
92	2	0	0	0.65	0.1	0
93	0	0	0	0.12	0.07	0
94	0	0	0	0.3	0.16	0
95	0	0	0	0.42	0.31	0
96	0	0	0	0.38	0.15	0
97	0	0	0	0.15	0.09	0
98	0	0	0	0.34	0.08	0
99	2	-0.42	0	0	0	0
100	2	2.52	0	0.37	0.18	0
101	0	0	0	0.22	0.15	0
102	0	0	0	0.05	0.03	0
103	2	0.4	0	0.23	0.16	0
104	2	0	0	0.38	0.25	0
105	2	0	0	0.31	0.26	0.2
106	0	0	0	0.43	0.16	0
107	2	-0.22	0	0.28	0.12	0.06
108	0	0	0	0.02	0.01	0
109	0	0	0	0.08	0.03	0
110	2	0	0	0.39	0.3	0
111	2	0.36	0	0	0	0
112	2	-0.43	0	0.25	0.13	0

Continued on the next page

Table B.7 – continued from the previous page

113	2	-0.06	0	0	0	0
114	0	0	0	0.08	0.03	0
115	0	0	0	0.22	0.07	0
116	2	-1.84	0	0	0	0
117	0	0	0	0.2	0.08	0
118	0	0	0	0.33	0.15	0

Table B.8: The 118-bus Power System Parameters

From Bus	To Bus	r_{ij} (p.u.)	x_{ij} (p.u.)	Line Charging (p.u.)	Tap Ratio
1	2	0.0303	0.0999	0.0254	0
1	3	0.0129	0.0424	0.01082	0
4	5	0.00176	0.00798	0.0021	0
3	5	0.0241	0.108	0.0284	0
5	6	0.0119	0.054	0.01426	0
6	7	0.00459	0.0208	0.0055	0
8	9	0.00244	0.0305	1.162	0
8	5	0	0.0267	0	0.985
9	10	0.00258	0.0322	1.23	0
4	11	0.0209	0.0688	0.01748	0
5	11	0.0203	0.0682	0.01738	0
11	12	0.00595	0.0196	0.00502	0
2	12	0.0187	0.0616	0.01572	0
3	12	0.0484	0.16	0.0406	0
7	12	0.00862	0.034	0.00874	0
11	13	0.02225	0.0731	0.01876	0
12	14	0.0215	0.0707	0.01816	0

Continued on the next page

Table B.8 – continued from the previous page

13	15	0.0744	0.2444	0.06268	0
14	15	0.0595	0.195	0.0502	0
12	16	0.0212	0.0834	0.0214	0
15	17	0.0132	0.0437	0.0444	0
16	17	0.0454	0.1801	0.0466	0
17	18	0.0123	0.0505	0.01298	0
18	19	0.01119	0.0493	0.01142	0
19	20	0.0252	0.117	0.0298	0
15	19	0.012	0.0394	0.0101	0
20	21	0.0183	0.0849	0.0216	0
21	22	0.0209	0.097	0.0246	0
22	23	0.0342	0.159	0.0404	0
23	24	0.0135	0.0492	0.0498	0
23	25	0.0156	0.08	0.0864	0
26	25	0	0.0382	0	0
25	27	0.0318	0.163	0.1764	0
27	28	0.01913	0.0855	0.0216	0
28	29	0.0237	0.0943	0.0238	0
30	17	0	0.0388	0	0
8	30	0.00431	0.0504	0.514	0
26	30	0.00799	0.086	0.908	0
17	31	0.0474	0.1563	0.0399	0
29	31	0.0108	0.0331	0.0083	0
23	32	0.0317	0.1153	0.1173	0
31	32	0.0298	0.0985	0.0251	0
27	32	0.0229	0.0755	0.01926	0
15	33	0.038	0.1244	0.03194	0
19	34	0.0752	0.247	0.0632	0
35	36	0.00224	0.0102	0.00268	0

Continued on the next page

Table B.8 – continued from the previous page

35	37	0.011	0.0497	0.01318	0
33	37	0.0415	0.142	0.0366	0
34	36	0.00871	0.0268	0.00568	0
34	37	0.00256	0.0094	0.00984	0
38	37	0	0.0375	0	0.935
37	39	0.0321	0.106	0.027	0
37	40	0.0593	0.168	0.042	0
30	38	0.00464	0.054	0.422	0
39	40	0.0184	0.0605	0.01552	0
40	41	0.0145	0.0487	0.01222	0
40	42	0.0555	0.183	0.0466	0
41	42	0.041	0.135	0.0344	0
43	44	0.0608	0.2454	0.06068	0
34	43	0.0413	0.1681	0.04226	0
44	45	0.0224	0.0901	0.0224	0
45	46	0.04	0.1356	0.0332	0
46	47	0.038	0.127	0.0316	0
46	48	0.0601	0.189	0.0472	0
47	49	0.0191	0.0625	0.01604	0
42	49	0.0715	0.323	0.086	0
42	49	0.0715	0.323	0.086	0
45	49	0.0684	0.186	0.0444	0
48	49	0.0179	0.0505	0.01258	0
49	50	0.0267	0.0752	0.01874	0
49	51	0.0486	0.137	0.0342	0
51	52	0.0203	0.0588	0.01396	0
52	53	0.0405	0.1635	0.04058	0
53	54	0.0263	0.122	0.031	0
49	54	0.073	0.289	0.0738	0

Continued on the next page

Table B.8 – continued from the previous page

49	54	0.0869	0.291	0.073	0
54	55	0.0169	0.0707	0.0202	0
54	56	0.00275	0.00955	0.00732	0
55	56	0.00488	0.0151	0.00374	0
56	57	0.0343	0.0966	0.0242	0
50	57	0.0474	0.134	0.0332	0
56	58	0.0343	0.0966	0.0242	0
51	58	0.0255	0.0719	0.01788	0
54	59	0.0503	0.2293	0.0598	0
56	59	0.0825	0.251	0.0569	0
56	59	0.0803	0.239	0.0536	0
55	59	0.04739	0.2158	0.05646	0
59	60	0.0317	0.145	0.0376	0
59	61	0.0328	0.15	0.0388	0
60	61	0.00264	0.0135	0.01456	0
60	62	0.0123	0.0561	0.01468	0
61	62	0.00824	0.0376	0.0098	0
63	59	0	0.0386	0	0.96
63	64	0.00172	0.02	0.216	0
64	61	0	0.0268	0	0.985
38	65	0.00901	0.0986	1.046	0
64	65	0.00269	0.0302	0.38	0
49	66	0.018	0.0919	0.0248	0
49	66	0.018	0.0919	0.0248	0
62	66	0.0482	0.218	0.0578	0
62	67	0.0258	0.117	0.031	0
65	66	0	0.037	0	0.935
66	67	0.0224	0.1015	0.02682	0
65	68	0.00138	0.016	0.638	0

Continued on the next page

Table B.8 – continued from the previous page

47	69	0.0844	0.2778	0.07092	0
49	69	0.0985	0.324	0.0828	0
68	69	0	0.037	0	0.935
69	70	0.03	0.127	0.122	0
24	70	0.00221	0.4115	0.10198	0
70	71	0.00882	0.0355	0.00878	0
24	72	0.0488	0.196	0.0488	0
71	72	0.0446	0.18	0.04444	0
71	73	0.00866	0.0454	0.01178	0
70	74	0.0401	0.1323	0.03368	0
70	75	0.0428	0.141	0.036	0
69	75	0.0405	0.122	0.124	0
74	75	0.0123	0.0406	0.01034	0
76	77	0.0444	0.148	0.0368	0
69	77	0.0309	0.101	0.1038	0
75	77	0.0601	0.1999	0.04978	0
77	78	0.00376	0.0124	0.01264	0
78	79	0.00546	0.0244	0.00648	0
77	80	0.017	0.0485	0.0472	0
77	80	0.0294	0.105	0.0228	0
79	80	0.0156	0.0704	0.0187	0
68	81	0.00175	0.0202	0.808	0
81	80	0	0.037	0	0.935
77	82	0.0298	0.0853	0.08174	0
82	83	0.0112	0.03665	0.03796	0
83	84	0.0625	0.132	0.0258	0
83	85	0.043	0.148	0.0348	0
84	85	0.0302	0.0641	0.01234	0
85	86	0.035	0.123	0.0276	0

Continued on the next page

Table B.8 – continued from the previous page

86	87	0.02828	0.2074	0.0445	0
85	88	0.02	0.102	0.0276	0
85	89	0.0239	0.173	0.047	0
88	89	0.0139	0.0712	0.01934	0
89	90	0.0518	0.188	0.0528	0
89	90	0.0238	0.0997	0.106	0
90	91	0.0254	0.0836	0.0214	0
89	92	0.0099	0.0505	0.0548	0
89	92	0.0393	0.1581	0.0414	0
91	92	0.0387	0.1272	0.03268	0
92	93	0.0258	0.0848	0.0218	0
92	94	0.0481	0.158	0.0406	0
93	94	0.0223	0.0732	0.01876	0
94	95	0.0132	0.0434	0.0111	0
80	96	0.0356	0.182	0.0494	0
82	96	0.0162	0.053	0.0544	0
94	96	0.0269	0.0869	0.023	0
80	97	0.0183	0.0934	0.0254	0
80	98	0.0238	0.108	0.0286	0
80	99	0.0454	0.206	0.0546	0
92	100	0.0648	0.295	0.0472	0
94	100	0.0178	0.058	0.0604	0
95	96	0.0171	0.0547	0.01474	0
96	97	0.0173	0.0885	0.024	0
98	100	0.0397	0.179	0.0476	0
99	100	0.018	0.0813	0.0216	0
100	101	0.0277	0.1262	0.0328	0
92	102	0.0123	0.0559	0.01464	0
101	102	0.0246	0.112	0.0294	0

Continued on the next page

Table B.8 – continued from the previous page

100	103	0.016	0.0525	0.0536	0
100	104	0.0451	0.204	0.0541	0
103	104	0.0466	0.1584	0.0407	0
103	105	0.0535	0.1625	0.0408	0
100	106	0.0605	0.229	0.062	0
104	105	0.00994	0.0378	0.00986	0
105	106	0.014	0.0547	0.01434	0
105	107	0.053	0.183	0.0472	0
105	108	0.0261	0.0703	0.01844	0
106	107	0.053	0.183	0.0472	0
108	109	0.0105	0.0288	0.0076	0
103	110	0.03906	0.1813	0.0461	0
109	110	0.0278	0.0762	0.0202	0
110	111	0.022	0.0755	0.02	0
110	112	0.0247	0.064	0.062	0
17	113	0.00913	0.0301	0.00768	0
32	113	0.0615	0.203	0.0518	0
32	114	0.0135	0.0612	0.01628	0
27	115	0.0164	0.0741	0.01972	0
114	115	0.0023	0.0104	0.00276	0
68	116	0.00034	0.00405	0.164	0
12	117	0.0329	0.14	0.0358	0
75	118	0.0145	0.0481	0.01198	0
76	118	0.0164	0.0544	0.01356	0

Appendix C

Simulation Conditions

C.1 Small-Scale Networks

C.1.1 The IEEE 5 Bus Power Network

Two measurement sets are considered for experiments on the 5 bus network. The redundancy ratio on set A is 2.875 and the redundancy ratio in Set B is 2.625. Each set contains three sets of bad data points, which mostly includes outliers of the measurement set.
Tables C.1 and C.3, present the number of measurements used in simulations for each type.
Tables C.2 and C.4, show the type and place of bad measurements.

Table C.1: The 5-Bus System-Measurement Set A

Set	Measurement Type	Measurement
	Active Power Injection	3
A	Active Power Flow	8
	Reactive Power Injection	3
	Reactive Power Flow	9

Table C.2: The 5-Bus System-Bad Data in Set A

Sub Set	Bad Data Type	Description
A_1	Active Power Injection	p_2 is reversed
A_2	Active Power Flow	p_{3-1} is inverted
	Reactive Power Flow	q_{5-4} is halved
A_3	Active Power Flow	p_{3-1} is inverted
	Active Power Flow	p_{5-4} is set to zero
	Reactive Power Flow	q_{5-4} is halved

Table C.3: The 5-Bus System-Measurement Set B

Set	Measurement Type	Measurement
	Active Power Injection	4
B	Active Power Flow	7
	Reactive Power Injection	4
	Active Power Flow	6

Table C.4: The 5-Bus System-Bad Data in Set B

Sub Set	Bad Data Type	Description
B_1	Active Power Injection	p_2 is inverted
	Active Power Flow	p_{3-4} is inverted
	Reactive Power Injection	q_3 is halved
B_2	Active Power Injection	p_5 is halved
	Active Power Flow	p_{3-4} is doubled
		Continued on the next page

Table C.4 – continued from the previous page

	Reactive Power Injection	q_4 is set to zero
	Reactive Power Flow	q_{3-4} is set to zero
B_3	Active Power Injection	p_5 is halved
	Active Power Flow	p_{3-4} is doubled
	Active Power Flow	p_{2-4} is doubled
	Reactive Power Injection	q_4 is set to zero
	Reactive Power Flow	q_{3-4} is set to zero
	Reactive Power Flow	q_{4-2} is inverted

C.1.2 The IEEE 10 Bus Power Network

The measurement sets A and B are used for 10 bus system that have the redundancy ratios of 2.94 and 3.00 accordingly. The network is tested with the original LAV algorithm (the proposed algorithm), and the LS-based algorithm. The results are compared to show the inefficiency of proposed algorithm for larger networks. The more developed version of the original LAV algorithm (the modified algorithm) is tested for one of the measurement sets. The advantage to the LS-based estimator is shown through related figures.

Table C.5 and C.7 express the specifications of measurement set. The place and type of bad data is also shown in tables C.6 and C.8.

Table C.5: The 10-Bus System-Measurement Set A

Set	Measurement Type	Measurement
	Active Power Injection	9
A	Active Power Flow	15
	Reactive Power Injection	9
	Reactive Power Flow	20

Table C.6: The 10-Bus System-Bad Data in Set A

Sub Set	Bad Data Type	Description
A_1	Active Power Flow	p_{10-4} is reversed
	Reactive Power Flow	q_{5-6} is reversed
A_2	Active Power Flow	p_{10-4} is reversed
	Reactive Power Injection	q_7 is halved
	Reactive Power Injection	q_9 is halved
	Reactive Power Flow	q_{1-3} is doubled
	Reactive Power Flow	q_{5-6} is reversed

Continued on the next page

Table C.6 – continued from the previous page

	Reactive Power Flow	q_{8-9} is set to zero
A_3	Active Power Injection	p_3 is doubled and reversed
	Active Power Injection	p_9 is set to zero
	Reactive Power Flow	q_{2-4} is halved

Table C.7: The 10-Bus System-Measurement Set B

Set	Measurement Type	Measurement
	Active Power Injection	7
B	Active Power Flow	23
	Reactive Power Injection	7
	Reactive Power Flow	17

Table C.8: The 10-Bus System-Bad Data in Set B

Sub Set	Bad Data Type	Description
B	Active Power Injection	p_2 is reversed
	Active Power Injection	p_6 is halved
	Active Power Flow	p_{5-7} is reversed
	Reactive Power Flow	q_{4-9} is set to zero

C.2 Large-Scale Networks

In these series of experiments and for large networks, bad data points are measurements corrupted with noise. This noise can either be Gaussian or Rayleigh. The measurement error variance, σ^2, is presented for different types of measurements and noises, to reflect the expected accuracy of the meter used.

The measurements included in simulations, are active and reactive power injections and active and reactive power flows. A portion of each type of measurements is corrupted with noise. These noisy measurements are generated first by calculating true measurements of system based on the true states. Then the noise is added to the true measurements to produce bad data. For Gaussian noise, mean is set to zero and variance is set to one. For Rayleigh noise, unit variance is considered.

C.2.1 The IEEE 14 Bus Power Network

The important features of measurement sets and bad data, used in 14 bus network simulations, are given in Table C.9. In simulations, noise is mainly placed on the generation buses of the system and their related branches. For PBD equals to 1/6, bad data set includes buses one to three and their related branches. For PBD equals to 1/5, bad data set includes buses one to four and their connected branches. For PBD equals to 1/4, the set consists of noisy measurements from buses one to five and their related branches. PBD equals to 2/3, involves the first nine buses of the system and their branches.

Table C.9: The 14-Bus System-Measurement Set

PBD	Measurement Type	Total Meas	Num of Bad Meas	σ^2	Noise Type
1/5	Active Power Injection	14	3	1×10^{-3}	Gaussian
	Active Power Flow	20	4	1×10^{-4}	
	Reactive Power Injection	14	3	1×10^{-3}	
	Reactive Power Flow	20	4	1×10^{-4}	

Continued on the next page

Table C.9 – continued from the previous page

1/4	Active Power Injection	14	3	1×10^{-3}	Gaussian
	Active Power Flow	20	5	1×10^{-4}	
	Reactive Power Injection	14	3	1×10^{-3}	
	Reactive Power Flow	20	5	1×10^{-4}	
2/3	Active Power Injection	14	9	1×10^{-3}	Gaussian
	Active Power Flow	20	13	1×10^{-4}	
	Reactive Power Injection	14	9	1×10^{-3}	
	Reactive Power Flow	20	13	1×10^{-4}	
1/6	Active Power Injection	14	2	1×10^{-3}	Rayleigh
	Active Power Flow	20	3	1×10^{-4}	
	Reactive Power Injection	14	2	1×10^{-3}	
	Reactive Power Flow	20	3	1×10^{-4}	
1/5	Active Power Injection	14	3	1×10^{-3}	Rayleigh
	Active Power Flow	20	5	1×10^{-4}	
	Reactive Power Injection	14	3	1×10^{-3}	
	Reactive Power Flow	20	5	1×10^{-4}	
2/3	Active Power Injection	14	9	1×10^{-3}	Rayleigh
	Active Power Flow	20	13	1×10^{-4}	
	Reactive Power Injection	14	9	1×10^{-3}	
	Reactive Power Flow	20	13	1×10^{-4}	

C.2.2 The IEEE 30 Bus Power Network

Table C.10 shows the main features of measurement set and bad data for the IEEE 30 bus system. The network size is approximately twice the size of IEEE 14 bus system, and so is the number of measurements and bad data points. The Gaussian noise mostly affects the buses four to fourteen and their branches for smaller portions of bad data (1/6 and 1/5). However, for PBD equals to 1/2, most of the buses in the system, from bus four to twenty-four are affected. Rayleigh noise is placed slightly different within the set. For the smaller portions, measurements from buses one to seven are affected . For the measurement set with half noisy measurements, all the generation buses (buses number 1, 2, 5, 8, 11, 13), and their related branches, are affected.

Table C.10: The 30-Bus System-Measurement Set

PBD	Measurement Type	Total Meas	Num of Bad Meas	σ^2	Noise Type
1/6	Active Power Injection	30	5	1×10^{-3}	Gaussian
	Active Power Flow	41	7	1×10^{-4}	
	Reactive Power Injection	30	5	1×10^{-3}	
	Reactive Power Flow	41	7	1×10^{-4}	
1/5	Active Power Injection	30	6	1×10^{-3}	Gaussian
	Active Power Flow	41	8	1×10^{-4}	
	Reactive Power Injection	30	6	1×10^{-3}	
	Reactive Power Flow	41	8	1×10^{-4}	
1/2	Active Power Injection	30	15	1×10^{-3}	Gaussian
	Active Power Flow	41	21	1×10^{-4}	
	Reactive Power Injection	30	15	1×10^{-3}	
	Reactive Power Flow	41	21	1×10^{-4}	
1/6	Active Power Injection	30	5	1×10^{-3}	Rayleigh
	Active Power Flow	41	7	1×10^{-4}	
	Reactive Power Injection	30	5	1×10^{-3}	

Continued on the next page

Table C.10 – continued from the previous page

	Reactive Power Flow	41	7	1×10^{-4}	
1/5	Active Power Injection	30	6	1×10^{-3}	Rayleigh
	Active Power Flow	41	8	1×10^{-4}	
	Reactive Power Injection	30	6	1×10^{-3}	
	Reactive Power Flow	41	8	1×10^{-4}	
1/2	Active Power Injection	30	15	1×10^{-3}	Rayleigh
	Active Power Flow	41	21	1×10^{-4}	
	Reactive Power Injection	30	15	1×10^{-3}	
	Reactive Power Flow	41	21	1×10^{-4}	

C.2.3 The IEEE 57 Bus Power Network

The main characteristics of measurement set and the generated bad data for the IEEE 57 bus are presented in Table C.11. In this set, two different scenarios are tested, for each type of noise. In both cases, the noise is widely distributed within the measurement set, corrupting power injection and power flow measurements in different parts of the network. For PBD equals to 1/9, power injections at the first six buses of system are considered noisy. But noise also corrupts power flow measurements from branches between buses nineteen to twenty-eight. For PBD equals to 1/3, power injection measurements gained from buses thirty to forty-nine are affected by noise. Also power flow measurements related to branches between buses eighteen to forty-four are corrupted.

Table C.11: The 57-Bus System-Measurement Set

PBD	Measurement Type	Total Meas	Num of Bad Meas	σ^2	Noise Type
	Active Power Injection	57	6	1×10^{-3}	
1/9	Active Power Flow	80	9	1×10^{-4}	Gaussian
	Reactive Power Injection	57	6	1×10^{-3}	
	Reactive Power Flow	80	9	1×10^{-4}	
	Active Power Injection	57	6	1×10^{-3}	
1/3	Active Power Flow	80	8	1×10^{-4}	Gaussian
	Reactive Power Injection	57	19	1×10^{-3}	
	Reactive Power Flow	80	27	1×10^{-4}	
	Active Power Injection	57	6	1×10^{-3}	
1/9	Active Power Flow	80	9	1×10^{-4}	Rayleigh
	Reactive Power Injection	57	6	1×10^{-3}	
	Reactive Power Flow	80	9	1×10^{-4}	
	Active Power Injection	57	19	1×10^{-3}	
1/3	Active Power Flow	80	27	1×10^{-4}	Rayleigh

Continued on the next page

Table C.11 – continued from the previous page

	Reactive Power Injection	57	19	1×10^{-3}	
	Reactive Power Flow	80	27	1×10^{-4}	

C.2.4 The IEEE 118 Bus Power Network

Table C.12 describes the features of measurement set used in simulation on 118 bus system. The Gaussian noise corrupts 1/6, and 1/3 of the measurement set for the first round of experiments. The noise has been added to the measurements of the system such that when the portion of bad data is 1/6, noisy measurements involve buses thirty to fifty . They also affect measurements related to branches between buses twenty to forty-five. For the ratio of 1/3, buses thirty to sixty-nine are involved and related branch measurements between buses twenty-three to sixty-nine, including bus seven, bus eight and bus nineteen.

Table C.12: The 118-Bus System-Measurement Set

PBD	Measurement Type	Total Meas	Num of Bad Meas	σ^2	Noise Type
	Active Power Injection	118	20	1×10^{-3}	
1/6	Active Power Flow	186	31	1×10^{-4}	Gaussian
	Reactive Power Injection	118	20	1×10^{-3}	
	Reactive Power Flow	186	31	1×10^{-4}	
	Active Power Injection	118	39	1×10^{-3}	
1/3	Active Power Flow	186	62	1×10^{-4}	Gaussian
	Reactive Power Injection	118	39	1×10^{-3}	
	Reactive Power Flow	186	62	1×10^{-4}	
	Active Power Injection	118	20	1×10^{-3}	
1/6	Active Power Flow	186	31	1×10^{-4}	Rayleigh

Continued on the next page

Table C.12 – continued from the previous page

	Reactive Power Injection	118	20	1×10^{-3}	
	Reactive Power Flow	186	31	1×10^{-4}	
1/3	Active Power Injection	118	39	1×10^{-3}	Rayleigh
	Active Power Flow	186	62	1×10^{-4}	
	Reactive Power Injection	118	39	1×10^{-3}	
	Reactive Power Flow	186	62	1×10^{-4}	

Appendix D

Average Errors for Large-Scale Power Networks

It is noted that PBD stands for Portion of Bad Data.

D.1 The IEEE 14 Bus Test System with Gaussian Noise

Table D.1: Average Voltage Magnitude and Phase Angle Errors for IEEE 14 bus with Gaussian Noise

PBD[1]	LS Estimator ΔV_{avg}	LAV Estimator ΔV_{avg}	LS Estimator $\Delta\theta_{avg}$	LAV Estimator $\Delta\theta_{avg}$
1/5	0.1849	0.0353	4.0195	0.0982
1/4	0.2491	0.0352	2.7664	0.0515
2/3	0.5418	0.0379	10.72340	0.0934

[1] Portion of Bad Data

D.2 The IEEE 14 Bus Test System with Rayleigh Noise

Table D.2: Average Voltage Magnitude and Phase Angle Errors for IEEE 14 bus with Rayleigh Noise

PBD	LS Estimator ΔV_{avg}	LAV Estimator ΔV_{avg}	LS Estimator $\Delta\theta_{avg}$	LAV Estimator $\Delta\theta_{avg}$
1/6	0.1593	0.0385	3.6014	0.3213
1/5	0.3045	0.0467	0.7942	0.5289
2/3	0.7220	0.5206	19.8397	15.3305

D.3 The IEEE 30 Bus Test System with Gaussian Noise

Table D.3: Average Voltage Magnitude and Phase Angle Errors for IEEE 30 bus with Gaussian Noise

PBD	LS Estimator ΔV_{avg}	LAV Estimator ΔV_{avg}	LS Estimator $\Delta\theta_{avg}$	LAV Estimator $\Delta\theta_{avg}$
1/6	0.3714	0.2357	1.0295	0.1092
1/5	0.3717	0.2415	3.8169	0.5197
1/2	0.4051	0.2556	5.4841	0.6095

D.4 The IEEE 30 Bus Test System with Rayleigh Noise

Table D.4: Average Voltage Magnitude and Phase Angle Errors for IEEE 30 bus with Rayleigh Noise

PBD	LS Estimator ΔV_{avg}	LAV Estimator ΔV_{avg}	LS Estimator $\Delta\theta_{avg}$	LAV Estimator $\Delta\theta_{avg}$
1/6	0.3548	0.2779	17.4558	2.1448
1/5	0.3981	0.3400	32.0206	2.4806
1/2	0.7745	0.6482	67.325	7.9797

D.5 The IEEE 57 Bus Test System with Gaussian Noise

Table D.5: Average Voltage Magnitude and Phase Angle Errors for IEEE 57 bus with Gaussian Noise

PBD	LS Estimator ΔV_{avg}	LAV Estimator ΔV_{avg}	LS Estimator $\Delta\theta_{avg}$	LAV Estimator $\Delta\theta_{avg}$
1/9	0.2049	0.0595	5.7228	0.0558
1/3	0.3018	0.1620	4.1333	1.6884

D.6 The IEEE 57 Bus Test System with Rayleigh Noise

Table D.6: Average Voltage Magnitude and Phase Angle Errors for IEEE 57 bus with Rayleigh Noise

PBD	LS Estimator ΔV_{avg}	LAV Estimator ΔV_{avg}	LS Estimator $\Delta\theta_{avg}$	LAV Estimator $\Delta\theta_{avg}$

1/9	0.2562	0.0701	8.5619	0.1431
1/3	0.6406	0.3706	67.4604	23.9899

D.7 The IEEE 118 Bus Test System with Gaussian Noise

Table D.7: Average Voltage Magnitude and Phase Angle Errors for IEEE 118 bus with Gaussian Noise

PBD	LS Estimator ΔV_{avg}	LAV Estimator ΔV_{avg}	LS Estimator $\Delta\theta_{avg}$	LAV Estimator $\Delta\theta_{avg}$
1/6	0.2938	0.0570	24.5846	0.1273
1/3	0.3966	0.2063	51.3523	0.5538

D.8 The IEEE 118 Bus Test System with Rayleigh Noise

Table D.8: Average Voltage Magnitude and Phase Angle Errors for IEEE 118 bus with Rayleigh Noise

PBD	LS Estimator ΔV_{avg}	LAV Estimator ΔV_{avg}	LS Estimator $\Delta\theta_{avg}$	LAV Estimator $\Delta\theta_{avg}$
1/6	0.4388	0.0384	16.1060	0.5111
1/3	0.6231	0.4591	77.7831	4.9641

Appendix E

Selected Tables of Simulation Results

E.1 5 Bus Power System - Measurement Set A2

	LS-based	Exact Solution	Proposed LAV
V1	1.06	1.06	1.06
V2	1.0428	1.0474	1.0472
V3	1.0156	1.0242	1.0167
V4	1.019	1.0236	1.022
V5	1.0169	1.0179	1.017
θ_1	0	0	0
θ_2	-0.0307	-0.049	-0.0484
θ_3	-0.0207	-0.0872	-0.099
θ_4	-0.0301	-0.093	-0.131
θ_5	-0.0672	-0.1073	-0.188

E.2 5 Bus Power System - Measurement Set B1

	LS-based	Exact Solution	Proposed LAV
V1	1.06	1.06	1.06
V2	1.04658	1.0474	1.0476
V3	1.02823	1.0242	1.0243
V4	1.02802	1.02374	1.0237
V5	1.02063	1.01797	1.0179
θ_1	0	0	0
θ_2	-0.05459	-0.04897	-0.0485
θ_3	-0.0867	-0.08728	-0.0866
θ_4	-0.08908	-0.09305	-0.0924
θ_5	-0.10329	-0.1073	-0.1067

E.3 10 Bus Power System - Measurement Set A3

	LS-based	Exact Solution	Proposed LAV
V1	1.03	1.03	1.03
V2	0.9703	1.045	0.9497
V3	0.9836	1.04397	0.9687
V4	0.8934	1.03637	0.9076
V5	1.0337	1.03967	1.0276
V6	1.0336	1.04649	1.0121
V7	1.0154	1.03046	1.0455
V8	0.9762	1.03059	1.0479
V9	0.8571	1.02807	0.8199
V10	0.5593	1.02028	0.8082
$\theta 1$	0	0	0
$\theta 2$	0.0772	0.0889	0.1102
$\theta 3$	0.0539	0.06145	0.0749
$\theta 4$	0.0846	0.06834	0.0902
$\theta 5$	-0.0466	-0.03899	-0.0542
$\theta 6$	-0.0858	-0.07894	-0.1007
$\theta 7$	-0.1419	-0.12617	-0.1974
$\theta 8$	-0.1231	-0.21839	-0.2126
$\theta 9$	-0.0118	-0.06047	-0.0628
$\theta 10$	0.4521	-0.00472	0.0227

E.4 14 Bus Power System-Gaussian Noise on 1/4 data set

	LS-based	Exact Solution	Modified LAV
V1	1.06	1.06	1.06
V2	0.123018322	1.045	0.998365407
V3	1.002056944	1.01	1.007297028
V4	1.034184131	1.026092698	0.999708854
V5	0.909500579	1.032597949	0.994262162
V6	1.065420325	1.07	1.035057704
V7	1.060359366	1.044811975	0.998964849
V8	1.055077042	1.09	0.995736548
V9	1.035146468	1.027630894	1.007310227
V10	1.026217803	1.027543353	1.031256369
V11	1.067581224	1.044943317	1.035933452
V12	1.075339119	1.05301731	1.051048064
V13	1.077311388	1.046234106	1.046615712
V14	1.02493943	1.017433253	1.034779609
θ1	0	0	0
θ2	2.544934562	-0.086507559	-0.065529681
θ3	2.598956643	-0.220484417	-0.118353168
θ4	2.559592865	-0.180919937	-0.143322038
θ5	2.548491682	-0.156149826	-0.137595588
θ6	2.671272905	-0.25969414	-0.249429692
θ7	2.659363602	-0.234752199	-0.181448263
θ8	2.682356734	-0.234752199	-0.180758846
θ9	2.66906461	-0.263019004	-0.192682027
θ10	2.673524361	-0.267351867	-0.210873809
θ11	2.672412738	-0.265524606	-0.225649602
θ12	2.663699199	-0.274360116	-0.234984493
θ13	2.669344089	-0.274684504	-0.232935488

θ14	2.67807589	-0.286129123	-0.211183421

E.5 14 Bus Power System-Rayleigh Noise on 1/5 data set

	LS-based	Exact Solution	Modified LAV
V1	1.06	1.06	1.06
V2	-0.072402145	1.045	0.936886244
V3	0.828729474	1.01	1.033244339
V4	1.023520108	1.026092698	0.999857482
V5	0.916122277	1.032597949	0.947298551
V6	1.069528387	1.07	1.060526049
V7	1.061631515	1.044811975	1.007273654
V8	1.052797284	1.09	0.99910137
V9	1.035877477	1.027630894	1.007350414
V10	1.02547623	1.027543353	1.027797159
V11	1.064234474	1.044943317	1.045571184
V12	1.071973449	1.05301731	1.052428895
V13	1.074370579	1.046234106	1.05255677
V14	1.02243525	1.017433253	1.029665848
θ1	0	0	0
θ2	0.205302141	-0.086507559	-0.360656364
θ3	0.869085007	-0.220484417	-1.010651886
θ4	0.483504552	-0.180919937	-0.746740777
θ5	0.506675747	-0.156149826	-0.678540027
θ6	0.57965485	-0.25969414	-0.788954054
θ7	0.604985505	-0.234752199	-0.798836471
θ8	0.636949877	-0.234752199	-0.796326541

$\theta 9$	0.61077309	-0.263019004	-0.80948628
$\theta 10$	0.612595373	-0.267351867	-0.811810231
$\theta 11$	0.594566873	-0.265524606	-0.805216097
$\theta 12$	0.564848904	-0.274360116	-0.800893487
$\theta 13$	0.576330353	-0.274684504	-0.798618226
$\theta 14$	0.608969466	-0.286129123	-0.807021386

E.6 30 Bus Power System-Gaussian Noise on 1/2 data set

	LS-based	Exact Solution	Modified LAV
V1	1.06	1.06	1.06
V2	1.049511641	1.043	1.034099277
V3	1.045740302	1.024830371	1.009289913
V4	1.012161288	1.016826096	0.986372979
V5	1.04992021	1.01	1.02564211
V6	0.818174834	1.011194194	1.00202704
V7	1.086933919	1.002936554	0.966032808
V8	0.138875193	1.01	1.00603183
V9	0.269945333	1.023775239	1.002162128
V10	0.953550233	1.000932447	0.982767924
V11	-0.054548444	1.082	1.050593778
V12	0.388288354	1.026077684	0.42061883
V13	0.066654001	1.071	0.075906453
V14	0.69663625	1.008640225	0.707887821
V15	0.72390057	1.002086652	0.754092722
V16	0.41701829	1.007627307	0.838613731
V17	0.959449134	0.997746168	1.053439379

V18	0.455496594	0.98904376	0.504078586
V19	0.944988511	0.984580269	0.919405332
V20	1.074613107	0.98785947	1.04831807
V21	0.990972077	0.987570317	1.001106777
V22	0.99245921	0.988002551	1.00323024
V23	1.016942098	0.986437097	1.393859865
V24	0.99459182	0.974280764	1.046260617
V25	0.963589703	0.974551204	0.972594308
V26	0.88356075	0.956065253	0.976058974
V27	1.088982249	0.983686075	0.981228343
V28	1.018566965	1.006808871	1.006149879
V29	0.931576674	0.962956394	0.961928092
V30	0.906682204	0.950970371	0.969303116
$\theta 1$	0	0	0
$\theta 2$	-0.037547029	-0.09329216	-0.086085469
$\theta 3$	9.64E-05	-0.132485069	-0.152820606
$\theta 4$	0.01180972	-0.163229133	-0.161581198
$\theta 5$	-0.098121668	-0.247028312	-0.111658982
$\theta 6$	0.082677491	-0.193153261	-0.118680802
$\theta 7$	-0.069713299	-0.224467749	-0.150033693
$\theta 8$	6.509819095	-0.20596692	-0.134215772
$\theta 9$	1.536216426	-0.249366218	0.230350957
$\theta 10$	1.35233135	-0.279387696	0.494648703
$\theta 11$	-388.9557864	-0.249366218	0.183058303
$\theta 12$	-0.31824857	-0.271529508	-0.801522052
$\theta 13$	30.62299937	-0.271529508	0.582467279
$\theta 14$	-0.083392277	-0.287507314	-0.712290231
$\theta 15$	0.496189917	-0.287795622	-0.268102929
$\theta 16$	0.760498736	-0.279288537	0.325292558

θ17	1.33167163	-0.283605355	0.495809239
θ18	0.863933455	-0.297927113	0.558204514
θ19	1.381998055	-0.300355653	1.423405957
θ20	1.403587198	-0.296174488	1.433421363
θ21	1.324387856	-0.287545739	0.448416249
θ22	1.315154608	-0.287181315	0.428643731
θ23	0.880345946	-0.292707744	-0.201346292
θ24	1.156774468	-0.292757965	0.047142462
θ25	1.126386803	-0.286277964	-0.193167647
θ26	1.216770436	-0.294272601	-0.200908904
θ27	1.01664893	-0.277267582	-0.186816005
θ28	0.14951535	-0.203901876	-0.138292524
θ29	1.233004228	-0.300534844	-0.197419791
θ30	1.277196628	-0.31728093	-0.191930222

E.7 30 Bus Power System-Rayleigh Noise on 1/2 data set

	LS-based	Exact Solution	Modified LAV
V1	1.06	1.06	1.06
V2	-0.085174554	1.043	-0.271350549
V3	0.026211018	1.024830371	0.607743569
V4	-0.151807364	1.016826096	0.696716379
V5	-0.044051781	1.01	-0.148479317
V6	-0.014656585	1.011194194	0.953664392
V7	0.025790772	1.002936554	0.652155007
V8	0.11501933	1.01	1.106844112
V9	-0.037803981	1.023775239	0.685554021
V10	0.818735519	1.000932447	0.993407295
V11	0.606140407	1.082	-0.014394381
V12	0.112669405	1.026077684	-0.107136523
V13	-1.018337759	1.071	-0.422064679
V14	-0.058854624	1.008640225	0.714369287
V15	-0.228829231	1.002086652	0.071158298
V16	0.004052401	1.007627307	0.124115334
V17	0.850445551	0.997746168	1.1096753
V18	0.960947167	0.98904376	0.982882667
V19	0.977588771	0.984580269	1.005273745
V20	1.035769662	0.98785947	0.950161081
V21	0.996628049	0.987570317	0.997257108
V22	0.98891326	0.988002551	0.991651819
V23	0.819693434	0.986437097	2.554704967
V24	0.64637948	0.974280764	0.739284628
V25	0.918282323	0.974551204	0.957674212
V26	0.90095127	0.956065253	1.023975695
V27	0.882193401	0.983686075	0.953512974

V28	0.890108833	1.006808871	1.15596
V29	0.949405622	0.962956394	0.960467203
V30	0.939474722	0.950970371	0.966747372
θ1	0	0	0
θ2	3.534627825	-0.09329216	0.117575919
θ3	3.899774757	-0.132485069	2.467113428
θ4	-3.885327412	-0.163229133	1.380438853
θ5	-10.89941153	-0.247028312	-8.192657847
θ6	26.06667759	-0.193153261	1.661360953
θ7	4.053029642	-0.224467749	1.3108623
θ8	5.830064824	-0.20596692	1.861725028
θ9	-7.635678256	-0.249366218	0.918425707
θ10	8.68323403	-0.279387696	0.25425659
θ11	105.2024265	-0.249366218	-5.179947473
θ12	31.41993615	-0.271529508	-5.101674401
θ13	603.1683508	-0.271529508	-3.684004867
θ14	-4.202732641	-0.287507314	-37.25833456
θ15	4.937120622	-0.287795622	12.34431467
θ16	50.82071191	-0.279288537	14.28540991
θ17	6.942991351	-0.283605355	0.050279129
θ18	8.794855045	-0.297927113	-0.334142088
θ19	8.912285803	-0.300355653	-0.084932426
θ20	8.942795392	-0.296174488	-0.001021665
θ21	8.662305974	-0.287545739	0.251088677
θ22	8.657703461	-0.287181315	0.252870004
θ23	8.629899908	-0.292707744	-1.558534891
θ24	7.381752159	-0.292757965	1.474728396
θ25	7.75019645	-0.286277964	1.572670169
θ26	9.406911361	-0.294272601	1.548010269

θ27	6.720081665	-0.277267582	1.671027844
θ28	5.94420317	-0.203901876	1.886257937
θ29	5.481022656	-0.300534844	1.667413574
θ30	5.457677931	-0.31728093	1.674132387

E.8 57 Bus Power System-Gaussian Noise on 1/3 data

	LS-based	Exact Solution	Modified LAV
V1	1.04	1.04	1.04
V2	0.980757908	1.01	0.973851414
V3	0.993319198	0.985	0.989328628
V4	1.005503415	0.978030655	1.002647629
V5	1.01337006	0.975586	1.01027367
V6	1.006518738	0.98	1.001027896
V7	0.741543836	0.979898193	0.734829101
V8	1.003349995	1.005	1.097822496
V9	1.004034128	0.98	1.018228082
V10	0.985636921	0.982966137	0.981335602
V11	0.975258524	0.972328182	0.966949029
V12	0.992628534	1.015	0.994021474
V13	0.982003513	0.98070898	1.001161388
V14	0.969268052	0.972578287	1.000269353
V15	0.988468862	0.986526095	0.999000127
V16	1.01568326	1.013341786	0.976374644
V17	0.991439214	1.01742339	0.884936207
V18	0.961686332	0.946354595	0.971612892
V19	0.166141643	0.915210221	0.889052161

V20	0.429707834	0.909254583	0.989450537
V21	0.079211938	0.913916791	1.01304506
V22	0.54054952	0.915508548	1.003330861
V23	0.552116602	0.913445339	0.986277958
V24	0.134294014	0.895132992	0.980648215
V25	0.411153399	0.838468271	0.647499089
V26	0.01771532	0.89750851	1.043177005
V27	0.611447065	0.930278477	0.834375154
V28	0.620877222	0.949505685	0.681247316
V29	0.435484078	0.965768673	0.419264952
V30	0.466655973	0.81703591	0.482481732
V31	0.214465961	0.790535149	0.349875003
V32	0.63192878	0.814960146	0.625495795
V33	0.617211514	0.812283873	0.634817073
V34	0.609686832	0.865156145	1.016320005
V35	0.619917299	0.87406903	0.984672785
V36	0.571961614	0.885533817	0.999547694
V37	0.583850412	0.894314049	1.00061978
V38	0.832346528	0.919923531	1.002151413
V39	0.579868427	0.892801041	0.998441173
V40	0.647091082	0.884432635	1.001386472
V41	0.38324955	0.930880734	0.331001368
V42	0.82049151	0.887935295	0.734312893
V43	0.906310175	0.959303509	0.751649114
V44	0.998793777	0.933222087	0.999757749
V45	1.000056253	0.973171437	1.015737566
V46	0.953344515	0.957676066	1.002617604
V47	0.938624579	0.934138475	1.000498743
V48	0.936347379	0.93005649	0.998383293

V49	0.97814934	0.936874996	1.008771681
V50	0.94150029	0.928827667	0.992815845
V51	0.972891473	0.971370537	0.974059754
V52	0.907170261	0.921228418	0.908331456
V53	0.958434634	0.904362618	0.960814652
V54	0.91612761	0.930742426	0.907296229
V55	1.043868406	0.966923491	1.006168773
V56	0.814170383	0.879165235	0.930228316
V57	0.912720966	0.870121684	0.871311099
θ1	0	0	0
θ2	-0.030310526	-0.020899268	-0.031622022
θ3	-0.112288283	-0.105193273	-0.136922883
θ4	-0.129349166	-0.128226607	-0.141780976
θ5	-0.139505554	-0.150529003	-0.14387996
θ6	-0.134788451	-0.153302238	-0.151159841
θ7	-0.226320847	-0.134428539	-0.252190529
θ8	-0.221752345	-0.079901504	-0.294920502
θ9	-0.205719198	-0.168543573	-0.29613915
θ10	-0.209211216	-0.201818494	-0.292129612
θ11	-0.188963364	-0.178815195	-0.268070793
θ12	-0.151501072	-0.183454586	-0.245241677
θ13	-0.177969299	-0.171625151	-0.253784966
θ14	-0.179045442	-0.163126247	-0.243327822
θ15	-0.135036675	-0.125659078	-0.179063497
θ16	-0.117252655	-0.15511647	-0.155936309
θ17	-0.062642523	-0.094435404	-0.055909414
θ18	-0.186718143	-0.211641945	-0.176011798
θ19	-2.068718037	-0.241634038	-0.33038684
θ20	-9.352675991	-0.246355127	-0.390657547

θ21	9.645847794	-0.236120803	-0.458694717
θ22	-0.905938525	-0.235077181	-0.476312746
θ23	-0.083392396	-0.236061874	-0.510823722
θ24	0.309200992	-0.236907045	-1.93630895
θ25	0.454134752	-0.348019436	-2.049483154
θ26	26.42323232	-0.230610874	-2.041582385
θ27	-3.458654496	-0.207050223	-3.325573891
θ28	-2.598296699	-0.188981257	-2.98123736
θ29	-1.427607263	-0.176621005	-1.833321709
θ30	-0.22096704	-0.362441303	10.77925072
θ31	5.822813328	-0.381813513	-1.955307164
θ32	-1.604061396	-0.365841904	0.213365266
θ33	-1.016966517	-0.366783324	0.772459458
θ34	-3.233538455	-0.263271936	-0.236344744
θ35	-2.419114625	-0.258776887	-0.317524685
θ36	-1.262347489	-0.253612228	-0.348138585
θ37	-0.466559899	-0.249096533	-0.366071137
θ38	-0.423529736	-0.232921358	-0.420013051
θ39	0.437282139	-0.250115671	-0.361639796
θ40	-0.636648085	-0.254966904	-0.342279902
θ41	0.485181706	-0.26146603	-0.579393537
θ42	0.216837895	-0.287315638	-0.209254959
θ43	-0.20221832	-0.20290602	-0.29703105
θ44	-0.298111619	-0.216955401	-0.384124283
θ45	-0.209054341	-0.169634061	-0.265777613
θ46	-0.242221504	-0.197870981	-0.304990659
θ47	-0.290355168	-0.226502547	-0.366196324
θ48	-0.313324968	-0.229007633	-0.383134426
θ49	-0.276130054	-0.23345252	-0.3586404

θ50	-0.247748856	-0.243682181	-0.35291974
θ51	-0.22774512	-0.22555181	-0.319525266
θ52	-1.492653558	-0.203054381	-1.609934993
θ53	-1.369303681	-0.214102228	-1.489379361
θ54	-0.830985245	-0.206573564	-0.959766893
θ55	-0.352371245	-0.191502946	-0.458978231
θ56	-0.01598398	-0.294323326	-0.275780237
θ57	-0.081296934	-0.304977679	-0.223969984

E.9 57 Bus Power System-Rayleigh Noise on 1/3 data

	LS-based	Exact Solution	Modified LAV
V1	1.04	1.04	1.04
V2	1.026755836	1.01	1.024154742
V3	0.987509069	0.985	0.987349733
V4	0.980315281	0.978030655	0.987172294
V5	0.990991596	0.975586	0.990091562
V6	0.992295513	0.98	0.989285246
V7	0.633911479	0.979898193	0.643488868
V8	0.992403312	1.005	1.064148494
V9	1.012418866	0.98	1.035344327
V10	0.985992577	0.982966137	0.980832257
V11	0.881353947	0.972328182	0.881457504
V12	1.012261348	1.015	1.002620595
V13	0.985761444	0.98070898	1.032879555
V14	0.965725506	0.972578287	0.996521836
V15	0.986347388	0.986526095	0.993705321

V16	1.041117436	1.013341786	1.008868555
V17	1.04363284	1.01742339	1.024966919
V18	0.930847271	0.946354595	0.940829468
V19	-0.027494321	0.915210221	0.318143683
V20	-0.0423557	0.909254583	0.405957309
V21	0.050363939	0.913916791	0.932598319
V22	0.21322869	0.915508548	0.997457763
V23	0.483286588	0.913445339	1.003056211
V24	-0.0066921	0.895132992	0.979909966
V25	0.127570707	0.838468271	0.055143994
V26	-0.093811119	0.89750851	0.866667197
V27	-0.114203251	0.930278477	0.210659217
V28	-0.008770279	0.949505685	0.272572437
V29	0.088819866	0.965768673	0.031679478
V30	-0.024337054	0.81703591	-0.135777261
V31	0.057753042	0.790535149	-0.019100585
V32	0.050025883	0.814960146	-0.08441519
V33	-0.074872279	0.812283873	0.284543489
V34	-0.419721125	0.865156145	0.331948418
V35	0.028916834	0.87406903	0.939213572
V36	0.083933239	0.885533817	0.94440997
V37	0.058606736	0.894314049	0.93253764
V38	0.188773177	0.919923531	0.985605702
V39	-0.010949902	0.892801041	0.955954865
V40	-0.204217797	0.884432635	0.94780675
V41	-0.455500866	0.930880734	0.503404671
V42	0.431648092	0.887935295	0.057079585
V43	0.009546674	0.959303509	0.150527566
V44	0.27527402	0.933222087	1.00211356

V45	0.040447921	0.973171437	0.940150698
V46	0.428819104	0.957676066	0.986714286
V47	0.83478092	0.934138475	0.996789772
V48	0.798724689	0.93005649	0.996537896
V49	-0.029494239	0.936874996	0.991343321
V50	0.829056332	0.928827667	0.97149464
V51	0.93971364	0.971370537	0.969648908
V52	0.890652017	0.921228418	0.892774673
V53	0.942938729	0.904362618	0.941555671
V54	0.870240271	0.930742426	0.874635204
V55	0.9799895	0.966923491	0.832741988
V56	0.467261995	0.879165235	0.626846745
V57	0.287938218	0.870121684	0.765872113
θ1	0	0	0
θ2	-0.028376141	-0.020899268	-0.027169108
θ3	-0.118491414	-0.105193273	-0.113465148
θ4	-0.124140409	-0.128226607	-0.145797239
θ5	-0.115606744	-0.150529003	-0.187349461
θ6	-0.106015252	-0.153302238	-0.198111051
θ7	-0.070154767	-0.134428539	-0.23783265
θ8	-0.192013469	-0.079901504	-0.321085286
θ9	-0.191825875	-0.168543573	-0.31839792
θ10	-0.196585983	-0.201818494	-0.263028294
θ11	-0.252589637	-0.178815195	-0.665325899
θ12	-0.156406128	-0.183454586	-0.19264803
θ13	-0.222282059	-0.171625151	-0.236343103
θ14	-0.251677232	-0.163126247	-0.161731702
θ15	-0.179339443	-0.125659078	-0.126527598
θ16	-0.114432782	-0.15511647	-0.125570875

θ17	-0.058451692	-0.094435404	-0.063741125
θ18	-0.206522279	-0.211641945	-0.218094917
θ19	-128.0378551	-0.241634038	-13.86684951
θ20	-222.459545	-0.246355127	-0.907808851
θ21	142.4216111	-0.236120803	-0.20052634
θ22	-369.7359284	-0.235077181	-0.182327198
θ23	-0.705626688	-0.236061874	-0.220236774
θ24	6.36554139	-0.236907045	-0.927225371
θ25	53.94683378	-0.348019436	-3.280963171
θ26	-24.06581294	-0.230610874	-0.848311508
θ27	4.563029938	-0.207050223	-3.011886909
θ28	16.89858911	-0.188981257	17.8936808
θ29	17.81708307	-0.176621005	7.86115018
θ30	16.61594421	-0.362441303	-33.33968646
θ31	6.697726457	-0.381813513	-164.4568277
θ32	-85.95740061	-0.365841904	46.74582322
θ33	80.86191874	-0.366783324	-0.238246971
θ34	38.52621842	-0.263271936	4.035466737
θ35	-29.13176207	-0.258776887	2.404360143
θ36	21.32718109	-0.253612228	0.930388684
θ37	-11.06155709	-0.249096533	-0.762546303
θ38	8.936480413	-0.232921358	-0.135661667
θ39	-0.784529365	-0.250115671	-1.110960017
θ40	10.51715134	-0.254966904	-0.158409742
θ41	2.963589287	-0.26146603	2.690781947
θ42	-10.03008807	-0.287315638	-43.37701414
θ43	-28.65924268	-0.20290602	6.09824557
θ44	-118.5807419	-0.216955401	-0.15612551
θ45	3.858535183	-0.169634061	-0.154874604

θ46	3.689466391	-0.197870981	-0.161738967
θ47	0.415039878	-0.226502547	-0.158535606
θ48	1.015605704	-0.229007633	-0.157474706
θ49	12.484887	-0.23345252	-0.178230513
θ50	-0.75724557	-0.243682181	-0.220593859
θ51	-0.230544529	-0.22555181	-0.281705319
θ52	-0.530311704	-0.203054381	-0.50489944
θ53	-0.474218489	-0.214102228	-0.494410817
θ54	-0.365464677	-0.206573564	-0.404436678
θ55	-0.236523778	-0.191502946	-0.369011922
θ56	8.237614749	-0.294323326	1.186412565
θ57	5.459241928	-0.304977679	6.469110284

E.10 118 Bus Power System-Gaussian Noise on 1/6 data

	LS-based	Exact Solution	Modified LAV
V1	0.997395104	1	0.999999032
V2	0.994366653	0.994841533	1.00000441
V3	1.007067549	0.996538035	0.999993899
V4	1.002165545	1	0.999994334
V5	1.002147741	1.002289624	1.000017224
V6	1.001542787	1	0.999997638
V7	0.999019132	0.999336917	1.000000621
V8	0.929005942	1	1.000039832
V9	1.028508173	1.009180031	0.999989771
V10	1.031072637	1	0.999986112
V11	0.99648226	0.992799715	0.999996589
V12	0.996265046	1	0.999996769
V13	1.018969603	0.98135513	0.999934204
V14	1.035466496	0.99896324	0.999935216
V15	0.976474755	1	1.000008694
V16	1.054558303	0.994405011	0.999944443
V17	0.913790169	1.006285752	1.000169187
V18	1.03973333	1	0.999914308
V19	1.010375949	1	0.999860218
V20	0.99856299	0.985261032	0.999940496
V21	0.994950462	0.978786897	1.000028048
V22	0.964852507	0.981467787	1.000026235
V23	0.384320293	0.997601169	0.999756579
V24	0.630826953	1	1.001776005
V25	0.156212266	1	0.999407474
V26	0.031827925	1	1.000283263
V27	0.654068902	1	0.999994758

V28	-0.060996461	0.994277782	1.000031662
V29	0.378562826	0.996238628	1.000008461
V30	0.075236719	1.009114636	1.000467039
V31	0.51531387	1	0.999970111
V32	0.891433297	1	0.999980022
V33	0.157931763	0.993558137	1.002008924
V34	0.354221806	1	0.999190968
V35	0.26409611	0.99938369	1.00013742
V36	0.371043653	1	0.99953546
V37	0.312423751	1.004239965	1.004545686
V38	0.441225238	1.009042539	0.997873962
V39	0.309801402	0.994093869	1.057246881
V40	0.170804392	1	0.96260647
V41	0.390458833	0.993092208	0.391558539
V42	0.818945447	1	0.911390856
V43	0.07464292	0.97727436	0.935123343
V44	0.909506598	0.961432203	0.956999845
V45	1.006242711	0.964055407	0.979175344
V46	0.991651586	1	0.984718848
V47	1.002096257	0.996138427	1.014637317
V48	0.999779341	0.993479906	1.005985147
V49	0.996012747	1	1.002283233
V50	1.006379383	0.99321852	0.991652942
V51	0.982470267	0.980799366	0.97955225
V52	0.975802807	0.976373108	0.978954156
V53	0.986332628	0.980645253	0.986248637
V54	1.000068108	1	0.998014771
V55	1.000387699	1	1.002682595
V56	0.999302234	1	1.000486004

V57	0.999622084	0.993988772	1.000748895
V58	0.986847463	0.986732548	0.990806335
V59	1.004736842	1	1.009516794
V60	0.998937129	0.998315192	0.998856742
V61	0.998655444	1	0.999086816
V62	0.997798355	1	0.999437158
V63	0.999085949	0.999464417	1.000567708
V64	0.999478114	1.001239905	1.00014195
V65	1.0042035	1	0.999361543
V66	0.994004072	1	1.003478283
V67	1.000047661	0.993395183	0.999318053
V68	1.002862409	1.003274483	1.000042062
V69	1.035	1	1.035
V70	0.999430343	1	0.999187399
V71	1.002694992	1.00048439	1.000421139
V72	1.088954465	1	0.998598885
V73	0.990236461	1	1.000803047
V74	0.995177794	1	1.000104905
V75	0.997405886	0.992506749	0.999220053
V76	0.996648509	1	1.000871012
V77	0.996987899	1	0.999533922
V78	0.996328594	0.991675598	1.001055266
V79	0.990437911	0.986287303	1.006731112
V80	0.997679828	1	0.997180458
V81	1.003210586	1.007889227	0.999828714
V82	0.976658668	0.973736576	0.980455845
V83	0.973299852	0.976123762	0.982127073
V84	0.990958519	0.987266035	0.991565176
V85	0.990444037	1	0.990709846

V86	1.00490723	0.990628769	1.004499478
V87	0.98191084	1	0.981668139
V88	0.997219428	0.990587404	0.997182696
V89	0.998251248	1	0.998236265
V90	1.00330258	1	1.003345446
V91	1.002127942	1	1.002143445
V92	0.996104685	1	0.99610176
V93	0.985735771	0.984205884	0.985674432
V94	0.979655999	0.978662495	0.979748731
V95	0.968574913	0.965589554	0.96877599
V96	0.973698296	0.973399732	0.976640681
V97	0.985263912	0.981773147	0.982329051
V98	1.006744243	0.991700754	1.002070453
V99	1.003618246	1	1.002888811
V100	0.994070113	1	0.99374439
V101	0.994065095	0.986103729	0.994314569
V102	1.000429344	0.994120909	1.000522721
V103	1.001378334	1	1.001533973
V104	1.000562131	1	1.000595318
V105	0.998107387	1	0.998131828
V106	1.001776601	0.9907116	1.001818922
V107	0.989525094	1	0.989563145
V108	0.99786526	0.998164241	0.99786078
V109	0.998423516	0.997678348	0.998424383
V110	1.000686826	1	1.000720683
V111	0.997478602	1	0.997458501
V112	0.997217379	1	0.997165429
V113	1.169658211	1	0.999719779
V114	0.999124078	0.995217672	1.000000112

V115	0.987298264	0.994806449	1.000002402
V116	1.001156013	1	0.999911525
V117	0.963018327	0.9840504	1.000045397
V118	0.994806231	0.989790679	1.002277875
θ1	-2.800314481	-0.346942794	-0.376928132
θ2	-2.808934801	-0.33244518	-0.376967452
θ3	-2.790554597	-0.32758539	-0.376893838
θ4	-2.750211975	-0.257542568	-0.376607498
θ5	-2.744313511	-0.249476925	-0.376557265
θ6	-2.77615012	-0.298703714	-0.376865013
θ7	-2.786950639	-0.306304318	-0.37692855
θ8	-2.683875063	-0.159323822	-0.375802963
θ9	-2.630097683	-0.025100185	-0.376438421
θ10	-2.612682399	0.11979921	-0.376662066
θ11	-2.781584444	-0.303145224	-0.376969263
θ12	-2.795828266	-0.312428613	-0.377029731
θ13	-2.801514783	-0.328049143	-0.377603364
θ14	-2.805261838	-0.326136037	-0.377796634
θ15	-2.806340456	-0.335185915	-0.382658507
θ16	-2.788500514	-0.317793004	-0.377043409
θ17	-2.810618327	-0.287334257	-0.376053076
θ18	-2.82908242	-0.329112247	-0.379646582
θ19	-2.82560912	-0.339998816	-0.383406113
θ20	-2.863934725	-0.324802945	-0.369568151
θ21	-2.855979739	-0.297781393	-0.361383878
θ22	-2.832543395	-0.253902919	-0.351512352
θ23	-3.057797946	-0.167667708	-0.330852491
θ24	-1.502219746	-0.172231804	-0.300686808
θ25	261.4790657	-0.033445792	-0.350692405

θ26	49.60557529	-0.000711098	-0.357128189
θ27	-3.684050459	-0.270885166	-0.35513261
θ28	-4.819832712	-0.298649716	-0.357773011
θ29	-5.121416381	-0.31436343	-0.360260315
θ30	4.513421647	-0.197287832	-0.371584641
θ31	-4.031076509	-0.312282958	-0.360970913
θ32	-3.587520594	-0.280685968	-0.354177939
θ33	-0.477933949	-0.343575933	-0.410008181
θ34	-3.723275081	-0.331242472	-0.448599378
θ35	-4.401877173	-0.339678764	-0.450634702
θ36	-3.596568736	-0.339980353	-0.450364168
θ37	-2.401235232	-0.322767015	-0.452935799
θ38	-1.294923027	-0.23066925	-0.363629298
θ39	-5.603962051	-0.385010082	-0.651954966
θ40	-3.001717701	-0.405887114	-0.722748382
θ41	-1.984774014	-0.412945687	-1.099695644
θ42	-0.473129382	-0.38531827	-0.329626735
θ43	-10.43552033	-0.332556559	-0.368539423
θ44	-0.304421285	-0.288807851	-0.245945572
θ45	-0.213712122	-0.257969572	-0.159883999
θ46	-0.179023713	-0.21403429	-0.122494855
θ47	-0.148672109	-0.170003123	-0.094194296
θ48	-0.188223525	-0.181479439	-0.122533915
θ49	-0.184383116	-0.163921055	-0.111951433
θ50	-0.189132059	-0.204411005	-0.122167637
θ51	-0.212964162	-0.254361477	-0.157591872
θ52	-0.222570738	-0.271835064	-0.169859333
θ53	-0.2195477	-0.290301572	-0.18906785
θ54	-0.180264663	-0.276966208	-0.195760388

$\theta 55$	-0.180162701	-0.282057505	-0.19048719
$\theta 56$	-0.179805314	-0.278928889	-0.195803014
$\theta 57$	-0.202606992	-0.254596737	-0.167023967
$\theta 58$	-0.213149134	-0.269885069	-0.176255693
$\theta 59$	-0.100958648	-0.196453108	-0.107539344
$\theta 60$	-0.067396212	-0.128534675	-0.059242251
$\theta 61$	-0.072534348	-0.112840458	-0.055355579
$\theta 62$	-0.050500428	-0.123760008	-0.047206194
$\theta 63$	-0.081832595	-0.135136036	-0.06529688
$\theta 64$	-0.072367553	-0.103293746	-0.054763587
$\theta 65$	-0.088390749	-0.043777251	-0.069389659
$\theta 66$	-0.11809979	-0.041424131	-0.069226048
$\theta 67$	-0.021388615	-0.094502569	-0.020753199
$\theta 68$	-0.049025891	-0.046018061	-0.046671115
$\theta 69$	0	0	0
$\theta 70$	-0.17835689	-0.145823361	-0.100764793
$\theta 71$	-0.214559634	-0.152462808	-0.114200455
$\theta 72$	-0.494605858	-0.173840533	-0.208982188
$\theta 73$	-0.205749485	-0.155192917	-0.111856271
$\theta 74$	-0.127746386	-0.169493203	-0.09425263
$\theta 75$	-0.111379336	-0.144026551	-0.082336955
$\theta 76$	-0.111667222	-0.171378132	-0.082119131
$\theta 77$	-0.037977922	-0.070408802	-0.031330739
$\theta 78$	-0.039900658	-0.073974231	-0.034840347
$\theta 79$	-0.039234645	-0.065824752	-0.035309913
$\theta 80$	-0.045277557	-0.019563862	-0.02764318
$\theta 81$	-0.039622015	-0.036910324	-0.043884196
$\theta 82$	0.03421474	-0.056990754	0.014627637
$\theta 83$	0.07327771	-0.037146182	0.050021682

θ84	0.152445092	0.002245626	0.117462271
θ85	0.171093273	0.026478738	0.131051611
θ86	0.217229789	0.006256778	0.177442097
θ87	0.229930874	0.013493552	0.190233774
θ88	0.183418629	0.082726591	0.133401044
θ89	0.069431977	0.155443041	0.014788729
θ90	0.106278084	0.039755831	0.050154315
θ91	0.07128853	0.038681819	0.014426282
θ92	0.053856292	0.050968267	-0.003399119
θ93	0.031635587	0.001985967	-0.025910333
θ94	0.014086665	-0.033254176	-0.041151598
θ95	0.018616533	-0.049498343	-0.031211946
θ96	0.019919395	-0.050978271	-0.016655648
θ97	0.011224174	-0.04191227	-0.023373541
θ98	0.012938974	-0.050828706	-0.038492195
θ99	-0.000134123	-0.062114934	-0.065285104
θ100	-0.036281774	-0.042969946	-0.10276097
θ101	0.014631048	-0.0180183	-0.050647298
θ102	0.037305923	0.026401239	-0.022550141
θ103	-0.060777939	-0.110964581	-0.133070139
θ104	-0.053214873	-0.165586758	-0.12901931
θ105	-0.064528832	-0.18568229	-0.141179532
θ106	-0.060195019	-0.188306014	-0.136879766
θ107	-0.067928646	-0.238566462	-0.14650056
θ108	-0.094255646	-0.204274004	-0.171798381
θ109	-0.100917639	-0.21128549	-0.178512363
θ110	-0.10636046	-0.224144295	-0.1834922
θ111	-0.11957207	-0.194777896	-0.197105152
θ112	-0.118287987	-0.274660309	-0.19577115

θ113	-2.861907292	-0.28653782	-0.374634695
θ114	-3.677206657	-0.285737006	-0.354896423
θ115	-3.682257251	-0.285806918	-0.354950991
θ116	-0.048007896	-0.053226333	-0.047112288
θ117	-2.823721745	-0.33879035	-0.376887641
θ118	-0.123593425	-0.1643856	-0.081041546

E.11 118 Bus Power System-Rayleigh Noise on 1/6 data

	LS-based	Exact Solution	Modified LAV
V1	0.997337164	1	1.000006719
V2	0.992134803	0.994841533	1.000100505
V3	1.00756903	0.996538035	1.000002278
V4	1.002592958	1	1.000012978
V5	1.001634675	1.002289624	0.999953099
V6	1.00189928	1	1.00000265
V7	0.99831291	0.999336917	0.999992167
V8	0.911020905	1	0.999988722
V9	1.030986648	1.009180031	0.99999215
V10	1.037581057	1	1.000003813
V11	0.996316685	0.992799715	1.000003912
V12	0.995139209	1	1.000004928
V13	1.041560935	0.98135513	0.999973352
V14	1.055741729	0.99896324	0.999936077
V15	0.93748537	1	1.000414987
V16	1.07197752	0.994405011	0.999927356
V17	0.897617556	1.006285752	1.000092278

V18	1.050238374	1	1.000277396
V19	0.97226271	1	0.999051626
V20	1.005719744	0.985261032	1.006620297
V21	1.001819881	0.978786897	1.011759985
V22	0.925846859	0.981467787	1.005379536
V23	-0.002183541	0.997601169	1.000323519
V24	0.533100656	1	1.000443446
V25	0.018809815	1	1.003225513
V26	-0.108184706	1	0.998997381
V27	0.387087768	1	1.000211303
V28	0.054379607	0.994277782	1.000049421
V29	-0.062460452	0.996238628	1.000063218
V30	-0.07457776	1.009114636	0.999861162
V31	0.041507638	1	0.999885741
V32	0.665815657	1	0.999132207
V33	-0.022059985	0.993558137	1.011552468
V34	0.042955889	1	1.000943593
V35	-0.024364228	0.99938369	1.000018461
V36	0.055435278	1	1.00003553
V37	-0.144798431	1.004239965	0.992445879
V38	0.079167175	1.009042539	1.006442848
V39	-0.028031526	0.994093869	0.99910991
V40	0.189284077	1	0.945992098
V41	0.265630648	0.993092208	0.699529825
V42	-0.085138934	1	0.956599817
V43	-0.408745115	0.97727436	1.023112902
V44	-0.012349817	0.961432203	0.973100951
V45	0.150823218	0.964055407	0.993065388
V46	0.026550427	1	0.772390591

V47	0.449402968	0.996138427	1.120033989
V48	0.393364123	0.993479906	1.029586052
V49	0.919738533	1	1.065153158
V50	1.106892879	0.99321852	0.985268167
V51	0.993661805	0.980799366	0.980275921
V52	0.982367261	0.976373108	0.975351729
V53	0.987642295	0.980645253	0.984243697
V54	0.999608322	1	0.99976891
V55	0.999999266	1	0.99970164
V56	1.001519405	1	0.997457241
V57	1.042170054	0.993988772	0.999022992
V58	0.995747046	0.986732548	0.987370301
V59	1.003125556	1	1.000678685
V60	0.998686331	0.998315192	0.998018339
V61	0.998758324	1	0.999309156
V62	1.006863255	1	0.99892063
V63	0.999415419	0.999464417	0.999886626
V64	1.000940313	1.001239905	1.000035331
V65	0.998531192	1	0.998410298
V66	1.041825806	1	0.985453187
V67	1.067603783	0.993395183	0.968196919
V68	1.002946433	1.003274483	1.000081507
V69	1.035	1	1.035
V70	0.997855129	1	1.001171763
V71	1.001312133	1.00048439	0.998871812
V72	0.991340304	1	0.98193783
V73	1.001565719	1	1.001569083
V74	0.99571802	1	0.995369931
V75	0.997785066	0.992506749	0.996471557

V76	0.996652808	1	0.99762445
V77	0.997013223	1	0.999886573
V78	0.996310077	0.991675598	0.992085356
V79	0.990458592	0.986287303	0.985390287
V80	0.997466599	1	0.998434658
V81	1.004111856	1.007889227	1.000314487
V82	0.976648928	0.973736576	0.973851486
V83	0.973286648	0.976123762	0.978571193
V84	0.990942976	0.987266035	0.991770363
V85	0.990442042	1	0.990740288
V86	1.0048986	0.990628769	1.004819983
V87	0.98192168	1	0.981706873
V88	0.997218353	0.990587404	0.997245041
V89	0.998251545	1	0.998232178
V90	1.003301688	1	1.003330041
V91	1.00212615	1	1.002145
V92	0.996104277	1	0.996180622
V93	0.9857332	0.984205884	0.986155743
V94	0.979655979	0.978662495	0.980119423
V95	0.968571538	0.965589554	0.970708072
V96	0.973711846	0.973399732	0.966144918
V97	0.985393771	0.981773147	0.989576016
V98	1.006860557	0.991700754	0.998741736
V99	1.003633786	1	1.00363984
V100	0.994078466	1	0.993786822
V101	0.994063886	0.986103729	0.994313148
V102	1.00042783	0.994120909	1.000475735
V103	1.001373639	1	1.001577004
V104	1.000561917	1	1.00059471

V105	0.998107017	1	0.998130769
V106	1.001776483	0.9907116	1.001829535
V107	0.989524668	1	0.989547403
V108	0.997865255	0.998164241	0.997861092
V109	0.998423554	0.997678348	0.998423758
V110	1.000686614	1	1.000716937
V111	0.997478871	1	0.997456573
V112	0.997217389	1	0.997171777
V113	1.167666228	1	0.999424252
V114	1.001531787	0.995217672	0.999852363
V115	0.980367415	0.994806449	0.999908478
V116	1.001586153	1	0.999879691
V117	0.926011758	0.9840504	1.000221794
V118	0.994865166	0.989790679	0.992808586
θ1	-1.66916851	-0.346942794	0.443346468
θ2	-1.681248407	-0.33244518	0.443077365
θ3	-1.660055501	-0.32758539	0.443299192
θ4	-1.625107346	-0.257542568	0.442583801
θ5	-1.619985885	-0.249476925	0.442444253
θ6	-1.649255421	-0.298703714	0.443138311
θ7	-1.660595879	-0.306304318	0.443122817
θ8	-1.573986885	-0.159323822	0.440433801
θ9	-1.515897768	-0.025100185	0.442722661
θ10	-1.497517561	0.11979921	0.443528092
θ11	-1.657904436	-0.303145224	0.442668099
θ12	-1.672069235	-0.312428613	0.442706012
θ13	-1.687838431	-0.328049143	0.441968782
θ14	-1.694077143	-0.326136037	0.441828185
θ15	-1.789571556	-0.335185915	0.441153657

θ16	-1.669555885	-0.317793004	0.439816008
θ17	-1.703606179	-0.287334257	0.422034904
θ18	-1.742035725	-0.329112247	0.427945033
θ19	-1.772886156	-0.339998816	0.431062016
θ20	-1.746338629	-0.324802945	0.322940555
θ21	-1.717204923	-0.297781393	0.311499528
θ22	-1.683288149	-0.253902919	0.311576155
θ23	-3.290244382	-0.167667708	0.181769944
θ24	0.429697139	-0.172231804	0.074300513
θ25	7.872399923	-0.033445792	0.274141871
θ26	5.824088382	-0.000711098	0.315114413
θ27	-2.985983309	-0.270885166	0.279903761
θ28	21.87761978	-0.298649716	0.293182375
θ29	-9.056494227	-0.31436343	0.310518677
θ30	-1.429334544	-0.197287832	0.426532491
θ31	-41.92338027	-0.312282958	0.316740879
θ32	-1.949416431	-0.280685968	0.279691833
θ33	-13.51940372	-0.343575933	0.537743369
θ34	18.88823324	-0.331242472	0.630987598
θ35	11.966264	-0.339678764	0.655394704
θ36	27.23422809	-0.339980353	0.653915381
θ37	-14.85307969	-0.322767015	0.642910369
θ38	-24.43711007	-0.23066925	0.464256317
θ39	-38.12676674	-0.385010082	1.105916574
θ40	44.86204955	-0.405887114	1.099746027
θ41	-40.54424463	-0.412945687	0.860941131
θ42	-91.53911111	-0.38531827	-0.669155748
θ43	-9.839551557	-0.332556559	0.097389474
θ44	110.4510754	-0.288807851	-0.590872809

θ45	-11.40874823	-0.257969572	-1.195575154
θ46	-2.515315465	-0.21403429	-1.629555009
θ47	3.120100283	-0.170003123	-0.855544743
θ48	-0.952463779	-0.181479439	-0.843739161
θ49	-0.426536618	-0.163921055	-0.476416845
θ50	-0.190174758	-0.204411005	-0.242519077
θ51	-0.109145196	-0.254361477	-0.228852132
θ52	-0.075149166	-0.271835064	-0.224677212
θ53	-0.0756135	-0.290301572	-0.228645474
θ54	-0.10722499	-0.276966208	-0.236340791
θ55	-0.100349671	-0.282057505	-0.220455096
θ56	-0.100865935	-0.278928889	-0.228760178
θ57	-0.10977037	-0.254596737	-0.224718167
θ58	-0.090158312	-0.269885069	-0.224920227
θ59	-0.081664135	-0.196453108	-0.150168164
θ60	-0.077160333	-0.128534675	-0.117892586
θ61	-0.083567618	-0.112840458	-0.116071607
θ62	-0.069592622	-0.123760008	-0.120088918
θ63	-0.086137361	-0.135136036	-0.120289012
θ64	-0.088916757	-0.103293746	-0.106576716
θ65	-0.138008842	-0.043777251	-0.069544344
θ66	-0.204500478	-0.041424131	-0.222751305
θ67	-0.072744108	-0.094502569	-0.154683495
θ68	-0.080113026	-0.046018061	-0.062698874
θ69	0	0	0
θ70	-0.113809598	-0.145823361	-0.05364428
θ71	-0.135469281	-0.152462808	-0.071990863
θ72	-0.214563296	-0.173840533	-0.091501547
θ73	-0.137108948	-0.155192917	-0.07801662

θ74	-0.106882093	-0.169493203	-0.067056067
θ75	-0.096800477	-0.144026551	-0.063459101
θ76	-0.110165564	-0.171378132	-0.081425292
θ77	-0.054082544	-0.070408802	-0.077406363
θ78	-0.057130663	-0.073974231	-0.083189234
θ79	-0.057616877	-0.065824752	-0.075440361
θ80	-0.066589958	-0.019563862	-0.071981431
θ81	-0.067339223	-0.036910324	-0.069463464
θ82	0.012505382	-0.056990754	-0.024231667
θ83	0.050806462	-0.037146182	0.01229025
θ84	0.129385804	0.002245626	0.080109245
θ85	0.14804226	0.026478738	0.093726147
θ86	0.193953775	0.006256778	0.140201064
θ87	0.20653112	0.013493552	0.153071278
θ88	0.160416016	0.082726591	0.096016593
θ89	0.046513423	0.155443041	-0.022776519
θ90	0.083353773	0.039755831	0.012754763
θ91	0.048366866	0.038681819	-0.022897178
θ92	0.031014461	0.050968267	-0.04132224
θ93	0.008894352	0.001985967	-0.064713804
θ94	-0.008462472	-0.033254176	-0.082327925
θ95	-0.003885524	-0.049498343	-0.073876954
θ96	-0.002298178	-0.050978271	-0.064665618
θ97	-0.010633206	-0.04191227	-0.070239382
θ98	-0.008650649	-0.050828706	-0.080110474
θ99	-0.022280606	-0.062114934	-0.11281118
θ100	-0.058700708	-0.042969946	-0.143162898
θ101	-0.008052979	-0.0180183	-0.088720393
θ102	0.014472767	0.026401239	-0.060124958

θ103	-0.083241431	-0.110964581	-0.172032556
θ104	-0.075705043	-0.165586758	-0.167107903
θ105	-0.087025361	-0.18568229	-0.179058191
θ106	-0.082691278	-0.188306014	-0.174750841
θ107	-0.09043843	-0.238566462	-0.183904128
θ108	-0.116759904	-0.204274004	-0.209452197
θ109	-0.123422574	-0.21128549	-0.216152395
θ110	-0.128862594	-0.224144295	-0.221245491
θ111	-0.142077641	-0.194777896	-0.234757214
θ112	-0.140793105	-0.274660309	-0.233435631
θ113	-1.708392207	-0.28653782	0.412780667
θ114	-1.759488113	-0.285737006	0.276724575
θ115	-1.749180533	-0.285806918	0.275930759
θ116	-0.078967602	-0.053226333	-0.064054242
θ117	-1.699255359	-0.33879035	0.444878223
θ118	-0.115813469	-0.1643856	-0.080626657

Bibliography

[1] A.J. Wood, and B.F. Wollenberg, *Power system generation, operation and control*, Wiley, New York, 1996.

[2] A. Monticelli, *State Estimation in Electric Power Systems, A Generalized Approach*, Kluwer Academic Publishers, Boston, 1999.

[3] A. Abur, and A.G. Exposito, *Power system state estimation: theory and implementation*, Marcel Dekker Inc., Switzerland, 2004.

[4] D.G. Luenberger, *Optimization by vector space methods*, Wiley-Interscience, 1997.

[5] J.D. Glover, M.S. Sarma, and T.J. Overbye, *Power system analysis and design*, Thomoson Learning, Toronto, 2008.

[6] A. Monticelli, ”Electric power system state estimation”, *Proceedings of the IEEE*, vol. 88, no. 2, pp. 262-282, 2000.

[7] G.S. Christensen, M. Saif, and S.A. Soliman, ”A new algorithm for finding the optimal solution of the least absolute value estimation probelm”, *Canadian Journal of Electrical and Computer Engineering*, vol. 32, no. 1, pp. 5-8, 2007.

[8] S.A. Soliman, G.S. Christensen, and A.H. Rouhi, ”A new algorithm for nonlinear L1-norm minimization with nonlinear equality constraints”, *Computational Statistics and Data Analysis*, vol. 11, no. 1, pp. 97-109, 1991.

[9] G.S. Christensen, S.A. Soliman, and M.Y. Mohamed, ”Power systems state estimation based on least absolute value”, *Control and Dynamic Systems (Advances in Theory and Applications)*, vol. 44, no. 4, pp. 345-481, 1991.

[10] N.M. Nor, R. Jegatheesan, and P. Nallagownden, ”Newton-raphson state estimation solution employing systematically constructed Jacobian matrix”, in *IEEE 2nd International Power and Energy Conference*, Johor Bahru (Malaysia), 2008, pp. 180-185.

[11] S.A. Soliman, G.S. Christensen, and A. Rouhi, ”A new technique for curve fitting based on minimum absolute deviations”, *Computational Statistics and Data Analysis*, vol. 6, no. 4, 1988.

[12] M.A. Herce, ”An example showing that a new technique for LAV estimation breaks down in certain cases”, *Computational Statistics and Data Analysis*, vol. 9, no. 2, pp. 197-202, 1990.

[13] S.A. Soliman, G.S. Christensen, and A. Rouhi, ”Discussion of ”An example showing that a new technique for LAV estimation breaks down in some cases” ”, *Computational Statistics and Data Analysis*, vol. 9, no. 2, pp. 203-213, 1990.

[14] C. Gonzalez-Perez, and B. Wollenberg, ”Analysis of massive measurement loss in large-scale power system state estimation”, *IEEE Power Engineering Review*, vol. 21, no. 10, 2001.

[15] A. Aboonabi, M. Saif, and S.M.M. Alavi, ”Power system least absolute value state estimation using contraction mapping”, in *Proceedings of the 12th IASTED International Conference*, vol. 697, Banff (Canada), 2010.

[16] A. Aboonabi, ”Power System state estimation using contraction mapping and singular value decomposition”, accepted at *18th IFAC World Congrs.*, Milan, Italy, 2011.

[17] C. Madtharad, S. Premrudeepreechacharn, and N.R. Watson, ”Power system state estimation using singular value decomposition”, *Electric Power Systems Research, Elsevier*, vol. 67, no. 2, 2003.

[18] R. Christie, *Power System Test Case Archive*, 1993. [Online]. Available: http://www.ee.washington.edu/research/pstca/

[19] M.E. El-Hawary, *Electrical power systems: design and analysis*, Wiley-IEEE Press, 1995.

[20] F.C. Schweppe, and J. Wildes, ”Power system static-state estimation, part I: Exact model”, *IEEE Transactions on Power Apparatus and Systems*, vol. PAS-89, no. 1, pp. 125-130, 1970.

[21] F.C. Schweppe, and J. Wildes, ”Power system static-state estimation, part II: Approximate model”, *IEEE Transactions on Power Apparatus and Systems*, PAS-89, no. 3, pp. 345-352, 1970.

[22] F.C. Schweppe, and E.J. Handschin, ”Static state estimation in electric power systems”, *Proceedings of the IEEE,* vol. 62, no. 7, pp. 972-882, 1974.

[23] D. Zhengchun, N. Zhenyong, and F. Wanliang, ”Block QR decomposition based power system state estimation algorithm”, *Electric Power Systems Research*, vol. 76, no. 1-3, pp. 86-92, 2005.

[24] H.B. Sun, and B.M. Zhang, ”Global state estimation for whole transmission and distribution networks”, *Electric Power Systems Research*, vol. 74, no. 2, pp. 187-195, 2005.

[25] R.A. Jabr, and B.C. Pal, ”Iteratively reweighted least-squares implementation of the WLAV state-estimation method”, *IEEE Proceedings Generation, Transmission and Distribution*, vol. 151, no. 1, pp. 103-108, 2004.

[26] A. Abur, F.H. Magnago, and F.L. Alvarado, ’Elimination of leverage measurements via matrix stretching”, *International Journal of Electrical Power and Energy Systems*, vol. 19, no. 8, pp. 557-562, 1997.

[27] R.A. Jabr, ”Power system state estimation using an iteratively reweighted least squares method for sequential L1-regression”, *International Journal of Electrical Power and Energy Systems* , vol. 28, no. 2, pp. 86-92, 2006.

[28] R. Neela, and R. Ashokkumar, and P. Arvaindhababu, ”A robust decoupled WLAV state estimation for power systems”, *International Journal of Engineering Science and Technology*, vol. 2, no. 8, pp. 3590-3596, 2010.

[29] A. Papoulis, S.U. Pillai, and S. Unnikrishna, *Probability, random variables, and stochastic processes*, McGraw-Hill, 2002.

[30] W. Willy Kotiuga, and M. Vidyasagar, ”Bad data rejection properties of weighted least absolute value techniques applied to static state estimation”, *IEEE Transactions on Power Apparatus and Systems*, vol. 4, pp. 844-853, 2007.

[31] J.M. Lin, S.J. Huang, and K.R. Shih, ”Application of sliding surface-enhanced fuzzy control for dynamic state estimation of a power system”, *IEEE Transactions on Power Systems*, vol. 18, no. 2, pp. 570-577, 2003.

[32] A. Abur, ”A bad data identification method for linear programming state estimation”, *IEEE Transactions on Power Systems*, vol. 5, no. 3, pp. 894-901, 1990.

[33] Y. Deng, Y. He, and B. Zhang, ”A branch-estimation-based state estimation method for radial distribution systems”, *IEEE Transactions on Power Delivery*, vol. 17, no. 4, pp. 1057-1062, 2002.

[34] M.K. Celik, and A. Abur, ”A robust WLAV state estimator using transformations”, *IEEE Transactions on Power Systems*, vol. 7, no. 1, pp. 106-113, 2002.

[35] N.G. Bretas, and J.B.A. London, ”Network observability: the critical measurement identification using the symbolic Jacobian matrix”, in *International Conference on Power System Technology*, Beijing (China), Aug 1998, pp. 1222-1226.

[36] A.P.S. Meliopoulos, B. Fardanesh, and S. Zelingher, ”Power system state estimation: modeling error effects and impact on system operation”, in *Proceedings of the 34th Annual Hawaii International Conference on System Sciences*, Hawaii (USA), Jan 2001, pp. 682-690.

[37] M.R. Irving, R.C. Owen, and M.J.H. Sterling, ”Power system state estimation using linear programming”, *Proceeding of IEEE*, vol. 125, no. 9, pp. 879-885, 1978.

[38] F.F. Wu, ”Power system state estimation: a survey”, *International Journal of Electrical Power Energy Systems*, vol. 12, no. 2, pp. 80-87, 1990.

[39] L. Holten, A. Gjelsvik, S. Aam, F.F. Wu, and W.H.E. Liu, ”Comparison of different methods for state estimation”, *IEEE Transactions on Power Systems*, vol. 3, no. 4, pp. 1798-1806, 2002.

[40] H.J. Koglin, G. Neisius, G. Beibler, and K.D. Schmitt, ”Bad data detection and identification”, *International Journal of Electrical Power and Energy Systems*, vol. 12, no. 2, pp. 94-103, 1990.

[41] M. Filho, AML da Silva, and D.M. Falcao, ”Bibliography on power system state estimation (1968-1989)”, *IEEE Transactions on Power Systems*, vol. 5, no. 3, pp. 950-961, 1990.

[42] O. Alsac, N. Vempati, B. Stott, and A. Monticelli, ”Generalized state estimation”, *IEEE Transactions on Power Systems*, vol. 13, no. 3, pp.1069-1075, 2002.

[43] A. Bose, and K.A. Clements,”Real-time modeling of power networks”, *Proceedings of the IEEE*, vol. 75, no. 12, pp. 1607-1622, 2005.

[44] E. Handschin, F.C. Schweppe, J. Kohlas, and A. Fiechter, ”Bad data analysis for power system state estimation”, *IEEE Transactions on Power Apparatus and Systems*, vol. 94, no. 2, pp. 329-337, 1975.

[45] W. Jiang, V. Vittal, and G.T. Heydt, ”Diakoptic state estimation using phasor measurement units”, *IEEE Transactions on Power Systems*, vol. 23, no. 4, pp. 1580-1589, 2008.